

If you have discovered material in AURA which is unlawful e.g. breaches copyright, (either yours or that of a third party) or any other law, including but not limited to those relating to patent, trademark, confidentiality, data protection, obscenity, defamation, libel, then please read our [Takedown Policy](#) and [contact the service](#) immediately

THE SEDIMENTOLOGY AND DIAGENESIS OF LOWER PERMIAN  
(ROTLIEGEND) SEDIMENTS:  
(ONSHORE U.K. AND SOUTHERN NORTH SEA).

VOLUME I

DAVID JEREMY PROSSER  
DOCTOR OF PHILOSOPHY

THE UNIVERSITY OF ASTON IN BIRMINGHAM

AUGUST 1988

This copy of the thesis has been supplied on condition that anyone who consults it is understood to recognise that its copyright rests with its author and that no quotation from the thesis and no information derived from it may be published without the author's prior, written consent.

THE UNIVERSITY OF ASTON IN BIRMINGHAM.  
THE SEDIMENTOLOGY AND DIAGENESIS OF LOWER PERMIAN  
(ROTLIEGEND) SEDIMENTS:  
(ONSHORE U.K. AND SOUTHERN NORTH SEA).

DAVID JEREMY PROSSER

DOCTOR OF PHILOSOPHY

AUGUST 1988

SUMMARY.

The thesis provides a comparative study of both sedimentology and diagenesis of Lower Permian (Rotliegend) strata, onshore and offshore U.K. (Southern North Sea). Onshore formations studied include the Bridgnorth, Penrith and Hopeman Sandstone, and are dominated by aeolian facies, with lesser amounts of interbedded fluvial sediments. Aeolian and fluvial strata in onshore basins typically grade laterally into alluvial fan breccias at basin margins. Onshore basins represent proximal examples of Rotliegend desert sediments.

The Leman Sandstone Formation of the Ravenspurn area in the Southern North Sea displays a variety of facies indicative of a distal sedimentological setting; Aeolian, fluvial, sabkha, and playa lake sediments all being present. "Sheet-like" geometry of stratigraphical units within the Leman Sandstone, and alternation of fluvial and aeolian deposition was climatically controlled. Major first order bounding surfaces are laterally extensive and were produced by lacustrine transgression and regression from the north-west.

Diagenesis within Permian strata was studied using standard petrographic microscopy, scanning electron microscopy, cold cathodo-luminescence, X-ray diffraction clay analysis, X-ray fluorescence spectroscopy, fluid inclusion microthermometry, and K-Ar dating of illites.

The diagenesis of Permian sediments within onshore basins is remarkably similar, and a paragenetic sequence of early haematite, illitic clays, feldspar, kaolinite, quartz and late calcite is observed. In the Leman Sandstone formation, authigenic mineralogy is complex and includes early quartz, sulphates and dolomite, chlorite, kaolinite, late quartz, illite and siderite.

Primary lithological variation, facies type, and the interdigitation and location of facies within a basin are important initial controls upon diagenesis. Subsequently, burial history, structure, the timing of gas emplacement, and the nature of sediments within underlying formations may also exercise significant controls upon diagenesis within Rotliegend strata.

KEY WORDS: PERMIAN, DIAGENESIS, SEDIMENTOLOGY, AEOLIAN, SANDSTONE.

### ACKNOWLEDGMENTS.

Well data for the Leman Sandstone Formation of the Southern North Sea was made available for study by Hamilton Brothers Oil and Gas Limited. The Author is also grateful for the help and guidance provided throughout the course of this study by Dr Peter Turner, and staff and friends at Aston University. Draughting of lithological logs was carried out by Mrs M. Prosser.

### STATEMENT

With the exception of appendices one to eight all the work presented within this dissertation has been carried out by the candidate. Reference to the work of others is specifically noted at the appropriate place in the text. Appendices one to eight comprise part of a joint paper, to be submitted for publication, written in co-operation with the project supervisor Dr. P. Turner. The authors consider that they have contributed equally to the content and interpretation of data to be submitted for publication.

Neither this dissertation, nor one substantially similar has been submitted for any degree, diploma or other qualification at any university.

D. J. Prosser

*D. J. Prosser*

Dr. P. Turner

*P. Turner*

For Alison.....

CONTENTS

	PAGE
(i) List of Contents.	4
(ii) List of Figures.	12
(iii) List of Tables.	22
(iv) List of Plates.	28
(v) List of Appendices	37

(i) LIST OF CONTENTS.

(VOLUME ONE)

CHAPTER ONE

1.0 INTRODUCTION.....	39
-----------------------	----

CHAPTER TWO

2.0 THE SEDIMENTOLOGY AND STRATIGRAPHY OF THE LEMAN SANDSTONE FORMATION (U.K. SECTOR, SOUTHERN NORTH SEA).....	41
2.1 INTRODUCTION.....	41
2.2 STRUCTURAL SETTING.....	41
2.3 THE SEDIMENTOLOGY OF LITHOFACIES TYPES PRESENT WITHIN THE LEMAN SANDSTONE.....	43
2.3.1 AEOLIAN SANDSTONES.....	43
2.3.1.1 AEOLIAN DUNE BASE.....	44
2.3.1.2 AEOLIAN DUNE.....	45
2.3.1.3 AEOLIAN INTERDUNE.....	45
2.3.2 FLUVIAL SANDSTONES.....	45
2.3.2.1 STRUCTURELESS FLUVIAL SHEETFLOODS..	47
2.3.2.2 STRUCTURED FLUVIAL SHEETFLOODS.....	47
2.3.2.3 CHANNELISED OR "SEMI-CONFINED" FLUVIAL DEPOSITS.....	47
2.3.3 SABKHA SANDSTONES AND SILTSTONES.....	49

2.3.4	PLAYA LAKE DEPOSITS.....	50
2.4	THE IDENTIFICATION OF FACIES TYPES ON THE BASIS OF WIRELINE LOG RESPONSE.....	50
2.5	STRATIGRAPHY: THE MULTISTOREY INTERDIGITATION OF FACIES TYPES .....	51
2.5.1	U.K. BLOCK 43/26.....	51
2.5.1.1	STRATIGRAPHIC UNIT ONE.....	51
2.5.1.2	STRATIGRAPHIC UNIT TWO.....	52
2.5.1.3	STRATIGRAPHIC UNIT THREE.....	54
2.5.1.4	STRATIGRAPHIC UNIT FOUR.....	55
2.5.1.5	STRATIGRAPHIC UNIT FIVE.....	57
2.5.1.6	STRATIGRAPHIC UNIT SIX.....	58
2.5.2	AMOCO WELL 48/2-1.....	58
2.5.3	AMERADA HESS WELL 48/3-3.....	61
2.5.4	PHILLIPS PETROLEUM WELL 47/5-1.....	63
2.6	SEDIMENTOLOGICAL MODEL.....	63
2.7	CONCLUSIONS.....	65

### CHAPTER THREE

3.0	THE PETROLOGY AND DIAGENESIS OF THE LEMAN SANDSTONE FORMATION.....	67
3.1	DETRITAL MINERALOGY.....	67
3.1.1	QUARTZ.....	67
3.1.2	FELDSPAR.....	69
3.1.3	LITHIC ROCK FRAGMENTS.....	70
3.1.4	ALLOGENIC CLAYS.....	71
3.2	AUTHIGENIC MINERALOGY.....	72
3.2.1	QUARTZ.....	72
3.2.2	DOLOMITE.....	73

3.2.3	ILLITE.....	75
3.2.4	CHLORITE.....	77
3.2.5	KAOLINITE.....	77
3.2.6	ANHYDRITE.....	78
3.2.7	BARYTE.....	78
3.2.8	SIDERITE.....	79
3.3	QUANTITATIVE PETROLOGY AND PREDICTED RESERVOIR CHARACTERISTICS.....	79
3.3.1	ANALYSIS OF POROSITY/PERMEABILITY DATA..	79
3.3.2	ANALYSIS OF POINT COUNT DATA.....	82
3.4	SEMI QUANTITATIVE X-RAY DIFFRACTION ANALYSIS OF THE "CLAY SIZED" SEDIMENT FRACTION WITHIN THE LEMAN SANDSTONE.....	89
3.5	K-AR DATING OF AUTHIGENIC ILLITE SEPARATES...	96
3.6	FLUID INCLUSION STUDIES.....	98
3.7	"WHOLE ROCK" GEOCHEMICAL ANALYSIS USING X-RAY FLUORESCENCE SPECTROSCOPY.....	101
3.8	THE DIAGENESIS OF THE LEMAN SANDSTONE.....	108
3.9	CONCLUSIONS.....	124

#### CHAPTER FOUR

4.0	THE SEDIMENTOLOGY AND STRATIGRAPHY OF THE PENRITH SANDSTONE.....	128
4.1	INTRODUCTION.....	128
4.2	STRUCTURAL SETTING AND STRATIGRAPHY.....	129
4.3	LITHOFACIES TYPES IN THE PENRITH SANDSTONE AND ASSOCIATED SEDIMENTS.....	132
4.4	LOCATION AND NATURE OF OUTCROPS STUDIED.....	134
4.4.1	AEOLIAN PENRITH SANDSTONE CROPPING OUT	

	IN THE REGION NORTH OF PENRITH.....	135
4.4.2	MIXED FLUVIAL AND AEOLIAN SEQUENCES CROPPING OUT IN THE REGION BETWEEN APPELBY AND KIRKBY STEPHEN.....	138
4.5	SEDIMENTOLOGICAL MODEL.....	146
4.6	CONCLUSIONS.....	149
 <u>CHAPTER FIVE</u>		
5.0	THE PETROLOGY AND DIAGENESIS OF THE PENRITH SANDSTONE AND ASSOCIATED SEDIMENTS.....	150
5.1	THE PETROLOGY OF AEOLIAN AND FLUVIAL SANDS...	150
5.1.1	DETRITAL MINERALOGY.....	150
5.1.1.1	QUARTZ.....	150
5.1.1.2	FELDSPAR.....	151
5.1.1.3	LITHIC ROCK FRAGMENTS.....	151
5.1.1.4	ALLOGENIC CLAY.....	152
5.1.2	AUTHIGENIC MINERALOGY .....	153
5.1.2.1	QUARTZ.....	153
5.1.2.2	FELDSPAR.....	154
5.1.2.3	ILLITE / SMECTITE CLAYS.....	154
5.1.2.4	DOLOMITE.....	155
5.1.2.5	CALCITE.....	156
5.1.2.6	KAOLINITE.....	156
5.1.2.7	GYPSUM.....	156
5.1.3	QUANTITATIVE PETROLOGY .....	157
5.1.4	SEMI - QUANTITATIVE X-RAY DIFFRACTION ANALYSIS OF THE "CLAY SIZED" SEDIMENT FRACTION WITHIN THE PENRITH SANDSTONE...	158
5.2	THE PETROLOGY OF CONGLOMERATES AND BRECCIAS	



	(BROCKRAM SEQUENCES).....	160
5.2.1	DETRITAL MINERALOGY - CONGLOMERATIC CHANNELS.....	160
5.2.1.1	QUARTZ.....	160
5.2.1.2	LITHIC ROCK FRAGMENTS.....	160
5.2.1.3	FELDSPAR.....	162
5.2.1.4	ALLOGENIC CLAYS.....	162
5.2.2	DETRITAL MINERALOGY: ALLUVIAL FAN BRECCIAS	162
5.2.2.1	LITHIC ROCK FRAGMENTS.....	162
5.2.2.2	QUARTZ.....	163
5.2.2.3	FELDSPAR.....	163
5.2.2.4	ALLOGENIC CLAY.....	163
5.2.3	AUTHIGENIC MINERALOGY - CONGLOMERATIC CHANNELS AND ALLUVIAL FAN BRECCIAS.....	163
5.2.3.1	CALCITIC CEMENTS.....	163
5.2.3.2	GYPSUM.....	166
5.2.3.3	AUTHIGENIC CLAYS.....	166
5.3	DIAGENESIS.....	167
5.3.1	DIAGENESIS WITHIN BROCKRAM CHANNELS OF RIVER BELAH AND HILTON BECK.....	167
5.3.2	DIAGENESIS WITHIN ALLUVIAL FAN BRECCIAS OF SKENKRITH BECK AND BURRELLS QUARRY...	170
5.3.3	DIAGENESIS WITHIN THE PENRITH SANDSTONE.	172
5.4	CONCLUSIONS .....	179
 <u>CHAPTER SIX</u>		
6.0	THE SEDIMENTOLOGY AND DIAGENESIS OF THE BRIDGNORTH SANDSTONE.....	181
6.1	INTRODUCTION.....	181

6.2	STRUCTURAL SETTING.....	181
6.3	THE STRATIGRAPHY OF THE BRIDGNORTH SANDSTONE.	182
6.4	THE SEDIMENTOLOGY OF THE BRIDGNORTH SANDSTONE FORMATION - LOCATION AND NATURE OF OUTCROP...	184
6.4.1	THE PERMIAN BRECCIAS.....	184
6.4.1.1	BASAL PERMIAN BRECCIAS.....	184
6.4.1.2	HIGHER PERMIAN BRECCIAS.....	188
6.4.2	THE BRIDGNORTH SANDSTONE.....	193
6.4.2.1	THE REGION AROUND BRIDGNORTH.....	194
6.4.2.2	THE REGION AROUND ENVILLE AND KINVER.....	197
6.4.2.3	THE REGION AROUND KIDDERMINSTER, BEWDLEY AND HIGH HABBERLEY.....	200
6.4.2.4	THE REGION SOUTH OF WEM .....	201
6.4.2.5	SUBSURFACE DATA .....	203
6.5	SEDIMENTOLOGICAL MODEL.....	207
6.6	CONCLUSIONS.....	210

## CHAPTER SEVEN

7.0	THE PETROLOGY AND DIAGENESIS OF THE BRIDGNORTH SANDSTONE.....	212
7.1	DETRITAL MINERALOGY.....	212
7.1.1	QUARTZ.....	212
7.1.2	FELDSPAR.....	213
7.1.3	ROCK FRAGMENTS.....	213
7.1.4	HEAVY MINERALS AND DETRITAL OPAQUES.....	214
7.2	AUTHIGENIC MINERALOGY.....	215
7.2.1	FELDSPAR.....	215
7.2.2	QUARTZ.....	216

7.2.3	ILLITE / SMECTITE CLAY.....	216
7.2.4	KAOLINITE.....	217
7.2.5	CARBONATE CEMENTS.....	217
7.2.6	ANHYDRITE.....	218
7.2.7	BARYTE.....	219
7.3	QUANTITATIVE MINERALOGY.....	219
7.3.1	ANALYSIS OF POINT COUNT DATA .....	219
7.3.2	SEMI - QUANTITATIVE X-RAY DIFFRACTION ANALYSIS OF THE "CLAY SIZED" SEDIMENT FRACTION IN THE BRIDGNORTH SANDSTONE....	221
7.3.3	WHOLE ROCK GEOCHEMICAL ANALYSIS USING X-RAY FLUORESCENCE SPECTROSCOPY .....	222
7.4	THE DIAGENESIS OF THE BRIDGNORTH SANDSTONE...	223
7.5	CONCLUSIONS.....	227

#### CHAPTER EIGHT

8.0	THE SEDIMENTOLOGY AND STRATIGRAPHY OF THE HOPEMAN SANDSTONE.....	230
8.1	INTRODUCTION.....	230
8.2	STRUCTURAL SETTING.....	230
8.3	STRATIGRAPHY.....	231
8.4	SEDIMENTOLOGY - LOCATION AND NATURE OF OUTCROPS.....	234
8.5	SEDIMENTOLOGICAL MODEL.....	241
8.6	CONCLUSIONS .....	247

#### CHAPTER NINE

9.0	THE PETROLOGY AND DIAGENESIS OF THE HOPEMAN SANDSTONE.....	249
9.1	DETRITAL MINERALOGY.....	249

9.1.1	QUARTZ.....	249
9.1.2	FELDSPAR.....	250
9.1.3	ROCK FRAGMENTS.....	250
9.1.4	HEAVY MINERALS.....	250
9.2	AUTHIGENIC MINERALOGY.....	251
9.2.1	QUARTZ.....	251
9.2.2	FELDSPAR.....	251
9.2.3	ILLITIC CLAYS.....	251
9.2.4	KAOLINITE.....	252
9.2.5	CALCITE.....	252
9.2.6	FLUORITE.....	252
9.2.7	BARYTE.....	252
9.3	QUANTITATIVE PETROLOGY.....	253
9.3.1	POINT COUNT ANALYSIS.....	253
9.3.2	SEMI - QUANTITATIVE X-RAY DIFFRACTION ANALYSIS OF THE "CLAY SIZED" SEDIMENT FRACTION WITHIN THE HOPEMAN SANDSTONE...	254
9.3.3	"WHOLE ROCK" GEOCHEMICAL ANALYSIS OF THE HOPEMAN SANDSTONE USING X-RAY FLUORESENCE SPECTROSCOPY.....	254
9.4	DIAGENETIC MODEL.....	255
9.5	CONCLUSIONS .....	258

## CHAPTER TEN

10.0	THE DIAGENESIS OF LOWER PERMIAN (ROTLIEGEND) DESERT SEDIMENTS - DISCUSSION.....	261
11.0	REFERENCES.....	279

(ii)

LIST OF FIGURES

PAGE

(VOLUME TWO)

<u>FIGURE</u>	<u>TITLE</u>	<u>PAGE</u>
<u>CHAPTER TWO</u>		
2.2.1	SKETCH MAP ILLUSTRATING THE REGION OF STUDY AND LOCATION OF WELLS.....	31
2.3.1	ENVIRONMENTAL MODEL - FLUVIAL DEPOSITION	32
2.5.1	CORRELATION DIAGRAM FOR STRATIGRAPHIC UNITS IN NORTH RAVENSPURN.....	33
2.6.1	CORRELATION OF LITHOLOGICAL AND DIPMETER LOGS FOR LOWER AEOLIAN SAND COMPLEX IN WELL 43/26-4.....	34
2.6.2	CARTOON SKETCH OF THE GEOLOGICAL MODEL PROPOSED FOR THE LEMAN SANDSTONE.....	35
<u>CHAPTER THREE</u>		
3.1.1	TERNARY PLOT ILLUSTRATING THE COMPOSITION OF THE LEMAN SANDSTONES IN WELL 43/26-1..	36
3.1.2	TERNARY PLOT ILLUSTRATING THE COMPOSITION OF THE LEMAN SANDSTONES IN WELL 43/26-2..	37
3.1.3	TERNARY PLOT ILLUSTRATING THE COMPOSITION OF THE LEMAN SANDSTONES IN WELL 43/26-3..	38
3.1.4	TERNARY PLOT ILLUSTRATING THE COMPOSITION OF THE LEMAN SANDSTONES IN WELL 43/26-4..	39
3.1.5	TERNARY PLOT ILLUSTRATING THE COMPOSITION OF THE LEMAN SANDSTONES IN WELL 43/26-5..	40
3.1.6	TERNARY PLOT ILLUSTRATING THE COMPOSITION	

<u>FIGURE</u>	<u>TITLE</u>	<u>PAGE</u>
	OF THE LEMAN SANDSTONES IN WELL 48/3-3...	41
3.1.7	TERNARY PLOT ILLUSTRATING THE COMPOSITION OF THE LEMAN SANDSTONES IN WELL 48/2-1...	42
3.1.8	TERNARY PLOT ILLUSTRATING THE COMPOSITION OF THE LEMAN SANDSTONES IN WELL 47/5-1...	43
3.1.9	FOUR VARIABLE QUARTZ PROVENANCE DIAGRAM FOR WELL 43/26-1.....	44
3.1.10	FOUR VARIABLE QUARTZ PROVENANCE DIAGRAM FOR WELL 43/26-2.....	45
3.1.11	FOUR VARIABLE QUARTZ PROVENANCE DIAGRAM FOR WELL 43/26-3.....	46
3.1.12	FOUR VARIABLE QUARTZ PROVENANCE DIAGRAM FOR WELL 43/26-4.....	47
3.1.13	FOUR VARIABLE QUARTZ PROVENANCE DIAGRAM FOR WELL 43/26-5.....	48
3.1.14	FOUR VARIABLE QUARTZ PROVENANCE DIAGRAM. FOR WELL 48/3-3.....	49
3.1.15	FOUR VARIABLE QUARTZ PROVENANCE DIAGRAM FOR WELL 48/2-1.....	50
3.1.16	FOUR VARIABLE QUARTZ PROVENANCE DIAGRAM FOR WELL 47/5-1.....	51
3.3.1	CORE GRAPH 43/26-1.....	52
3.3.2	CORE GRAPH 43/26-2.....	53
3.3.3	CORE GRAPH 43/26-3.....	54
3.3.4	CORE GRAPH 43/26-4.....	55
3.3.5	CORE GRAPH 43/26-5.....	56
3.3.6	CORE GRAPH 48/3-3.....	57

<u>FIGURE</u>	<u>TITLE</u>	<u>PAGE</u>
3.3.7	CORE GRAPH 48/2-1.....	58
	THE SIGNIFICANCE OF POROSITY/PERMEABILITY TYPES.....	59
3.3.9	COMPARISON OF HELIUM POROSITY DATA WITH POROSITY DATA OBTAINED DURING POINT COUNTING, WELL 43/26-1.....	60
3.3.10	PETROGRAPHIC DATA, WELL 43/26-1, GRAIN SIZE, SORTING AND PACKING.....	61
3.3.11	PETROGRAPHIC DATA, WELL 43/26-1, POROSITY / PERMEABILITY.....	62
3.3.12	PETROGRAPHIC DATA, WELL 43/26-1, PORE OCCLUDING PHASES AND PREDICTED RESERVOIR QUALITY.....	63
3.3.13	PETROGRAPHIC DATA, WELL 43/26-2, GRAIN SIZE, SORTING AND PACKING.....	64
3.3.14	PETROGRAPHIC DATA, WELL 43/26-2, POROSITY / PERMEABILITY.....	65
3.3.15	PETROGRAPHIC DATA, WELL 43/26-2, PORE OCCLUDING PHASES AND PREDICTED RESERVOIR QUALITY.....	66
3.3.16	PETROGRAPHIC DATA, WELL 43/26-3, GRAIN SIZE, SORTING AND PACKING.....	67
3.3.17	PETROGRAPHIC DATA, WELL 43/26-3, POROSITY / PERMEABILITY.....	68
3.3.18	PETROGRAPHIC DATA, WELL 43/26-3, PORE OCCLUDING PHASES AND PREDICTED RESERVOIR QUALITY.....	69
3.3.19	PETROGRAPHIC DATA, WELL 43/26-4, GRAIN	

<u>FIGURE</u>	<u>TITLE</u>	<u>PAGE</u>
	SIZE, SORTING AND PACKING .....	70
3.3.20	PETROGRAPHIC DATA, WELL 43/26-4, POROSITY / PERMEABILITY.....	71
3.3.21	PETROGRAPHIC DATA, WELL 43/26-4, PORE OCCLUDING PHASES AND PREDICTED RESERVOIR QUALITY.....	72
3.3.22	PETROGRAPHIC DATA, WELL 43/26-5, GRAIN SIZE, SORTING AND PACKING.....	73
3.3.23	PETROGRAPHIC DATA, WELL 43/26-5, POROSITY / PERMEABILITY.....	74
3.3.24	PETROGRAPHIC DATA, WELL 43/26-5, PORE OCCLUDING PHASES AND PREDICTED RESERVOIR QUALITY.....	75
3.3.25	PETROGRAPHIC DATA, WELL 48/3-3, GRAIN SIZE, SORTING AND PACKING.....	76
3.3.26	PETROGRAPHIC DATA, WELL 48/3-3, POROSITY / PERMEABILITY.....	77
3.3.27	PETROGRAPHIC DATA, WELL 48/3-3, PORE OCCLUDING PHASES AND PREDICTED RESERVOIR QUALITY.....	78
3.3.28	PETROGRAPHIC DATA, WELL 48/2-1, GRAIN SIZE, SORTING AND PACKING.....	79
3.3.29	PETROGRAPHIC DATA, WELL 48/2-1, POROSITY / PERMEABILITY.....	80
3.3.30	PETROGRAPHIC DATA, WELL 48/2-1, PORE OCCLUDING PHASES AND PREDICTED RESERVOIR QUALITY.....	81
3.3.31	PETROGRAPHIC DATA, WELL 47/5-1, GRAIN	



<u>FIGURE</u>	<u>TITLE</u>	<u>PAGE</u>
	SIZE, SORTING AND PACKING.....	82
3.3.32	PETROGRAPHIC DATA, WELL 47/5-1, POROSITY / PERMEABILITY.....	83
3.3.33	PETROGRAPHIC DATA, WELL 47/5-1, PORE OCCLUDING PHASES AND PREDICTED RESERVOIR QUALITY.....	84
3.4.1	A TYPICAL SET OF DIFFRACTOGRAM TRACES FOR WELL 43/26-4.....	85
3.4.2	A TYPICAL SET OF DIFFRACTOGRAM TRACES FOR WELL 43/26-2.....	86
3.4.3	A TYPICAL SET OF DIFFRACTOGRAM TRACES FOR WELL 43/26-3.....	87
3.6.1	THREE DIMENSIONAL HISTOGRAM ILLUSTRATING THE DISTRIBUTION OF HOMOGENISATION TEMPERATURES FOR FLUID INCLUSIONS WITHIN QUARTZ, DOLOMITE AND SIDERITE.....	88
3.7.11	Ca : Mg PLOTS, "A" AND "B" STRUCTURE SANDSTONES.....	89
3.8.1	PARAGENETIC SEQUENCE FOR AUTHIGENIC MINERAL PHASES PRESENT IN WELLS 43/26-1 43/26-2, 43/26-4, AND 47/5-1.....	90
3.8.2	PARAGENETIC SEQUENCE FOR AUTHIGENIC MINERAL PHASES PRESENT IN WELLS 43/26-3 AND 43/26-5.....	91
3.8.3	PARAGENETIC SEQUENCE FOR AUTHIGENIC MINERAL PHASES PRESENT IN WELLS 43/26-4. 48/3-3, AND 48/2-1.....	92
3.8.4	EARLY DIAGENESIS WITHIN THE LEMAN	

<u>FIGURE</u>	<u>TITLE</u>	<u>PAGE</u>
	SANDSTONE - MODELLED AFTER GLENNIE ET AL (1978).....	93
3.8.5	EARLY DIAGENESIS WITHIN THE LEMAN SANDSTONE - ALTERNATIVE MODEL.....	94
3.8.6	CONDITIONS OF PRECIPITATION FOR CALCITE, DOLOMITE AND ARAGONITE / HIGH Mg CALCITE IN TERMS OF SALINITY AND Mg / Ca RATIO... ..	95
3.8.7	THE RELATIONSHIP BETWEEN pH AND THE SOLUBILITY OF QUARTZ.....	96
3.8.8	THE RELATIONSHIP BETWEEN pH AND THE SOLUBILITY OF KAOLINITE.....	96
3.8.9	Eh-pH DIAGRAM ILLUSTRATING THE STABILITY FIELDS FOR IRON MINERALS.....	97
3.8.10	Eh-pS <sub>2</sub> DIAGRAM ILLUSTRATING THE NECESSITY OF LOW SULPHUR ACTIVITY IN ORDER TO PRECIPITATE SIDERITE.....	98
3.8.11	Eh - P CO <sub>2</sub> DIAGRAM ILLUSTRATING THE STABILITY OF IRON MINERALS.....	99
3.8.12	COMBINATION DIAGRAM ILLUSTRATING THE RELATIONSHIP BETWEEN K - MICA (ILLITE), K - FELDSPAR AND KAOLINITE, IN TERMS OF K <sup>+</sup> / H <sup>+</sup> RATIO AND H <sub>4</sub> SiO <sub>4</sub> ACTIVITY.....	100
3.8.13	THE DIAGENESIS OF THE LEMAN SANDSTONE WITHIN U.K. BLOCK 43/26.....	101
3.8.14	"LATE" DIAGENESIS WITHIN THE LEMAN SANDSTONE FORMATION.....	102

<u>FIGURE</u>	<u>TITLE</u>	<u>PAGE</u>
 <u>CHAPTER FOUR</u>		
4.2.1	LOCATION MAP FOR VALE OF EDEN.....	103
4.2.2	SIMPLE CROSS SECTION FOR VALE OF EDEN....	104
4.4.1	SIMPLE STRATIGRAPHIC SECTION FOR GEORGE GILL.....	105
 <u>CHAPTER FIVE</u>		
5.1.1	TERNARY COMPOSITIONAL PLOT FOR THE PENRITH SANDSTONE.....	106
5.1.2	FOUR VARIABLE QUARTZ PROVENANCE DIAGRAM FOR THE PENRITH SANDSTONE.....	107
5.1.3	PETROGRAPHIC DATA - THE PENRITH SANDSTONE GRAIN SIZE, SORTING AND PACKING.....	108
5.1.4	PETROGRAPHIC DATA - THE PENRITH SANDSTONE POROSITY, AUTHIGENIC QUARTZ AND CALCITE..	109
5.3.1	PARAGENETIC SEQUENCE FOR AUTHIGENIC PHASES WITHIN CONGLOMERATIC CHANNEL FILLS	110
5.3.2	PARAGENETIC SEQUENCE FOR AUTHIGENIC PHASES WITHIN ALLUVIAL FAN BRECCIAS AT BURRELLS QUARRY AND STENKRITH BECK.....	111
5.3.3	PARAGENETIC SEQUENCE FOR AUTHIGENIC PHASES WITHIN UNSILICIFIED FLUVIAL AND AEOLIAN SANDS OF RIVER BELAH, GEORGE GILL AND HILTON BECK.....	112
5.3.4	PARAGENETIC SEQUENCE FOR AUTHIGENIC PHASES WITHIN THE SILICIFIED SANDS OF COWRAIK QUARRY, LAZONBY FELL, STONERAISE AND GEORGE GILL.....	113

<u>FIGURE</u>	<u>TITLE</u>	<u>PAGE</u>
5.3.5	MODEL TO EXPLAIN SILICA AUTHIGENESIS WITHIN THE PENRITH SANDSTONE, WHICH INVOLVES THE DISSOLUTION OF LABILE SILICATE CLASTS IN MARGINAL FACIES, AND RE-PRECIPITATION OF SILICA AS QUARTZ AT THE BASIN CENTER.....	114
5.3.6	MODEL TO EXPLAIN SILICA AUTHIGENESIS WITHIN THE PENRITH SANDSTONE, WHICH SUGGESTS ORGANIC MATURATION IN UPPER CARBONIFEROUS STRATA TO INTRODUCE LOW pH FLUIDS INTO POROUS AEOLIAN SANDS, AND PRECIPITATE QUARTZ AND KAOLINITE.....	115
 <u>CHAPTER SIX</u>		
6.2.1	LOCATION OF STUDY AREA FOR THE BRIDGNORTH SANDSTONE FORMATION.....	116
6.3.1	STRATIGRAPHIC NOMENCLATURE FOR THE REGION OF STUDY .....	117
6.4.1	LOCATION OF BRIDGNORTH SANDSTONE OUTCROP WITHIN THE ENGLISH MIDLANDS.....	118
6.4.2	INTERPRETATION OF COUNTER-DIPPING FORESETS IN EXPOSURES AT THE EASTERN SIDE OF CASTLE HILL, BRIDGNORTH.....	119
6.4.3	WEDGE SHAPED CROSS BEDDING FABRICS WITH OPPOSING FORESET DIP DIRECTIONS VISIBLE AT ROAD-CUTTINGS AT QUATFORD.....	120
6.4.4	LITHOLOGICAL LOGS FOR THE CORED PERMIAN SECTION WITHIN THE KEMPSEY BOREHOLE FROM	

<u>FIGURE</u>	<u>TITLE</u>	<u>PAGE</u>
	THE WORCESTER BASIN.....	121
6.4.5	CORRELATION OF BOREHOLE DATA AVAILABLE FOR THE BRIDGNORTH SANDSTONE (LINES ONE AND TWO IN APPENDIX NINE).....	122
6.4.6	CORRELATION OF BOREHOLE DATA AVAILABLE FOR THE BRIDGNORTH SANDSTONE (LINES THREE AND FOUR IN APPENDIX NINE).....	123
6.4.7	CORRELATION OF BOREHOLE DATA AVAILABLE FOR THE KEMPSEY AND SHERBORNE BOREHOLES IN THE WORCESTER BASIN.....	124

CHAPTER SEVEN

7.3.1	TERNARY COMPOSITIONAL PLOT FOR SURFACE SAMPLES OF THE BRIDGNORTH SANDSTONE.....	125
7.3.2	TERNARY COMPOSITIONAL PLOT FOR SUB-SURFACE SAMPLES OF THE BRIDGNORTH SANDSTONE FROM THE KEMPSEY BOREHOLE.....	126
7.3.3	FOUR VARIABLE QUARTZ PROVENANCE DIAGRAM FOR SURFACE SAMPLES OF BRIDGNORTH SANDSTONE.....	127
7.3.4	FOUR VARIABLE QUARTZ PROVENANCE DIAGRAM FOR SUB-SURFACE SAMPLES OF THE BRIDGNORTH SANDSTONE FROM THE KEMPSEY BOREHOLE.....	128
7.3.5	PETROGRAPHIC DATA: THE BRIDGNORTH SANDSTONE GRAIN SIZE, SORTING AND PACKING.....	129
7.3.6	PETROGRAPHIC DATA: THE BRIDGNORTH SANDSTONE AUTHIGENIC CEMENTS.....	130
7.3.7	PETROGRAPHIC DATA: THE BRIDGNORTH SANDSTONE	

<u>FIGURE</u>	<u>TITLE</u>	<u>PAGE</u>
	CLAY MINERALS.....	131
7.4.1	PARAGENETIC SEQUENCE FOR AUTHIGENIC PHASES PRESENT WITHIN THE BRIDGNORTH SANDSTONE...	132
 <u>CHAPTER EIGHT</u>		
8.2.1	LOCATION MAP OF THE MORAY FIRTH STUDY AREA	133
8.3.1	THE PERMO - TRIASSIC STRATIGRAPHY OF THE ELGIN REGION.....	134
 <u>CHAPTER NINE</u>		
9.3.1	TERNARY COMPOSITIONAL PLOT FOR THE HOPEMAN SANDSTONE FORMATION.....	135
9.3.2	FOUR VARIABLE QUARTZ PROVENANCE DIAGRAM FOR THE HOPEMAN SANDSTONE FORMATION.....	136
9.3.3	PETROGRAPHIC DATA: THE HOPEMAN SANDSTONE GRAIN SIZE, SORTING AND PACKING.....	137
9.3.4	PETROGRAPHIC DATA: THE HOPEMAN SANDSTONE AUTHIGENIC CEMENTS.....	138
9.4.1	PARAGENETIC SEQUENCE FOR AUTHIGENIC PHASES PRESENT WITHIN THE HOPEMAN SANDSTONE.....	139

## (VOLUME TWO)

<u>TABLE</u>	<u>TITLE</u>	<u>PAGE</u>
<u>CHAPTER TWO</u>		
2.4.1	IDENTIFICATION OF FACIES TYPE ON THE BASIS OF WIRELINE LOG RESPONSE.....	141
2.5.1	DEPTH TO TOP OF STRATIGRAPHIC UNITS RECOGNISED IN WELLS LOCATED UPON U.K. BLOCK 43/26.....	142
<u>CHAPTER THREE</u>		
3.3.1	POROSITY / PERMEABILITY DATA, 43/26-1....	143
3.3.2	POROSITY / PERMEABILITY DATA, 43/26-2....	144
3.3.3	POROSITY / PERMEABILITY DATA, 43/26-3....	145
3.3.4	POROSITY / PERMEABILITY DATA, 43/26-4....	146
3.3.5	POROSITY / PERMEABILITY DATA, 43/26-5....	147
3.3.6	POROSITY / PERMEABILITY DATA, 48/3-3.....	148
3.3.7	POROSITY / PERMEABILITY DATA, 48/2-1.....	149
3.3.8	RESULTS OF STATISTICAL ANALYSIS TO CHECK THE SIGNIFICANCE OF POROSITY/PERMEABILITY CORRELATIONS, WELL 43/26-1.....	150
3.3.9	RESULTS OF STATISTICAL ANALYSIS TO CHECK THE SIGNIFICANCE OF POROSITY/PERMEABILITY CORRELATIONS, WELL 43/26-2.....	151
3.3.10	RESULTS OF STATISTICAL ANALYSIS TO CHECK THE SIGNIFICANCE OF POROSITY/PERMEABILITY CORRELATIONS, WELL 43/26-3.....	152
3.3.11	RESULTS OF STATISTICAL ANALYSIS TO CHECK	

<u>TABLE</u>	<u>TITLE</u>	<u>PAGE</u>
	THE SIGNIFICANCE OF POROSITY/PERMEABILITY CORRELATIONS, WELL 43/26-4.....	153
3.3.12	RESULTS OF STATISTICAL ANALYSIS TO CHECK THE SIGNIFICANCE OF POROSITY/PERMEABILITY CORRELATIONS, WELL 43/26-5.....	154
3.3.13	RESULTS OF STATISTICAL ANALYSIS TO CHECK THE SIGNIFICANCE OF POROSITY/PERMEABILITY CORRELATIONS, WELL 48/3-3.....	155
3.3.14	RESULTS OF STATISTICAL ANALYSIS TO CHECK THE SIGNIFICANCE OF POROSITY/PERMEABILITY CORRELATIONS, WELL 48/2-1.....	156
3.4.1	RESULTS OF X-RAY DIFFRACTION ANALYSIS OF THE LESS THAN 2 MICRON SIZE FRACTION IN SEDIMENT SAMPLES FROM WELL 43/26-1.....	157
3.4.2	RESULTS OF X-RAY DIFFRACTION ANALYSIS OF THE LESS THAN 2 MICRON SIZE FRACTION IN SEDIMENT SAMPLES FROM WELL 43/26-2.....	158
3.4.3	RESULTS OF X-RAY DIFFRACTION ANALYSIS OF THE LESS THAN 2 MICRON SIZE FRACTION IN SEDIMENT SAMPLES FROM WELL 43/26-3.....	159
3.4.4	RESULTS OF X-RAY DIFFRACTION ANALYSIS OF THE LESS THAN 2 MICRON SIZE FRACTION IN SEDIMENT SAMPLES FROM WELL 43/26-4.....	160
3.4.5	RESULTS OF X-RAY DIFFRACTION ANALYSIS OF THE LESS THAN 2 MICRON SIZE FRACTION IN SEDIMENT SAMPLES FROM WELL 43/26-5.....	161
3.4.6	RESULTS OF X-RAY DIFFRACTION ANALYSIS OF	



<u>TABLE</u>	<u>TITLE</u>	<u>PAGE</u>
	THE LESS THAN 2 MICRON SIZE FRACTION IN SEDIMENT SAMPLES FROM WELL 48/3-3.....	162
3.4.7	RESULTS OF X-RAY DIFFRACTION ANALYSIS OF THE LESS THAN 2 MICRON SIZE FRACTION IN SEDIMENT SAMPLES FROM WELL 48/2-1.....	163
3.4.8	RESULTS OF X-RAY DIFFRACTION ANALYSIS OF THE LESS THAN 2 MICRON SIZE FRACTION IN SEDIMENT SAMPLES FROM WELL 47/5-1.....	164
3.4.9	MEAN PERCENTAGES OF DIFFERENT CLAY SPECIES WITHIN CATEGORIES ERECTED FOR WELLS STUDIED.....	165
3.4.10	SUMMARY OF X-RAY DIFFRACTOGRAMS OBTAINED FOR CLAY SIZED SEDIMENT FRACTIONS FROM WELLS 43/26-2 AND 47/5-1.....	166
3.4.11	SUMMARY OF X-RAY DIFFRACTOGRAMS OBTAINED FOR CLAY SIZED SEDIMENT FRACTIONS FROM WELLS 48/3-3, 43/26-4, AND 48/2-1.....	167
3.4.12	SUMMARY OF X-RAY DIFFRACTOGRAMS OBTAINED FOR CLAY SIZED SEDIMENT FRACTIONS FROM WELLS 43/26-3 AND 43/26-5.....	168
3.5.1	K / AR DATA FOR 0.5 MICRON ILLITE SEPARATES FROM WELL 43/26-2.....	169
3.6.1	FLUID INCLUSION DATA: TEMPERATURES OF HOMOGENISATION.....	170
3.7.1	GEOCHEMICAL DATA, "A" STRUCTURE, WELL 43/26-1.....	171
3.7.2	GEOCHEMICAL DATA, "A" STRUCTURE, WELL	

<u>TABLE</u>	<u>TITLE</u>	<u>PAGE</u>
	43/26-2.....	172
3.7.3	GEOCHEMICAL DATA, "A" STRUCTURE, WELL 43/26-4.....	173
3.7.4	GEOCHEMICAL DATA, "B" STRUCTURE, WELLS 43/26-3 AND 43/26-5.....	174
3.7.5	COMPARISONS OF MEAN ELEMENTAL ABUNDANCES FOR MAJOR ELEMENTS DETERMINED USING X-RAY FLUORESCENCE SPECTROSCOPY : AEOLIAN FACIES "A" STRUCTURE VERSUS "B" STRUCTURE.....	175
3.7.6	COMPARISONS OF MEAN ELEMENTAL ABUNDANCES FOR MAJOR ELEMENTS DETERMINED USING X-RAY FLUORESCENCE SPECTROSCOPY : FLUVIAL FACIES "A" STRUCTURE VERSUS "B" STRUCTURE.....	176
3.7.7	CORRELATION MATRIX "A" STRUCTURE WELLS: AEOLIAN FACIES.....	177
3.7.8	CORRELATION MATRIX "A" STRUCTURE WELLS: FLUVIAL FACIES.....	178
3.7.9	CORRELATION MATRIX "B" STRUCTURE WELLS: AEOLIAN FACIES.....	179
3.7.10	CORRELATION MATRIX "B" STRUCTURE WELLS: AEOLIAN FACIES.....	180

CHAPTER FIVE

5.1.1	RESULTS OF X-RAY FLUORESCENCE WHOLE ROCK GEOCHEMICAL ANALYSIS OF THE PENRITH SANDSTONE.....	181
5.1.2	RESULTS OF SEMI - QUANTITATIVE X-RAY DIFFRACTION ANALYSIS OF THE "CLAY SIZED"	

<u>TABLE</u>	<u>TITLE</u>	<u>PAGE</u>
	SEDIMENT FRACTION WITHIN THE PENRITH SANDSTONE.....	182
5.1.3	DESCRIPTIONS OF X-RAY DIFFRACTOGRAM TRACES OBTAINED FOR SAMPLES OF THE PENRITH SANDSTONE.....	183
 <u>CHAPTER SEVEN</u>		
7.2.1	RESULTS OF ELECTRON MICROPROBE ANALYSIS OF FELDSPAR CLASTS AND OVERGROWTHS PRESENT WITHIN THE BRIDGNORTH SANDSTONE.....	184
7.3.1	RESULTS OF INVESTIGATIONS INTO THE COMPOSITION OF THE "CLAY SIZED" SEDIMENT FRACTION OF THE BRIDGNORTH SANDSTONE AT SURFACE OUTCROP.....	185
7.3.2	RESULTS OF INVESTIGATIONS INTO THE COMPOSITION OF THE "CLAY SIZED" SEDIMENT FRACTION OF THE BRIDGNORTH SANDSTONE FROM THE KEMPSEY BOREHOLE.....	186
7.3.3	SUMMARY OF X-RAY DIFFRACTOGRAMS FOR CLAY MINERAL SEPARATES FROM THE BRIDGNORTH SANDSTONE.....	187
7.3.4	RESULT OF X-RAY FLUORESCENCE WHOLE ROCK GEOCHEMICAL ANALYSIS OF THE BRIDGNORTH SANDSTONE.....	188
7.3.5	COMPARISON OF GEOCHEMICAL DATA FOR AEOLIAN BRIDGNORTH SANDSTONE AT SURFACE OUTCROP WITH AEOLIAN SANDS FROM THE KEMPSEY BOREHOLE.....	189

<u>TABLE</u>	<u>TITLE</u>	<u>PAGE</u>
 <u>CHAPTER NINE</u>		
9.3.1	SUMMARY OF X-RAY DIFFRACTOGRAMS OBTAINED FOR CLAY MINERAL SEPARATES FROM THE HOPEMAN SANDSTONE.....	190
9.3.2	RESULTS OF SEMI - QUANTITATIVE X-RAY DIFFRACTION ANALYSIS OF THE "CLAY SIZED" SEDIMENT FRACTION WITHIN THE HOPEMAN SANDSTONE.....	191
9.3.3	RESULT OF X-RAY FLUORESCENCE WHOLE ROCK GEOCHEMICAL ANALYSIS OF THE BRIDGNORTH SANDSTONE.....	192
 <u>CHAPTER TEN</u>		
10.1	COMPARISON OF GEOCHEMICAL DATA FROM THE NORTH RAVENSPURN "A" STRUCTURE WITH AEOLIAN SANDS FROM THE KEMPSEY BOREHOLE...	193
10.2	COMPARISON OF GEOCHEMICAL DATA FOR AEOLIAN SANDS FROM THE BRIDGNORTH SANDSTONE WITH AEOLIAN SANDS FROM THE HOPEMAN SANDSTONE..	194
10.3	COMPARISON OF GEOCHEMICAL DATA FOR AEOLIAN SANDS FROM THE BRIDGNORTH SANDSTONE WITH AEOLIAN SANDS FROM THE PENRITH SANDSTONE..	195
10.4	COMPARISON OF GEOCHEMICAL DATA FOR AEOLIAN SANDS FROM THE HOPEMAN SANDSTONE WITH AEOLIAN SANDS FROM THE PENRITH SANDSTONE..	196

(iv)

LIST OF PLATES

(VOLUME TWO)

<u>PLATE</u>	<u>TITLE</u>	<u>PAGE</u>
<u>CHAPTER TWO</u>		
2.1	AEOLIAN FACIES SANDSTONE WITH ABUNDANT GRAIN FLOW LAMINAE. WELL 48/3-3.....	198
2.2	AEOLIAN FACIES SANDSTONE DOMINATED BY GRAIN FALL DEPOSITS. WELL 48/2-1.....	199
2.3	STRUCTURELESS FLUVIAL SANDSTONE WITH ABUNDANT INTRAFORMATIONAL MUD CLASTS. WELL 48/3-3.....	200
2.4	FLUVIAL SANDSTONE WITH ABUNDANT DEWATERING STRUCTURES. WELL 48/3-3.....	201
2.5	SABKHA AND FLUVIAL FACIES SANDSTONES. WELL 48/3-3.....	202
2.6	INTERBEDDED ADHESION RIPPLED SABKHA SILTS, AND PLANE BEDDED FLUVIAL SHEETFLOODS. WELL 48/3-3.....	203
<u>CHAPTER THREE</u>		
3.1	SCANNING ELECTRON MICROGRAPH ILLUSTRATING EUBEDRAL POREFILLING AUTHIGENIC QUARTZ. WELL 43/26-5.....	204
3.2	THIN SECTION PHOTOMICROGRAPH ILLUSTRATING LATE QUARTZ CEMENT REPLACING ANHYDRITE, AND ENCLOSING DOLOMITE. WELL 48/2-1.....	205
3.3	THIN SECTION PHOTOMICROGRAPH ILLUSTRATING COMPOSITIONALLY ZONED DOLOMITE CEMENTS.	

<u>PLATE</u> (Cont)	<u>TITLE</u>	<u>PAGE</u>
	WELL 48/2-1.....	206
3.4	SCANNING ELECTRON MICROGRAPH ILLUSTRATING THE PRESENCE OF MECHANICALLY INFILTRATED CLAYS AT GRAIN CONTACTS. WELL 43/26-1.....	207
3.5	SCANNING ELECTRON MICROGRAPH ILLUSTRATING THE DEVELOPMENT OF FIBROUS ILLITE AT GRAIN MARGINS. WELL 43/26-1.....	208
3.6	SCANNING ELECTRON MICROGRAPH ILLUSTRATING THE DEVELOPMENT OF GRAIN COATING ILLITE / CHLORITE CLAYS HAVING A BOXWORK TEXTURE. WELL 43/26-2.....	209
3.7	SCANNING ELECTRON MICROGRAPH ILLUSTRATING THE DEVELOPMENT OF POREFILLING KAOLINITE CEMENTS. WELL 43/26-5.....	210
3.8	COLD CATHODOLUMINESCENCE PHOTOMICROGRAPH ILLUSTRATING LUMINESCENCE PROPERTIES OF KAOLINITIC CLAYS. WELL 43/26-5.....	211
3.9	THIN SECTION PHOTOMICROGRAPH ILLUSTRATING THE PRESENCE OF LATE STAGE SIDERITE CEMENT ENCLOSING QUARTZ CEMENTS. WELL 43/26-5....	212

CHAPTER FOUR

4.1	UNSILICIFIED PENRITH SANDSTONE DOMINATED BY GRAINFALL STRATA, COWRAIK QUARRY. (NY 542 310).....	213
4.2	AEOLIAN BEDFORM WITH CONVEX UPWARD MORPHOLOGY, SILICIFIED PENRITH SANDSTONE, COWRAIK QUARRY (NY 542 310).....	214

<u>PLATE</u> (Cont)	<u>TITLE</u>	<u>PAGE</u>
4.3	LARGE SCALE TROUGH CROSS STRATIFICATION SETS , SILICIFIED PENRITH SANDSTONE, STONERAISE QUARRY (NY 533 352).....	215
4.4	SILICIFIED, AEOLIAN PENRITH SANDSTONE CROPPING OUT IN CRAGS ON THE SOUTHERN SIDE OF GEORGE GILL (NY 718 188).....	216
4.5	THE "LOWER BROCKRAM" HORIZON EXPOSED IN GEORGE GILL (NY 718 187).....	217
4.6	RED, UN-SILICIFIED FLUVIAL SANDSTONES AND CHANNEL FILL CONGLOMERATES EXPOSED IN SECTIONS AT RIVER BELAH (NY 7936 1210)....	218
4.7	COARSE ALLUVIAL FAN BRECCIAS EXPOSED AT BURRELLS QUARRY (NY 677 180).....	219
4.8	LIMESTONE RICH ALLUVIAL FAN BRECCIAS EXPOSED IN SECTIONS AT STENKRITH BECK (NY 7730 0735).....	220

CHAPTER FIVE

5.1	SCANNING ELECTRON MICROGRAPH ILLUSTRATING THE DEVELOPMENT OF ABUNDANT AUTHIGENIC QUARTZ OVERGROWTH WITHIN AEOLIAN PENRITH SANDSTONE SAMPLES FROM COWRAIK QUARRY (NY 542 310).....	221
5.2	THIN SECTION PHOTOMICROGRAPH ILLUSTRATING AUTHIGENIC QUARTZ CEMENT ENCLOSING AUTHIGENIC FELDSPAR OVERGROWTHS, COWRAIK QUARRY (NY 542 310).....	222
5.3	THIN SECTION PHOTOMICROGRAPH ILLUSTRATING	

<u>PLATE</u> (Cont)	<u>TITLE</u>	<u>PAGE</u>
	THE DEVELOPMENT OF AUTHIGENIC FELDSPAR PRIOR TO QUARTZ OVERGROWTH, AND THE PRESENCE OF MOULDIC POROSITY FORMED BY THE REMOVAL OF AUTHIGENIC FELDSPAR, COWRAIK QUARRY (NY 542 310) .....	223
5.4	SCANNING ELECTRON MICROGRAPH ILLUSTRATING AUTHIGENIC CLAYS (ILLITE / SMECTITE) WHICH POST DATE AUTHIGENIC QUARTZ OVERGROWTH. AEOLIAN PENRITH SANDSTONE, COWRAIK QUARRY (NY 542 310).....	224
5.5	THIN SECTION PHOTOMICROGRAPH ILLUSTRATING AUTHIGENIC DOLOMITE IN AEOLIAN SANDSTONES FROM STONERAISE QUARRY (NY 533 352).....	225
5.6	THIN SECTION PHOTOMICROGRAPH ILLUSTRATING THE PRESENCE OF RHOMBIC DISSOLUTION VOIDS WITHIN QUARTZ OVERGROWTHS AT COWRAIK QUARRY (NY 342 310).....	226
5.7	THIN SECTION PHOTOMICROGRAPH ILLUSTRATING POIKILOTOPIC CALCITE CEMENTS IN FLUVIAL SANDS FROM RIVER BELAH (NY 7936 1210)....	227
5.8	THIN SECTION PHOTOMICROGRAPH ILLUSTRATING DETAIL OF POIKILOTOPIC CALCITE CEMENT, RIVER BELAH (NY 7936 1210).....	228
5.9	THIN SECTION PHOTOMICROGRAPH ILLUSTRATING CORROSION OF SILICATE CLASTS BY CALCITE CEMENT, BURRELLS QUARRY, (NY 677 180).....	229
5.10	COLD CATHODOLUMINESCENCE PHOTOMICROGRAPH	



<u>PLATE</u> (Cont)	<u>TITLE</u>	<u>PAGE</u>
	ILLUSTRATING THE MULTIPLE ZONATION OF CARBONATE CEMENTS WITHIN ALLUVIAL FAN BRECCIAS, STENKRITH BECK (NY 7730 0735)...	230
5.11	THIN SECTION PHOTOMICROGRAPH AND COLD CATHODOLUMINESCENCE PHOTOMICROGRAPH OF CALCITE CEMENTS IN BROCKRAMS FROM HILTON BECK (NY 7151 2037).....	231
5.12	THIN SECTION PHOTOMICROGRAPH ILLUSTRATING SYNTAXIAL OVERGROWTHS ON ECHINODERM FRAGMENTS WITHIN ALLUVIAL FAN BRECCIAS, BURRELLS QUARRY (NY 677 180).....	232
5.13	THIN SECTION PHOTOMICROGRAPH ILLUSTRATING CARBONATE CEMENTS WITH MENISCUS TEXTURES, HILTON BECK (NY 7151 2037).....	233
5.14	THIN SECTION PHOTOMICROGRAPH OF A BROCKRAM FROM HILTON BECK, SHOWING DETAIL OF MENISCUS CEMENTS (NY 7151 2037).....	234
5.15	THIN SECTION PHOTOMICROGRAPH ILLUSTRATING EARLY GYPSUM CEMENT WITHIN ALLUVIAL FAN BRECCIAS AT STENKRITH BECK (NY 7730 0735).	235
5.16	THIN SECTION PHOTOMICROGRAPH ILLUSTRATING MOULDIC POROSITY FORMED BY THE REMOVAL OF EARLY GYPSUM, ALLUVIAL FAN BRECCIAS, STENKRITH BECK (NY 7730 0735).....	236
 <u>CHAPTER SIX.</u>		
6.1	TROUGH CROSS STRATIFICATION WITHIN THE HIGH HABBERLEY BRECCIA. (SO 8100 7590)....	237

<u>PLATE</u>	<u>TITLE</u>	<u>PAGE</u>
6.2	TROUGH CROSS STRATIFIED SETS WITHIN SHEETFLOOD DEPOSITS AT BARR BEACON QUARRIES (SO 0588 9644).....	238
6.3	LARGE SCALE TROUGH CROSS STRATIFICATION WITHIN THE BRIDGNORTH SANDSTONE AT CASTLE HILL, BRIDGNORTH (SO 7180 9315).....	239
6.4	"WEDGE-LIKE" CROSS BEDDING FABRICS VISIBLE IN EXPOSURES OF THE BRIDGNORTH SANDSTONE AT THE EASTERN SIDE OF CASTLE HILL, BRIDGNORTH (SO 7180 9315).....	240
6.5	THREE DIMENSIONAL EXPOSURES OF CROSS STRATIFIED AEOLIAN SANDS AT HOLY AUSTIN ROCK (SO 8350 8360).....	241
6.6	A RARE EXAMPLE OF AN INTERDUNE SHEETSAND EXPOSED AT HOLY AUSTIN ROCK (SO7350 8360)	242
6.7	DOWNWIND SHINGLING OF AEOLIAN DUNES WITH ASSOCIATED OVERLAP AND INCISION OF BEDFORMS, BEWDLEY (SO 8005 7595).....	243
6.8	PLANE BEDDED - WIND RIPPLED STRATA, ROCK HALL, PRESTON BROCKHURST (SJ 5400 2505)...	244

CHAPTER SEVEN

7.1	THIN SECTION PHOTOMICROGRAPH ILLUSTRATING AUTHIGENIC FELDSPAR WITHIN THE BRIDGNORTH SANDSTONE, BRIDGNORTH (SO 7175 9275).....	245
7.2	SCANNING ELECTRON MICROGRAPH ILLUSTRATING AUTHIGENIC FELDSPAR WITHIN THE BRIDGNORTH SANDSTONE, GAGS HILL (SO 7555 9058).....	246

<u>PLATE</u> (Cont)	<u>TITLE</u>	<u>PAGE</u>
7.3	SCANNING ELECTRON MICROGRAPH ILLUSTRATING AUTHIGENIC FELDSPAR GROWING WITHIN DISSOLUTION VOIDS IN DETRITAL FELDSPARS, AEOLIAN BRIDGNORTH SANDSTONE, GAGS HILL (SO 7555 9058).....	247
7.4	SCANNING ELECTRON MICROGRAPH ILLUSTRATING THE DEVELOPMENT OF ILLITE / SMECTITE CLAYS AND AUTHIGENIC FELDSPAR, IN BRIDGNORTH SANDSTONE OF THE KEMPSEY BOREHOLE.....	248
7.5	SCANNING ELECTRON MICROGRAPH ILLUSTRATING CORRODED DETRITAL FELDSPAR (F), KAOLINITE (K), AND AUTHIGENIC SILICA. AEOLIAN BRIDGNORTH SANDSTONE, KEMPSEY BOREHOLE....	249
7.6	THIN SECTION PHOTOMICROGRAPH ILLUSTRATING DOLOMITISATION OF CARBONATE CEMENTS IN THE BRIDGNORTH SANDSTONE, GAGS HILL (SO 7555 9058).....	250
7.7	THIN SECTION PHOTOMICROGRAPH ILLUSTRATING LATE BARYTE CEMENT WITHIN AEOLIAN BRIDGNORTH SANDSTONE, ROCK HALL, PRESTON BROCKHURST (SJ 540 250).....	251
7.8	THIN SECTION PHOTOMICROGRAPH SHOWING A GENERAL VIEW OF THE BRIDGNORTH SANDSTONE, WITH EVIDENCE OF SECONDARY POROSITY GENERATION, BRIDGNORTH (SO 7175 9275)....	252

<u>PLATE</u> (Cont)	<u>TITLE</u>	<u>PAGE</u>
 <u>CHAPTER EIGHT</u>		
8.1	INTERLOCKING "WEDGE-LIKE" CROSS STRATIFIED FABRICS WITHIN THE HOPEMAN SANDSTONE RODDACH BOW (NJ 1365 9620).....	253
8.2	"GROOVE-LIKE" CASTS WITHIN AEOLIAN SANDS AT RODDACH BOW (NJ 1365 6920).....	254
8.3	SOFT SEDIMENT DEFORMATION STRUCTURES IN THE HOPEMAN SANDSTONE, FORESHORE EAST OF OF HOPEMAN (NJ 1515 7010).....	255
8.4	ASYMMETRICAL CURRENT RIPPLES IN THIN, FLUVIAL HOPEMAN SANDSTONE BEDS EXPOSED IN THE FORESHORE TO THE EAST OF HOPEMAN (NJ 1550 7030).....	256
8.5	LARGE SCALE TROUGH CROSS STRATIFICATION EXPOSED IN CLIFFS EAST OF COVESEA QUARRIES (NJ 1718 7038).....	257
8.6	OPPOSING FORESET DIP DIRECTIONS WITHIN GRAINFALL DOMINATED STRATA AT CLASHACH QUARRY (NJ 1630 7026).....	258
8.7	OPPOSING FORESET DIP DIRECTIONS WITHIN GRAINFALL DOMINATED STRATA AT CLASHACH QUARRY (NJ 1630 7026).....	259
8.8	LATE CARBONATE CEMENTS WITHIN AEOLIAN SANDSTONES AT CLASHACH QUARRY (NJ 163 703).	260

CHAPTER NINE

9.1	SCANNING ELECTRON MICROGRAPH ILLUSTRATING	
-----	---	--

<u>PLATE</u> (Cont)	<u>TITLE</u>	<u>PAGE</u>
	WELL DEVELOPED QUARTZ OVERGROWTH WITHIN THE HOPEMAN SANDSTONE FROM COVESEA QUARRY (NJ 1718 7040).....	261
9.2	THIN SECTION PHOTOMICROGRAPH ILLUSTRATING AUTHIGENIC FELDSPAR WITHIN THE HOPEMAN SANDSTONE, CLASHACH QUARRY (NJ 1625 7025).	262
9.3	THIN SECTION PHOTOMICROGRAPH ILLUSTRATING AUTHIGENIC FELDSPAR AND CALCITE WITHIN THE HOPEMAN SANDSTONE (NJ 1625 7025).....	263
9.4	THIN SECTION PHOTOMICROGRAPH ILLUSTRATING POREFILLING FLUORITE CEMENT WITHIN THE HOPEMAN SANDSTONE (NJ 152 702).....	264

(v)

LIST OF APPENDICES

	<u>Page</u>
APPENDIX ONE	INSERT
COMPOSITE CORELOG WELL 43/26-1.....	INSERT
APPENDIX TWO	
COMPOSITE CORELOG WELL 43/26-2.....	INSERT
APPENDIX THREE	
COMPOSITE CORELOG WELL 43/26-3.....	INSERT
APPENDIX FOUR	
COMPOSITE CORELOG WELL 43/26-4.....	INSERT
APPENDIX FIVE	
COMPOSITE CORELOG WELL 43/26-5.....	INSERT
APPENDIX SIX	
COMPOSITE CORELOG WELL 48/3-3.....	INSERT
APPENDIX SEVEN	
COMPOSITE CORELOG WELL 48/2-1.....	INSERT
APPENDIX EIGHT	
COMPOSITE CORELOG WELL 47/5-1.....	INSERT
APPENDIX NINE	
SEDIMENTOLOGICAL LOG - BARR BEACON BEDS, BARR BEACON QUARRY.....	INSERT
APPENDIX TEN	
LOCATIONS OF BOREHOLES AND CORRELATION LINES USED IN STUDY OF THE BRIDGNORTH SANDSTONE.....	INSERT

APPENDIX ELEVEN

SEDIMENTOLOGICAL LOG - NEHELLS BOREHOLE..... INSERT

APPENDIX TWELVE

SEDIMENTOLOGICAL LOG - STOURBRIDGE (GREAT WESTERN  
RAILWAY GOODS YARD) BOREHOLE..... INSERT

APPENDIX THIRTEEN

SEDIMENTOLOGICAL LOG - BURCOTE PUMPING STATION. INSERT

APPENDIX FOURTEEN

MEAN DIFFERENCES BETWEEN OBSERVED AND EXPECTED  
COMPOSITIONS OF SIX STANDARD SAMPLES NOT USED IN  
MACHINE CALIBRATION OF THE X-RAY FLUORESCENCE  
SPECTROMETER..... 266

APPENDIX FIFTEEN

LOCATIONS OF BOREHOLES USED IN THE STUDY OF THE  
BRIDGNORTH SANDSTONE, AS GIVEN BY WHITEHEAD AND  
POCOCK (1946)..... 267

APPENDIX SIXTEEN

KEY TO LITHOLOGICAL LOGGING SYMBOLS USED IN  
APPENDICES ONE - EIGHT..... 269.

## CHAPTER ONE

### 1.0 INTRODUCTION.

The term Rotliegend is applied to red continental clastic sequences occurring beneath Permian Zechstein deposits (Rotliegend literally means "red-bed"). Rotliegend sediments are considered to be of Lower Permian age, and are interpreted as having formed in arid desert basins. In contrast to Rotliegend, the term Weisslegend ("white-bed") is used to describe Lower Permian sediments which are characteristically drab (grey or yellow / white). These sediments are also interpreted as having formed within arid desert basins, and in this report will be described with their red counterparts using the term Rotliegend as a stratigraphic or formational descriptor.

The aim of this study is to produce a comparative report documenting Rotliegend diagenesis in both onshore U.K. and offshore U.K. basins. Factors which combine to make this a viable objective include:

- (a) A basic similarity in the morphology of Rotliegend basins, i.e. sedimentation occurred within essentially fault bounded "graben-like" structures.
- (b) A close similarity in facies types between basins, i.e. one or more of the facies types recognised in any one basin will typically be present in other Rotliegend basins studied.
- (c) The basic mineralogy of framework clasts present



within U.K. Rotliegend sediments studied in this thesis appears to be very similar regardless of basin location.

Thus, it is proposed that differences observed in the diagenesis of sediments of the same facies type, either within or between basins, probably reflects differences in the burial history, and / or thermochemical regimes encountered by those sediments.

Rotliegend sediments studied from onshore U.K. basins include:

(i) The Bridgnorth Sandstone Formation of the Worcester, Stafford and Knowle basins in the English Midlands.

(ii) The Penrith Sandstone Formation of the Vale of Eden.

(iii) The Hopeman Sandstone Formation found cropping out along the southern margin of the Moray Firth Basin around Lossiemouth and Hopeman.

Rotliegend strata from the North Ravenspurn region of the Southern North Sea Basin provided a database for study of Lower Permian desert sediments in offshore U.K. basins.

Techniques utilised in this study include standard petrographic microscopy, scanning electron microscopy, fluid inclusion microthermometry, K / Ar dating of illitic clay minerals, X-ray diffraction analysis of clay mineral separates, and whole rock geochemical analysis using X-ray fluorescence spectroscopy.

THE SEDIMENTOLOGY AND STRATIGRAPHY OF THE LEMAN SANDSTONE  
FORMATION. (U.K. SECTOR, SOUTHERN NORTH SEA).

2.1 INTRODUCTION

Research has been based upon a study of eight wells including; Hamilton Brothers well 43/26-1, 43/26-2, 43/26-3, 43/26-4, 43/26-5 (North Ravenspurn area), Amoco well 48/2-1, Amerada Hess well 48/3-3, and Phillips Petroleum well 47/5-1.

2.2 STRUCTURAL SETTING.

The Southern North Sea basin (often referred to as the Southern Permian Basin) is a major sedimentary basin bounded by the Mid North Sea High in the north, the London Brabant Massif to the south, the Variscan Highlands to the east, and the Pennine High to the west.

The study area within the Southern North Sea basin lies within the southern portion of the Silverpit Basin, and is situated immediately to the north of the Sole Pit High - a major Cretaceous inversion structure which is the site of many gas producing Permian reservoirs. To the east the study area is bounded by the Cleaver Bank High, and to the west by the Dowsing fault zone. Northwards it extends into the Silverpit basin.

The location of the study wells and regional structural elements are shown in figure 2.2.1.

A structural history of the North Sea Basin area

may be summarised after Ziegler (1975, 1978, 1981, 1982), Glennie and Boegner (1981), and Glennie (1983) as follows:

Late Westphalian north - south compression resulted in the creation of the Variscan Highlands, a mountain chain which stretched from Southern Ireland through England to Poland and Germany. Associated with this, right lateral shearing in the U.K. sector of the Southern North Sea resulted in inversion of the Sole Pit region.

Collapse of the Variscan Highlands in the west gave rise to an east - west tensional regime and right lateral extensional movements in the Southern North Sea. This resulted in the formation of a horst and graben system which may possibly have been allied to a Proto-Atlantic fracture system. Subsidence in the Southern and Northern Permian basins resulted in the development of the Mid North Sea structural high, and formed en-echelon, northwest - southeast trending sub-basins (e.g. the Sole Pit Trough and the Broad Fourteens Basin), together with the formation of a northwest - southeast fracture system.

Erosion of Carboniferous highlands and deposition of Permian continental (Rotliegend) and marine (Zechstein) sequences within these basins was followed by the deposition of a predominantly continental clastic sequence during the Triassic, and marine sequences during the Jurassic. Active tectonics (extensional faulting and adjustments along pre-existing strike-slip faults) accompanied deposition of these sequences.

Cimmerian inversion (uplift of basin areas) took place during the Late Jurassic / Cretaceous by reverse displacement along previously existing fault lines. The Ravenspurh anticline is an inversion structure (positive flower structure) of this age.

During the Upper Cretaceous, chalks were deposited during a period of tectonic quiescence.

Further localised reverse movements along faults during the Cenozoic complete the structural scenario for the study area.

### 2.3 THE SEDIMENTOLOGY OF LITHOFACIES TYPES PRESENT WITHIN THE LEMAN SANDSTONE FORMATION.

The Leman Sandstone Formation is interpreted as having been deposited in an arid environment. Four principle depositional facies have been recognised i.e. a fluvial facies, an aeolian facies, a sabkha facies, and a playa lake facies .

The principle facies types listed above are similar to facies identified by *Glennie et al* (1978), and *Marie* (1975). They may be subdivided into "sub-facies" as follows:

#### 2.3.1 AEOLIAN SANDSTONES.

Aeolian sediments typically consist of red, fine - coarse, well sorted, porous, friable sandstones in which individual grains are highly rounded. Three subdivisions are recognised, i.e. aeolian dune base, aeolian dune and

aeolian interdune. (c.f. *Hunter (1977), Clemmensen and Abrahamsen (1983), and Kocurek and Dott (1981)*).

#### 2.3.1.1 AEOLIAN DUNE BASE.

Coarse grained, distinctly bimodal sediments dominated by grainflow laminae and generally low depositional dip angles ( $8^{\circ}$ ) are interpreted as those deposits which form towards the base of dunes. Grainflow and grainfall laminae (c.f. *Hunter 1977*) are readily distinguished in these aeolian sediments (see Plate 2.1). Grainflow laminae are formed by the downslope avalanching of coarse - medium sand particles on the slip faces of dunes. They commonly form asymptotic tongue-like laminae composed of well sorted clasts, and are separated by grainfall laminae. Grainflow laminae may exhibit normal or inverse grading. Inverse grading is produced as a result of kinetic sieving and dispersive pressures initiated by clast collisions which expand a moving (failed) layer of aeolian strata, and allow smaller clasts to filter downwards. Also, larger well rounded clasts flow to the "toe" of the foreset more quickly than smaller less rounded clasts, providing both lateral and vertical inverse grading (*Collinson and Thompson 1984*). Grainfall laminae are formed by the settling of fine wind borne / saltated sand and silt in the region downwind of the dune crest. Dune base deposits may sometimes be seen overlying a deflation surface with a poorly developed aeolian "lag" deposit.

#### 2.3.1.2 AEOLIAN DUNE.

Dune facies sandstones typically occur in sets ranging from 10cm - 4m in thickness. They display high angled cross bedding ( $20^{\circ}$  -  $30^{\circ}$ ), in which the dip angle of the foresets within each cross set increases upwards within the unit (see Plate 2.2). Internal lamination may be present on a mm or cm scale, the latter of which may be normal or reverse graded.

#### 2.3.1.3 AEOLIAN INTERDUNE.

Interdune facies sandstones occur as thin (typically 20 - 30cm) plane bedded sandbodies. The sandstones are fine grained, and typically occur interbedded with aeolian dune and dune base sandstones.

#### 2.3.2 FLUVIAL SANDSTONES.

Fluvial sediments consist mainly of pale coloured, red - grey, medium - coarse sandstones. The sandstones are commonly poorly sorted and are arranged in stacked fining upwards cycles up to 3m thick. Intraformational clay clasts and scattered granules are common (see Plate 2.3).

Three different types of fluvial sandstone are recognised. These are (1) structureless fluvial sheetfloods, (2) structured fluvial sheetfloods and (3) channelised fluvial sandstones.

##### 2.3.2.1 STRUCTURELESS FLUVIAL SHEETFLOODS.

Ephemeral fluvial sandbodies may occur in the form of (a) Essentially structureless sandstones in which

little or no original bedding fabric is recognisable, and in which abundant water escape features are common; or (b) Truly structureless sandstones, which often show normal grading.

Sandstones containing water escape structures in the form of dishes and vertical or subvertical stress pillars are considered to have been produced largely as a result of post depositional deformation processes in overpressured (undercompacted) sediments. These sandstones are typically up to 1m thick (See Plate 2.4). Truly structureless sandstones are interpreted as having formed within a flow regime where turbulence was too high to allow bedload traction. Both types of sandbody are commonly erosively based, and may contain abundant small intraformational rip-up clasts (see Plate 2.3). They range from less than 30cm to more than 3m in thickness. A bimodal texture, and the presence of well rounded grains points towards the possible presence of a fluvial reworked aeolian component within these sediments.

The development of overpressured zones in fluvial sediments may occur as a result of rapid deposition and/or a rapid rise in fluvial stage (Collinson and Thompson 1982). To summarise briefly, low permeabilities found in relatively fine grained, poorly sorted sediments deposited as a result of a rapid depositional event inhibit pore fluid movement to the extent that pore fluid pressures balance overburden pressure and the sediment distorts. Similarly the rapid rise in the level of

floodwaters above a sediment may increase pore fluid pressure to the point where liquefaction occurs.

#### 2.3.2.2 STRUCTURED FLUVIAL SHEETFLOODS.

These deposits commonly occur as fining upward units which are less than 3m thick. Like their structureless counterparts they often show an erosive base with intraformational mud clasts, but are different in that they may show a sharp transition into silt or mud grade material towards their upper limits.

Structured fluvial sediments often rapidly grade upwards into poorly sorted, adhesion rippled sandstones and siltstones of sabkha origin, and it is not uncommon for 30 cm - 1 m thick "cycles" of this type to be stacked vertically so that sabkha deposits may be described as "inter - fluvial" (see Plate 2.5).

Structured fluvial sandstones are interpreted as having been deposited in a less turbulent flow regime than their structureless counterparts. Traction currents in this less turbulent regime resulted in the formation of well developed bedforms characterised by low angle cross bedding, or plane bedding.

#### 2.3.2.3 CHANNELISED OR "SEMI-CONFINED" FLUVIAL DEPOSITS.

These consist of stacked sequences of medium grained, structureless, cross bedded or plane bedded sands. Individual units may be up to 2m or more thick and fine upwards. Stacked sequences frequently contain internal erosion surfaces, and tend to be common in stratigraphically lower parts of the Leman Sandstone.



The multistorey nature of these fluvial sequences (i.e. the fact that they are obviously stacked) points towards a higher degree of confinement of fluvial waters than is exhibited in other fluvial facies. However, considering the arid palaeoenvironmental setting, confined fluvial deposits are still likely to be ephemeral in nature, with individual units representing single sheetflood events within a confined or "semi confined", sandy "braided wadi" system.

The three subdivisions of the fluvial facies may be further used in order to draw inferences regarding proximity to source area, i.e. relative position within the fluvial regime. e.g.

Channelised fluvial sandstones may be thought of as occupying a proximal position within the fluvial regime, with sheetflood deposits occupying more distal environs and occurring as a result of a downstream decrease in channel confinement.

Within sheetflood deposits a downstream decrease in the turbulence of fluvial waters may lead to the development of traction induced bedforms, and the formation of a silt or mud grade "cap" to individual units as a result of the settling out of fine sediment fractions. Thus structured fluvial sheetfloods may be considered distal with respect to truly structureless fluvial sheetflood deposits. (See Figure 2.3.1)

### 2.3.3 SABKHA SILTS AND SANDSTONES.

Sabkha sediments are poorly sorted, red coloured, medium grained sandstones and silty sandstones (See Plate 2.6). Wavy - lenticular bedding is present throughout this facies, which is also characterised by the presence of adhesion ripples. Adhesion ripples are formed by the adhesion of fine - medium grained, wind blown sand to wet sabkha surfaces (Nagtegaal 1973, Glennie 1970). Evaporative action draws groundwater upward into the earliest accumulated layers of sand moistening them and allowing ripple growth to continue by what is probably a combination of trapping and adhesion. Desiccation of sabkha sediment is evident in some areas, and reflects periodic drying of the sabkha surface.

In strict terms, the sediments of the sabkha facies association may be divided into three sub-facies. These are (a) Lake Margin Sabkha, (b) Interfluvial Sabkha, and (c) Interdune Sabkha.

Sabkha facies sediments which appear to overly, or be overlain by shales or muds which might be attributed to a playa lake facies are interpreted as having been deposited in a lake margin setting.

Sabkha facies sediments which are effectively bound within thin fluvial sandstones (sheetfloods) are termed Interfluvial Sabkha.

Sabkha facies sediments which are effectively bound above and below by sediments of aeolian origin, are termed Interdune sabkha.

#### 2.3.4 PLAYA LAKE.

The sediments of this facies consist predominantly of red siltstones and silty mudstones. Desiccation of playa lake deposits is indicative of the ephemeral nature of these deposits. Thick playa siltstones with lenticular bedding may reflect the inflection of lacustrine wave base upon shore zone playa sediments.

The association of playa sediments with thin fluvial sheetfloods that appear distal in origin (i.e. Structured sheetfloods) is common.

#### 2.4 THE IDENTIFICATION OF FACIES TYPES ON THE BASIS OF WIRELINE LOG RESPONSE.

Four lithofacies are recognised on the basis of wireline log response. Identification of lithofacies types on the basis of gamma ray, neutron porosity and density log response is summarised in Table 2.4.1.

#### 2.5 STRATIGRAPHY: THE MULTISTOREY INTERDIGITATION OF FACIES TYPES AND ITS IMPLICATIONS FOR SEDIMENTOLOGICAL MODELLING.

##### 2.5.1 U.K BLOCK 43/26.

Six Stratigraphical units can be recognised within the Leman Sandstone formation in U.K. block 43/26. (See Figure 2.5.1 and Table 2.5.1). These stratigraphic

units are believed to reflect climatic variations occurring during the deposition of the Leman Sandstone. They contrast "wet" and "dry" facies, and are largely independent of tectonic control.

The six stratigraphic units recognised within U.K. block 43/26 and the sediments they contain may be summarised as follows:

#### 2.5.1.1 UNIT 1: DISTAL FAN SAND - PLAYA LAKE COMPLEX.

Stratigraphic unit one is composed chiefly of fluvial sheetfloods, distal "wet" alluvial fan sandstones, and playa lake siltstones and mudstones. (See Figure 2.5.1 and appendices one to five which illustrate logs for wells 43/26-1, 43/26-2, 43/26-3, 43/26-4, and 43/26-5). It occurs at the lowest stratigraphic level within the Leman Sandstone Formation, and is laterally very variable in terms of both thickness and sedimentology.

The sediments which typically form unit one are arranged in overall fining upward cycles, and rest directly upon eroded, and reddened Carboniferous basement.

The most informative section through unit one occurs in well 43/26-2, where a coarse grained matrix supported conglomerate (alluvial fan debris flow) rests directly upon Carboniferous strata, and passes upwards through an overall fining up cycle into a sequence of fluvial sandstones and playa lake mudstones. The alluvial

fan sandstones contain abundant internal erosion surfaces, and overall fining upward cycles are capped by mudstones. In this particular example, the intimate association of silty, distal fluvial "fan" sandstones containing abundant water escape features with playa lake sediments would suggest that during early Rotliegend deposition wet alluvial fans dominated by sheetflood deposition, were emplaced into or around a playa lake.

An important variation observed in this stratigraphic unit occurs in well 43/26-4, where aeolian sandstones are present. These sandstones may be inferred as being present in well 43/26-5 on the basis of electric log response. i.e. low gamma log response, high neutron porosity log response, and low density log response. It is suggested that aeolian deposits occur as sand pockets infilling depressions in the Carboniferous topography. The aeolian sandstones in well 43/26-5 overly and pass up into fluvial sediments which are in turn overlain by playa lake sediments. This sequence reflects the infilling of these topographic lows prior to the encroachment of lacustrine conditions.

#### 2.5.1.2 UNIT 2: FLUVIAL SANDSTONE COMPLEX.

Stratigraphic unit two is essentially a fluvial dominated unit, in which important lateral and vertical variation is evident. Sabkha and aeolian sediments may be interlayered with fluvial sediments in some wells.

In wells 43/26-2 and 43/26-3, unit two is composed entirely of fluvial sandstones which may be

divided into two fining upward cycles, i.e.

(a) A lower fining upward cycle (approximately 1m - 3m thick) of stacked cross bedded, plane bedded and essentially structureless sandstones which are interpreted as confined proximal sheetflood deposits.

(b) An upper fining upward cycle (approximately 3m thick) composed of essentially homogeneous sandstones with abundant water escape structures. These sandstones are interpreted as being proximal sheetflood deposits exhibiting much less evidence of multistorey stacking and "channelisation".

Evidence of confinement of fluvial deposits is also present in well 43/26-5 where fluvial sediments show an obvious multistorey structure reflecting a proximal fluvial regime. In well 43/26-4 however, reservoir unit two contains appreciable volumes of adhesion rippled sabkha deposits, and some aeolian style deposits are also present.

Analysis of data from wells in block 43/26 would suggest that the sediments of reservoir zone two exhibit a gradation from mainly fluvial sediments in the north and east, (e.g. wells 43/26-2, 43/26-3 and 43/26-5) to sediments of sabkha and aeolian origin in the south and west. (wells 43/26-1 and 43/26-4, See Figure 2.5.1). Fluvial dominated sections appear to show an upward gradation from "confined" fluvial sediments into a unit of apparently unconfined fluvial deposits which are interpreted as proximal sheetfloods, i.e. they show an upward gradation into more distal fluvial environments.

2.5.1.3 UNIT 3: LOWER AEOLIAN SANDSTONE COMPLEX.

Stratigraphic unit three forms the lower of two aeolian sandstone complexes existing within the Leman Sandstone Formation of block 43/26.

The upper and lower bounding surfaces which define this stratigraphic unit outline an essentially tabular sandstone which apparently thins in a northwesterly direction from well 43/26-5, through wells 43/26-3 and 43/26-2 to well 43/26-1.

In block 43/26 the lower bounding surface of stratigraphic unit three marks an upward passage from the "wet" fluvial dominated environments of stratigraphic unit two, into "dry" aeolian environments, i.e. it is a "drying" surface upon which aeolian reworking of fluvial sediments took place.

Similarly the upper bounding surface of stratigraphic unit three (lower surface of stratigraphic unit four) is considered to be a first order bounding surface produced by deflation to the water table within saturated aeolian dunes, during the onset of a climatically wet period. It is thus considered to be a first order bounding surface formed by primary climatic controls (c.f. Stokes 1968), i.e. it marks the transition from the dry climatic conditions of stratigraphic unit three into the wet climatic conditions of stratigraphic unit four.

Aeolian sediments dominate stratigraphic unit three in U.K. block 43/26, although subordinate fluvial

horizons are present in all wells studied. Typically these fluvial sandstones are thin (1m or less in thickness), erosively based, and may display wavy bedding, plane bedding or ripple lamination. Rarely fluvial sandstones display a mud grade cap. They are interpreted as distal ephemeral sheetflood deposits containing structures produced by bedload traction.

In wells 43/26-1 and 43/26-5, the fluvial sediments found within the upper regions of stratigraphic unit three are composed of thicker (typically greater than 2 m thick), essentially structureless sandstones. The sandstones appear to have erosive bases, and are less well sorted and generally "dirtier" than the aeolian sediments into which they are inserted. Intraformational mudclasts may be present. The presence of well rounded grains, a lack of internal structure, poor sorting, and generally bimodal size distribution, is interpreted as being indicative of rapid deposition in heavily laden ephemeral floodwaters, which achieved sediment saturation via the fluvial reworking of unconsolidated aeolian dunes.

#### 2.5.1.4 UNIT 4: AEOLIAN DUNE - FLUVIAL COMPLEX.

Stratigraphic unit four comprises an interbedded aeolian - fluvial - sabkha complex. Lateral facies variation is prominent within this unit, but the lowermost sediments directly overlying its sharp base always reflect the presence of an essentially wet climate.



The lowermost beds of this stratigraphic unit in wells 43/26-2 and 43/26-5 are cross bedded, stacked proximal type fluvial sandstones representing confined or "channel - like" deposits. In well 43/26-1 the beds at the base of this unit are plane bedded fluvial sandstones, whilst the lowermost beds of this unit in wells 43/26-3 and 43/26-4 consist of a broadly fining upward cycle of structureless fluvial sandstones interpreted as proximal sheetflood deposits.

The sediments of stratigraphic unit four reflect the presence of progressively more distal environments when traced towards the north and west. The lateral gradation into more distal fluvial environments also occurs as a vertical variation upwards within the sediments of stratigraphic unit four. i.e. The fluvial sandstones occurring towards the top of unit four appear to represent distal sheetflood deposition. They are composed of fining upward units of diffusely laminated, or poorly laminated sandstones having mudstone caps, and are interbedded with sabkha facies sediments.

Aeolian sandstones are present within stratigraphic unit four in wells 43/26-1, 43/26-2 and 43/26-5. These aeolian sediments appear to represent a discontinuous sand body which is present as a single unit in wells 43/26-2 and 43/26-5, but which splits into two thin aeolian sand bodies separated by a structured fluvial sandstone having an erosive base in well 43/26-1. Aeolian sandstones are absent in wells 43/26-3 and 43/26-4.

The presence of this aeolian sandstone in wells 43/26-1, 43/26-2 and 43/26-5 might be indicative of a geometry which is orientated approximately parallel to the strike of the Rotliegend section, i.e. elongated in an approximately east - west direction, broadly coincident with the palaeowind directions of Glennie (1983) and those inferred from the analysis of dipmeter logs. The aeolian sandbody present within stratigraphic unit four may represent a sief dune form.

#### 2.5.1.5 UNIT 5: UPPER AEOLIAN SANDSTONE COMPLEX.

Stratigraphic unit five comprises an essentially tabular aeolian sandbody which is present in all wells studied. In all wells studied, the base of stratigraphic unit five consists of aeolian dune deposits, and represents a major first order bounding surface separating the "dry" aeolian facies sediments of stratigraphic unit five from the "wet" fluvial facies sediments of stratigraphic unit four. Similarly the upper bounding surface of stratigraphic unit five marks a transition from sediments produced as a result of "dry" aeolian processes", into the "wet" fluvial and sabkha facies sediments of stratigraphic unit six.

In well 43/26-1 much of unit five lies within a "rubble" zone (10208 ft - 10240 ft log depth), but analysis of electric log response suggests the presence of two aeolian sandstones separated by sediments of sabkha origin (approx. 10218 ft log depth). i.e. There is an increase in gamma log response, and a loss of

aeolian type poro-perm characteristics as deduced from neutron porosity and density logs.

In wells 43/26-4 and 43/26-5 the aeolian sediments contain thin, apparently discontinuous fluvial sandstones, whilst in 43/26-3 the sandbody wedges to form two thinner aeolian units separated by sediments of sabkha origin.

The aeolian sandstone which dominates stratigraphic unit five appears to thin towards the north and west where it wedges into sediments of fluvial or sabkha origin.

#### 2.5.1.6 UNIT 6: LAKE MARGIN SABKHA - FLUVIAL COMPLEX.

Stratigraphic unit six in all wells studied is a highly variable unit dominated by lake margin sabkha facies sediments. Its lowermost bounding surface marks a transition from aeolian processes into fluvial and sabkha deposition.

#### 2.5.2 AMOCO WELL 48/2-1.

Amoco well 48/2-1 is located on the block immediately to the southeast of U.K. block 43/26 (See figure 2.2.1). The core interval studied from this well occurs between 11131.0 ft and 11419.0 ft (core depths) and consists predominantly of sediments belonging to the Leman Sandstone Formation. Interpretation of well logs available for well 48/2-1 indicates that the cored interval studied does not penetrate the Permo - Carboniferous unconformity. Well log interpretation

places this unconformity some 190 ft below the base of the cored section. (See Appendix Six)

Four stratigraphic divisions have been recognised within well 48/2-1. These are as follows:

(i) An interval between 11131.0 ft and 11197.0 ft (core depths) which is composed predominantly of lake margin sabkha deposits. The strata forming this interval are assigned to the Silverpit Formation and effectively grade downwards into the Leman Sandstone.

(ii) An interval between 11209.0 ft and 11321.0 ft (core depths) which is composed of interbedded fluvial and lake margin sabkha deposits. This interval forms an overall fining upward sequence which is considered to be the equivalent of stratigraphic unit 6 in block 43/26.

The lower portion of this stratigraphic unit comprises fluvial sheetflood deposits with water escape features (structured and structureless sheetfloods are present) which pass upward into a sequence of sabkha dominated fining upward cycles, the bases of which are fluvial in origin. The fluvial portions of these cycles consist of erosively based cross bedded sandstones, and the cycles are often capped by a thin mudstone horizon. One thin dune base deposit is also present within this stratigraphic division.

(iii) An interval between 11321.0 ft and 11377.0 ft (core depths) which is composed predominantly of aeolian deposits with minor fluvial intervals. This unit is

considered to be the equivalent of stratigraphic unit 5 in U.K. block 43/26 (upper aeolian sandstone complex).

In this well the aeolian sand body consists of two leaves separated by cross bedded, structured fluvial deposits, and the upper aeolian part of this stratigraphic unit contains a thin "interdune" sabkha.

It should be noted that "strike section" correlations of stratigraphy for wells 43/26-1, 43/26-2, 43/26-5 and 48/3-3 illustrate a northwest - southeast transition from: aeolian sandstone overlain by thin fluvial sandstones or playa lake deposits in 43/26-1, through to predominantly aeolian deposits in 43/26-2, aeolian deposits with thin discontinuous fluvial deposits in 43/26-5, and finally to two distinct aeolian sand bodies separated by well developed fluvial sheetfloods in 48/2-1, i.e. they document an increasing fluvial influence when this stratigraphic unit is traced southeast along strike.

(iv) An interval between 11377.0 ft and 11420.0 ft (core depths) which is composed of mixed fluvial and aeolian lithologies, and which is interpreted as the equivalent of stratigraphic unit 4 in block 43/26.

Fluvial lithologies within this unit consist of cross bedded sandstones which sometimes contain water escape structures, and an essentially structureless fluvial sandstone which forms the lowermost horizon within the cored interval. This sandstone is very tightly cemented and contrasts markedly with other sand

bodies present.

### 2.5.3 AMERADA HESS WELL 48/3-3

Amerada Hess well 48/3-3 is located to the southeast of U.K. block 43/26, adjacent to block 48/2 (See figure 2.2.1)

The recovered core interval (269 ft) for this well comprises entirely of the Lemna Sandstone Formation, and does not penetrate the Permo - Carboniferous unconformity (well log interpretation places this unconformity some 19 ft below the base of the cored interval). A detailed well log is provided in Appendix Seven.

Stratigraphic divisions recognised within this well are as follows:

(i) An interval between 11207.0 ft and 11260.0 ft (core depth) which is dominated by fluvial sediments, with minor aeolian and sabkha intervals. Fluvial sandstones are varied, but structured fluvial sheetfloods dominate. The strata present within this interval are considered to be the lateral equivalents of stratigraphic unit 6 in U.K. block 43/26.

(ii) An interval between 11260.0 ft and 11309.0 ft (core depths) comprising two leaves of fluvial sediments separated by adhesion rippled siltstones and mudstones of sabkha origin. The fluvial sandstones are predominantly structureless and frequently contain water escape columns. Bimodal textures in some portions of these beds indicate that some structureless units could

represent fluviually reworked dunes.

The sediments of this interval are believed to be the equivalent of stratigraphic unit 5 (upper aeolian sandstone complex) in U.K. block 43/26.

(iii) An interval between 11309.0 ft and 11356.0 ft (core depths) comprising a mixed succession of fluvial, sabkha and aeolian units.

Fluvial sandstones are predominantly structured units with erosive bases, although some structureless units with water escape columns are present.

The sediments of this interval appear to be the equivalent of stratigraphic unit 4 in U.K. block 43/26.

(iv) An interval between 11356.0 ft and 11415.0 ft (core depths) which is dominated by large scale structureless sand bodies. Individual fluvial units are large scale (up to 18 ft for one structureless sand unit) and form what are essentially stacked fining upward sequences. Single ephemeral sheetflood deposits of this thickness would be very unusual, and would probably be large enough to correlate on a basin wide scale. Since similar scale deposits have not been recognised in other wells studied, it is suggested that the scale and multistorey nature of these sandstones suggests the influence of some type of channelisation process. The presence of a bimodal texture in some sandstones may indicate that in part the deposits represent fluviually reworked dunes.

It is thought that this unit is the equivalent of

stratigraphic units 2 and 3 in U.K. block 43/26.

(v) An interval between 11309.0 ft and 11476.0 ft (core depths), the lower half of which is composed of essentially structureless, heavily dewatered sandstones which pass upward into a sequence of adhesion rippled siltstones of sabkha origin. This unit is probably the equivalent of stratigraphic unit 1 in U.K. block 43/26.

#### 2.5.4 PHILLIPS PETROLEUM WELL 47/5-1.

Phillips petroleum well 47/5-1 is located on the block immediately to the southwest of U.K. block 43/26. The cored interval available for this well is 136 ft thick. Aeolian dune base and aeolian dune are the only two lithofacies types present within this well. A detailed well log is provided in Appendix Eight.

#### 2.6 SEDIMENTOLOGICAL MODEL.

The study area is located within the Southern Permian Basin, at the northerly limit of Leman Sandstone deposition, in a setting marginal to the Silverpit Lake.

Analysis of dipmeter logs from the North Ravenspurn region indicates that aeolian dunes migrated in a W.S.W. direction within a predominantly easterly prevailing wind system (see Figure 2.6.1). Fluvial systems flowed northward into the Silverpit Lake. The close proximity of the study area to the Silverpit Lake and associated fluctuations in the water table influenced sedimentation and the development of sabkhas.



predominantly dry. During  
Aeolian dunes accumulated in a distal position  
with respect to the Silverpit Lake. Aeolian deposits  
thin towards the northwest, and have a "sheet-like"  
geometry which was probably controlled by climatic  
changes, perhaps as a result of Gondwanan deglaciations  
(Glennie 1984 and 1985).

Fluvial sediments are ephemeral, their deposition  
probably being controlled by seasonal variation in  
rainfall in upland areas to the south. Sheetflood  
events sometimes reworked aeolian sands, and would  
probably have been reworked themselves by later aeolian  
processes.

Sabkha sediments accumulated by the adhesion of  
wind blown sand to damp interdune areas, and to damp  
surfaces along the lake margin (Nagtegaal 1973, Glennie  
1970, Hummel and Kocurek 1984). Sabkha sediments become  
increasingly important both towards the top of the Leman  
Sandstone interval, and also when traced towards the  
northwest of the study area. This would suggest the  
southward encroachment of lacustrine conditions over  
predominantly aeolian and fluvial sequences.  
Lacustrine clays and lake margin sabkhas may be regarded  
as approximate datums (Kocurek 1981).

Major bounding surfaces in the North Ravenspurn  
area are parallel both to one another, and also to  
lithofacies variations, indicating that deposition is  
likely to have been climatically controlled. This  
implies that aeolian dune accumulation occurred during

periods when the climate was predominantly dry. During climatically wet periods the margin of the Silverpit Lake encroached southwards, water tables were elevated, and fluvial sedimentation was prevalent. During these periods the fluvial reworking of aeolian sands occurred, and the deflation of aeolian sediments to water table levels controlled the formation of first order bounding surfaces above aeolian sand accumulations, i.e. major first order bounding surfaces in North Ravenspurn are interpreted as forming by mechanisms analagous to those described by Stokes (1968) and Loope (1984). Further south (e.g. in Phillips Petroleum Well 47/5-1) the generation of first order bounding surfaces as a result of the migration and climbing of dunes and interdunes (Brookfield 1977, Mc Kee and Motola 1975, Rubin and Hunter 1982) is likely to be much more important.

A cartoon of the geological model is shown in figure 2.6.2.

## 2.7 CONCLUSIONS.

(i) The Lower Permian Lemn Sandstone Formation in the Southern North Sea represents the deposits of an arid desert environment, located marginal to a northerly lying saline lake. Three principle facies types are recognised within this desert setting, i.e. aeolian, fluvial and sabkha.

(ii) Aeolian dunes developed in a "proximal" environmental setting, and were deposited within an east-

north-easterly prevailing wind system. Fluvial systems (dominated by sheetflood deposition) flowed northward through more distal sabkha environments into the Silverpit Lake.

(iii) Six lithostratigraphic divisions have been recognised within the Leman Sandstone Formation of U.K. block 43/26. These units are (in descending order):

- 6 Lake margin sabkha - fluvial complex.
- 5 Upper aeolian sandstone complex.
- 4 Aeolian dune - fluvial complex.
- 3 Lower aeolian sandstone complex.
- 2 Fluvial sandstone complex.
- 1 Distal fan sandstone - playa lake.

(iv) Correlatable lithostratigraphic divisions within the Leman Sandstone Formation are separated by climatically controlled first order bounding surfaces. These boundaries mark periodic change from an arid to semi-arid environment, in which extensive sheetflood deposition took place. These climatic variations result in a broadly "sheet-like" aeolian sand body geometry.

THE PETROLOGY AND DIAGENESIS OF THE LEMAN SANDSTONE FORMATION.

Petrographic analysis of the Leman Sandstone has been carried out using thin sections, S.E.M. and cold cathodoluminescence in order to investigate detrital and diagenetic variables and their constraint on reservoir quality. Additional techniques utilised include X-ray diffraction analysis of clay minerals, K-Ar dating of authigenic illites, fluid inclusion microthermometric analysis, and whole rock geochemical analysis using X-ray fluorescence spectroscopy.

3.1 DETRITAL MINERALOGY.

The sediments of the Leman Sandstone are typically fine-medium grained, and may show varying degrees of sorting depending upon which facies association they belong to. Ternary plots illustrating the compositions of the sediments present within the Leman Sandstone Formation are shown in figures 3.1.1 - 3.1.8.

The sediments of the Leman Sandstone Formation consist of sublitharenites and orthoquartzitic sandstones. It should also be noted that plots for fluvial sands display the widest compositional spread, followed by aeolian and then sabkha sediments.

3.1.1 QUARTZ.

The Leman Sands are composed of subangular - well

rounded quartz clasts (50% - 60% on average) with minor lithic rock fragments and very rare feldspar.

Quartz clasts present may be divided into four groups using the classification proposed by Basu et Al (1975). i.e.

- (i) Non undulatory quartz,
- (ii) Strongly undulatory quartz,
- (iii) Polycrystalline quartz grains having two-three crystal units/grain,
- (iv) Polycrystalline quartz grains having greater than three crystal units/grain,

The relative percentages of each grain present can be plotted on a four variable diagram (see figures 3.1.9 to 3.1.16) and the work of Basu et al (1975) suggests that the position of each plot within this diagram is indicative of the nature of the rocks in the source area.

Figures 3.1.9 to 3.1.16 illustrate that non - undulatory quartz is the dominant quartz type, commonly forming 45%-75% of quartz present. Polycrystalline quartz grains having greater than three units per grain, commonly form 20%-30% of quartz present, whilst undulatory quartz commonly forms 10%-20% of the total quartz present. Polycrystalline quartz clasts having only 2 - 3 crystal units per grain are present in quantities less than 10%.

The inferred source using the four variable diagrams shown in figures 3.1.9 to 3.1.16 is one of middle - high rank metamorphic rocks; and palaeocurrent

/ palaeowind directions deduced from dipmeter logs would indicate that this source lay somewhere to the South and East.

Bubble trains are common within all quartz types present, and occasionally "en-echelon" Boehme Lamellae may be seen within quartz clasts. Very simply "bubble trains" and Boehme Lamellae are fluid inclusion trains produced as a result of "physical stress" imposed upon quartz within a rock. Bubble trains observed in wells studied are always confined within grain boundaries, and never pass continuously from one grain into another - suggesting that the stresses which resulted in the formation of the "bubble trains" affected the quartz at sometime prior to its utilisation, as a clastic constituent within the Lemn Sandstone Formation.

"En echelon" Boehme Strain Lamellae occur only in fluvial sediments. Their absence in aeolian sediments is probably due to the fact that such highly strained grains were not durable enough to withstand impact during aeolian transport. Clast - clast impacts are probably buffered in an aqueous transport medium, and highly strained grains are thus more likely to be preserved. Some quartz clasts present contain inclusions of vermicular chlorite, a feature probably indicative of a volcanic or hydrothermal origin (Folk 1974).

### 3.1.2 FELDSPAR.

Feldspar clasts are rare in the Lemn Sandstone Formation in all wells studied. When present it occurs

most commonly as alkali feldspar clasts constituting less than one percent of the total rock volume. Plagioclase feldspar is rare in samples studied from wells located upon UK block 43/26. However, samples studied from Amoco well 48/2-1 commonly contain both alkali and plagioclase feldspar.

### 3.1.3 LITHIC ROCK FRAGMENTS.

Lithic rock fragments occur within the Leman Sandstone Formation in all wells studied and include:

#### (a) Sedimentary Rock Fragments

Sedimentary rock fragments are the most common lithic clasts occurring within the Leman Sandstone Formation. Sandstone clasts often display clear lamination and may be well compacted. Features common within sedimentary rock fragments include clay pellicles, detrital mica clasts, carbonate cements and kaolinised feldspar clasts.

Bubble trains within compacted sandstone fragments frequently pass continuously through the boundaries of their own constituent clasts. This suggests bubble trains formed within quartz clasts some time after their incorporation into the sediment from which the lithic fragment was ultimately derived.

Chert clasts are common, and scanty evidence suggests chert is of sedimentary origin, e.g. spicule like forms within some clasts, and the presence of a chalcedonised bivalve fragment within one clast. Chert

clasts commonly form less than 1% of the total rock volume, and in some specimens are the most common lithic fragment after sandstone clasts.

(b) Metamorphic Rock Fragments.

Metamorphic rock fragments within the Lemna Sandstone Formation commonly form less than 1% of the total rock volume. Compositionally, metamorphic rock fragments appear to be the low grade metamorphic equivalent of the sandstone clasts described above.

(c) Igneous Rock Fragments.

Igneous rock fragments may occur as acid (rhyolitic) or basic lithologies. Rhyolitic fragments are light coloured and consist of fine grained quartz and feldspar intergrowths, sometimes exhibiting spherulitic textures. Basic rock fragments are typically fine grained, dark coloured, and iron rich with very little determinable mineralogy.

3.1.4 ALLOGENIC CLAYS.

Allogenic clays (pellicular coatings or "meniscus-like" bridges between grains) are present in most specimens studied. They are most common within sabkha and fluvial environments, and much less common in aeolian sands. Allogenic clays are typically of poorly crystalline illitic / chloritic composition.

The remaining detrital constituents within the Lemna Sandstone may include rare mica clasts (seen only in fluvial and sabkha sediments), heavy minerals and



detrital opaques. Heavy minerals typically occur as zircon and tourmaline.

### 3.2 AUTHIGENIC MINERALOGY.

Authigenic phases within the Leman Sandstone include (in order of decreasing abundance): quartz, dolomite, illite, kaolinite, chlorite, anhydrite and baryte. Siderite is present in considerable quantities within Hamilton Brothers wells 43/26-3 and 43/26-5. The paragenetic sequence is early quartz, dolomite, kaolinite, late quartz, illite and siderite.

#### 3.2.1 QUARTZ.

Authigenic quartz may be present in quantities varying from less than 10% to as much as 35% total rock volume. (Typically 10-20%).

Authigenic quartz may occur as:

- a) Complete, optically continuous overgrowths on detrital grains;
- b) Discrete, crystal units growing on the surface of detrital grains (see Plates 3.1, 3.5 and 3.9).

Complete overgrowths typically enclose a fine red/brown "dust rim" composed of mechanically infiltrated clays. This quartz is interpreted as having formed early during diagenesis. (Thin section evidence suggests that it is certainly earlier than dolomite and kaolinite, and probably earlier than anhydrite).

The majority of discrete quartz crystals are interpreted as having formed later during diagenesis,

(certainly later than some dolomite rhombs which they enclose, and also later than some kaolinite and illite porefilling phases, see Plate 3.2).

Quartz cements are common within fluvial and sabkha sediments, but less common in aeolian sands. Early quartz cements are well developed in fluvial sands containing water escape structures (dishes and pillars), and in some areas these sands contain pores which have been completely occluded by quartz (see Plate 3.2).

### 3.2.2 DOLOMITE.

Dolomite cements may occur as non-ferroan or ferroan (ankeritic) types. Different dolomite types reflect formation at different times under different diagenetic conditions, and are therefore mutually exclusive.

Euhedral dolomite rhombs having non-ferroan cores, but ferroan exteriors, indicate that the non-ferroan dolomite precipitated prior to ferroan dolomite. (see Plate 3.3).

Large "oversized" dolomite rhombs, i.e. larger than the average grain size of the sediment, may reflect direct replacement of silicate clasts by the carbonate cement, and / or the precipitation of carbonate cements within oversized voids formed as a result of earlier dissolution.

Poikilotopic porefills are most commonly observed in non-ferroan dolomite cements.

Textures observed between dolomite cements and

other authigenic and clastic constituents are important because they provide an insight into the relative timing of diagenetic phases. The following observations are relevant:

(a) Non-ferroan dolomite cements formed prior to ferroan cements.

(b) Dolomite cements may corrode silicate clasts and early authigenic silica phases which form continuous overgrowths. Corrosion is best developed at boundaries between silicates and non-ferroan dolomite, suggesting that precipitation of non-ferroan dolomite occurs under more strongly alkaline conditions than ferroan dolomite.

(c) Ferroan dolomite cements often contain isolated blebs of anhydrite, and occasionally small euhedral rhombs of ferroan dolomite occur within areas of anhydrite. This suggests the replacement of early anhydrite by later ferroan dolomite.

The relationship between anhydrite and non-ferroan dolomite is less easily established. Typically anhydrite replaces small areas of non-ferroan dolomite. However, this relationship is not unique and the reverse relationship (i.e. non-ferroan dolomite replacing anhydrite) is also observed. This suggests the formation of at least some anhydrite occurs prior to that of non-ferroan dolomite. Thus in a paragenetic sequence for the Lemna Sandstone, non-ferroan dolomite formation is essentially coeval with the formation of at least some anhydrite. The formation of anhydrite occurs under more strongly alkaline conditions than non-ferroan dolomite.

(d) Dolomite cements are "clear" and show no evidence for having formed via replacement of a precursor calcite cement.

(e) Dolomite cements provide important information regarding the timing of the authigenesis of clay minerals. i.e. dolomite cements are clearly earlier than illitic and kaolinitic clays.

### 3.2.3 ILLITE.

Illite is the commonest clay mineral within the Lemn Sandstone, and often occurs intimately associated with chloritic clays at pore margins / grain boundaries. Illite clays commonly constitute 90% of the clay sized sediment fraction, and occur in a number of forms. e.g.

(a) Very poorly crystalline, small irregular flakes tangentially coating grain surfaces. This type of illite is considered representative of an allogenic, mechanically infiltrated clay component. It is seen in thin section as red (haematite stained) pellicles which are continuous through grain contacts. In S.E.M allogenic illites sometimes form clay "bridges" between grains; the bridges being meniscus like forms (4 or 5 microns wide) formed from twisted amalgamations of illitic fibres and flakes, and having concave margins (see Plate 3.4).

(b) Fine "hair-like" fibres (up to a micron wide), which occur as "horns" projecting from the margins of larger more irregular perpendicularly orientated "flakes" (see Plate 3.5).

(c) Extensive pore dividing "networks" composed of sinuous bifurcating strands of illite (up to 30 or 40 microns wide) which subdivide larger intergranular pores into smaller micropores. This illite does not significantly decrease porosity, but does increase the tortuosity of pore throats, and has an adverse effect on permeability. This type of illite is best developed in aeolian facies sandstones.

(d) "Honeycombed" or "box-worked" illite/chlorite networks at the margins of intergranular pores. "Honeycombed" structures are formed as a result of extensive development of platy clay minerals (predominantly illitic) which are arranged perpendicular to grain boundaries. (see Plate 3.6). These clays may constitute recrystallised allogenic clay coatings.

Study of illitic clays using using standard microscopic and SEM techniques clearly illustrates that they are one of the latest authigenic phases to have formed. i.e.

(a) Illitic fibres commonly coat early authigenic silica phases. Less commonly, authigenic quartz may be seen to enclose illitic fibres, and in this case is thought to represent a late stage of silica authigenesis,

(b) Illitic clays enclose dolomite cements,

(c) Illitic clays enclose chlorite and kaolinite flakes,

(d) Illitic fibres traverse and subdivide large intergranular secondary pores,

Finally, wells located upon the "B" Structure of U.K. block 43/26 (43/26-3 and 43/26-5) contain significantly lower amounts of illite than "A" structure wells.

#### 3.2.4 CHLORITE.

Chloritic clays occur in minor amounts in all facies studied, and may constitute up to 23% of the total clay size fraction. The grey/green colouration observed in some sandstones appears due to the presence of chloritic clay.

Chloritic clays may occur as "rosette" like forms of roughly perpendicularly orientated pseudo-hexagonal chlorite platelets and associated fibrous illite; or as "honeycombed" or "boxworked" networks composed of pore-lining illitic/chloritic clay.

Fibrous projections which protrude from chlorite platelets are difficult to identify on morphology alone. They appear identical to fibrous illite, and are suggestive of the illitisation of chlorite. Green chloritic/illitic clays formed along grain/grain or grain/cement boundaries are interpreted as diagenetic alterations of earlier allogenic clay coatings.

#### 3.2.5 KAOLINITE.

Kaolinite commonly forms up to 10% of the total "clay sized" sediment fraction within the Lemna Sandstone, but is especially prolific in wells 43/26-3 and 43/26-5 where it may form as much as 45% of the total

clay fraction.

Kaolinite occurs as pseudo-hexagonal platelets up to 15 microns in diameter, commonly stacked to form short "strings" or "booklets" filling intergranular secondary pores; or as "pseudomorphs" (see Plates 3.7 and 3.8)

Kaolinite flakes may rarely be seen enclosed within euhedra of late stage authigenic quartz and are clearly later than dolomitic cements.

Kaolinite often occurs in close association with illitic and chloritic clays, but there is no evidence to suggest the illitisation or chloritisation of kaolinite. i.e. kaolinite platelets occur in pristine condition.

#### 3.2.6 ANHYDRITE.

Authigenic anhydrite is common within the Lemna Sandstone. It occurs as a blocky porefilling which replaces non ferroan dolomite cements. Anhydrite may severely corrode silicate clasts indicating precipitation from strongly alkaline groundwaters. Anhydrite cements frequently show extensive replacement by ferroan dolomite.

#### 3.2.7 BARYTE.

Baryte is one of the least common authigenic phases within the Lemna Sandstone, and occurs as small tabular crystals, or larger anhedral masses infilling intergranular pores. Petrographic evidence suggests the majority of baryte forms later than early porefilling quartz, but prior to dolomite and porefilling clays (see

Plate 3.3). However, wells 43/26-3 and 43/26-5 contain "lath-like" baryte crystals which are clearly much later in origin, and post date late quartz cements.

### 3.2.8 SIDERITE.

Siderite cements (see Plate 3.9) are common in Hamilton Brothers wells 43/26-3 and 43/26-5, but are absent or only very poorly developed in other wells studied.

When present, siderite is the latest diagenetic phase developed and occurs as poikilotopic cement "nodules". Silicate clasts in contact with siderite cements frequently show marked evidence of dissolution / replacement by siderite (see Plate 3.9). Inclusions of "wormy" pore filling kaolinite are common within sideritic cements, and these are also corroded. Siderite cements contain abundant fluid inclusions.

## 3.3 QUANTATIVE PETROLOGY AND PREDICTED RESERVOIR CHARACTERISTICS.

Quantative petrographic analysis was accomplished by :

- (i) Analysis of helium porosity and air (or nitrogen) permeability data obtained by conventional core analysis.
- (ii) Analysis of point count data obtained during standard petrographic study.

### 3.3.1 ANALYSIS OF POROSITY / PERMEABILITY DATA.

Porosity permeability data for wells studied are



summarised in Tables 3.3.1 to 3.3.7 and represented graphically in Figures 3.3.1 to 3.3.7. Data for Phillips Well 47/5-1 are not included in these tables because numerical data for individual core plugs were not available. However, interpolation of core graphs for this well indicates high mean porosities (20-25%), and permeabilities (75-100 mD).

Tables 3.3.8 to 3.3.14 provide a summary of porosity/permeability correlations. Correlations were tested statistically using the Students t test statistic:

$$t = r * \text{SQRT} \frac{(n - 2)}{(1 - r^2)}$$

in order to test the null hypothesis  $H_0: R = 0$ , at a 99% significance level i.e. to test whether a sample was drawn from a population in which there is zero correlation. The values of t obtained together with an acceptance or rejection of the null hypothesis are included in Tables 3.3.8 to 3.3.14.

Figures 3.3.1 to 3.3.7 indicate that aeolian sediments generally display higher porosities and permeabilities than fluvial and sabkha sediments. This is largely due to the fact that aeolian sediments had much higher depositional porosity than fluvial or sabkha sediments.

Of the fluvial samples studied, cross bedded sediments generally display higher porosities and permeabilities than plane bedded fluvial strata and

irregular / wavy bedded / homogeneous fluvial strata.

Two important facts emerge from analysis of porosity / permeability data, i.e.

(i) The best porosity / permeability relationships occur within better sorted clastic sediments such as aeolian dune sands and cross bedded fluvial sandstones. Sabkha sediments do not normally display good porosity / permeability relationships, because their high allogenic clay content means that an increase in porosity is not necessarily accompanied by an increase in permeability. i.e pore connectivity is very low.

(ii) Aeolian facies sandstones form the main reservoir units within the U.K. block 43/26, and higher correlation coefficients for the aeolian facies of well 43/26-5 when compared with those obtained for aeolian sediments from other wells are probably important. In all other wells studied (apart from well 48/3-3 where data for only six aeolian samples was available) the sediments of aeolian origin display good log-normal porosity / permeability correlations. i.e. correlations are evident only when logarithms are taken of porosity and permeability, indicating that porosity / permeability data is skewed and the bulk of values fall within a narrow range.

Aeolian sands from well 43/26-5, however, provide good porosity / permeability correlations irrespective of whether or not logarithms are taken for the data set. This phenomenon arises because well 43/26-5 contains lower proportions of pore dividing fibrous illite than any other well studied, i.e. although extensive

illitisation in other wells does not seriously reduce porosity within aeolian sediments, it does increase the tortuosity of pore throats and decreases pore throat diameters, adversely effecting permeability (Seeman, 1979). Hence high porosities within illitised wells do not necessarily correlate with high permeabilities. Where illite is absent or only poorly developed (as is the case in well 43/26-5) permeabilities are not adversely affected, and a better correlation exists between increasing porosity and permeability.

N.B. Hamilton Brothers well 43/26-3 is similar to well 43/26-5 in that it is located upon the northerly "B" structure within U.K. block 43/26, and contains significantly lower volumes of illite than wells located upon the "A" structure to the south. However, in the case of well 43/26-3, the difference in illite content is not as marked as that occurring in well 43/26-5, and it this results in it having similar porosity / permeability correlations to wells located upon the "A" structure

### 3.3.2 ANALYSIS OF POINT COUNT DATA.

Point counts of 250 points per thin section were carried out on specimens from all wells studied. A total of 250 points was chosen because although small, it allows the generation of reproducible data which are not significantly different from data obtained using larger totals of 350 or 500 points per thin section. This probably arises as a result of low variability and

relatively simple mineralogy within the Lemna Sandstone).

Compositional data was used in order to produce ternary compositional plots (Pettijohn, 1973), and four variable quartz type diagrams, which Basu et al (1975) suggest are indicative of rock types present within source areas. In addition to compositional data, point counting provides an indication of sediment size and sorting. This was achieved by measuring the apparent long axis of every fifth grain encountered during the point count.

Thin section point counts (together with data obtained using scanning electron microscopy) also provide important information concerning the nature and occurrence of different porosity types, and the varying methods of pore occlusion that took place following deposition.

Six porosity types were discriminated during point counting, and may be used to describe all types of porosity observed within the reservoir zones of all wells studied (see figure 3.3.8).

(a) Intergranular / intercrystalline primary porosity.

This describes areas of primary porosity occurring between clasts or cement ( $Ie_1$ ). Such pores are commonly small and restricted, and most easily recognised when bound by allogenic clay pellicles i.e. pellicles which are continuous along grain contacts. Generally, small scale pores existing between grains that are bound continuously by allogenic clay pellicles may be thought

of as being primary in origin. If the margins of the pore consist of allogenic grain coatings upon which a later phase of authigenic quartz has developed, then the pore is termed an intercrystalline primary pore, and represents a primary pore which has been modified by authigenic overgrowth. N.B. No "micro" equivalent of this porosity group is described in thin section point counts because of the difficulty in its recognition. However, areas of microporosity (typically 10 micron diameter pores) existing between mechanically infiltrated allogenic clay bridges are recognisable using SEM techniques. Small pores between infiltrated clay bridges are subject to diagenetic modification, i.e. in the proposed diagenetic scheme, it is suggested that much illite formation occurs by recrystallisation of allogenic components. Thus pores existing between illitic fibres observed along grain contacts using SEM techniques must be described as modified primary pores, or more correctly as intergranular / intercrystalline secondary micropores.

(b) Intergranular / intercrystalline secondary porosity.

This describes areas of macroporosity which occur between clasts or cement and which appear secondary in nature (Ie<sub>2</sub>). Porosity is recognised as secondary using criteria cited by *Schmidt et al* (1977) and *Burley et al* (1986), i.e. the presence of oversized pores, oversized carbonate cement rhombs, elongate and sinuous pores, floating and corroded grains, etc. Where (in thin section) a secondary pore is bound by authigenic cement phases, then it is termed an intercrystalline secondary

pore, denoting a secondary pore which has been modified by authigenic cement growth. Where at least one of the margins of the pore observed in thin section is a clast, then the porosity is termed intergranular secondary porosity.

(c) Intergranular/crystalline secondary microporosity.

This describes areas of microporosity which occur between clasts or cement, and which appear secondary in nature ( $Ie_m$ ). It typically describes areas of microporosity occurring between authigenic clay phases which infill larger secondary pores, e.g. between randomly stacked kaolinite flakes (see plate 3.3.8), illite fibres or chloritic platelets.

(d) Intragranular/crystalline secondary macroporosity.

This describes areas of macroporosity which occur within clasts or cements ( $Ia_2$ ).

(e) Intragranular/crystalline secondary microporosity

This describes areas of secondary microporosity which occur within clasts or cements ( $Ia_{2m}$ ).

(f) Fracture porosity ( $I_f$ ).

This describes porosity associated with fractures.

Comparison of helium porosity data with porosity estimates obtained during point counting (see figure 3.3.9) reveals that point count estimates of porosity commonly represent less than 15% of total porosity. This suggests that much of the porosity exists within micropores, and is not detected during standard petrographic analysis.

The bulk of macroporosity observed during point counting is interpreted as being secondary in origin, and is recognised as such on the basis of criteria cited by Schmidt et al (1977). Secondary porosity is best developed in facies which displayed the best depositional porosity and permeability. i.e. aeolian dunes.

In order to understand the mechanisms which control the porosity / permeability characteristics of a sediment, it is necessary to distinguish between pore dividing and pore occluding diagenetic phases, and to quantify these relative to a number of framework indices established by point counting. (N.B. This has been carried out using a method outlined in proprietary reports produced by Core Laboratories U.K. Ltd for Hamilton Brothers Oil and Gas Ltd in 1981)

Figures 3.3.10 to 3.3.33 illustrate how size, sorting and packing indices may be used to produce a framework index (I), providing an indication of original reservoir quality.

For Example:

For grain size	very fine	= 1.0
	fine	= 2.0
	medium	= 3.0
For sorting	poorly sorted	= 1.0
	moderately sorted	= 2.0
	well sorted	= 3.0

The packing index used in this report is defined by.....

$$\text{PACKING} = N / L * 10$$

Where N is the number of grains encountered in a traverse of length L.

If PACKING = 0.0 - 3.3,	Packing Index =	3 (LOOSE)
3.4 - 6.7,	Packing Index =	2 (MODERATE)
6.8 - 10.0	Packing Index =	1 (CLOSE)

The framework index (I) is equal to the sum of the size, sorting and packing indices. Having established a framework index which provides an indication of the original reservoir quality, then by quantifying the proportion of reservoir quality which was lost during diagenesis (Z), it becomes possible to provide an estimate of the present reservoir quality (Q). Distinguishing between pore occluding phases (eg quartz, dolomite, anhydrite and allogenic clays) which destroy porosity, and pore dividing phases (eg authigenic kaolinite and illite) which subdivide areas of porosity allows this to be done, i.e. if:

$$Z = \frac{\% \text{ Pore occluding material}}{\% \text{ Pore occluding} + \% \text{ pore dividing material}}$$

then the predicted reservoir quality (Q) is equal to the original reservoir quality minus the proportion of that quality which has lost pore occluding material, i.e.

$$Q = (I - (I*Z))$$

For the purpose of this report,



Q = 0 - 3.0	poor reservoir quality
Q = 4.0 - 6.0	Moderate reservoir quality
Q = 7.0 - 9.0	good reservoir quality

Figures 3.3.10 to 3.3.33 illustrate that using these relatively crude manipulations reveals a number of important facts:

(i) Better predicted reservoir quality (generally moderate) occurs in aeolian sandstones. Predicted reservoir quality for fluvial sands is poor - moderate, whilst in Sabkha sediments it is poor only. This is important because in the proposed sedimentological model for U.K. block 43/26, aeolian sands form correlatable, laterally extensive "sheet-like" reservoir units, and the extremely poor reservoir characteristics of Sabkha facies sediments leads to their acting as "seals" in what are effectively stratigraphic hydrocarbon traps.

(ii) Aeolian sediments contain the highest porosity / permeability values, and this conforms with their displaying the lowest volumes of "total pore occluding material". In particular they are characterised by much lower allogenic clay contents.

(iii) Predicted reservoir quality for aeolian sands is rarely good. Most commonly it is moderate or often poor, and this does not always agree with data obtained from core analysis or petrographic observation, e.g. samples from well 43/26-5 display excellent porosity and permeability determined during core analysis, and in thin section they are seen to contain abundant macroporosity. However, they also contain significant

quantities of pore occluding quartz and carbonate cement which result in the predicted loss of original reservoir quality being large. The extreme discrepancy between predicted reservoir quality (poor in this case) and actual reservoir quality (excellent) stems from the fact that much of the porosity is secondary in nature, and has developed as a result of grain dissolution (probably via a carbonate replacement stage).

The simple model used for predicting reservoir quality relies upon the occlusion of pores existing at deposition. When processes occur which result in the production of secondary porosity, the cement / framework balance is upset, and the clast/cement ratio is weighted in favour of the authigenic components. This can, and evidently does, occur without producing enough of an alteration in the packing index in order to allow the balance to be restored.

Thus, poor predicted reservoir quality in sediments which other data suggests should display excellent reservoir characteristics may be used to infer the development of secondary porosity.

### 3.4 SEMI-QUANTATIVE X-RAY DIFFRACTION ANALYSIS OF THE "CLAY SIZED" SEDIMENT FRACTION WITHIN THE LEMAN SANDSTONE.

X-ray diffraction analysis of specimens was carried out in order to establish the composition of the clay size fraction within the Leman Sandstone.

Samples were prepared by gently disaggregating the rock specimen with a pestle and mortar. Separation of the clay-fraction from the sand-fraction was achieved by allowing the disaggregated sediment to settle in a flask containing de-ionised water to which a deflocculating agent (sodium-hexa-meta-phosphate) had been added. The desired size fraction (less than two microns) was then pipetted from the flask at the appropriate time and depth. Orientated clay mounts were prepared by precipitating the clays onto porcelain disks using a Buckner Filter Funnel.

Air dried clay mounts were run at  $0.5^\circ$  theta / minute using cobalt K-alpha radiation. The samples were run following glycolation and again after heating to  $180^\circ\text{C}$  and  $500^\circ\text{C}$  for identification of clay phases present using procedures outlined by *Carroll* (1970).

The relative percentages of clay mineral phases present were established using simple calculations outlined in *Carver* (1974).

The results of investigations into the composition of clay size sediment fractions from all wells studied are tabulated in Tables 3.4.1 to 3.4.8. The values given in these tables reflect relative percentages of illite, kaolinite and "chloritic type" clays present.

Analysis of the percentages of clay types present within different wells (see Table 3.4.9), suggests that Hamilton Brothers wells 43/26-3 and 43/26-5 contain lower proportions of illite, and higher proportions of

chlorite and kaolinite than other wells studied. In order to test this observation the wells studied were divided into three categories:

(i) Hamilton Brothers wells 43/26-3 and 43/26-5, which are located to the north of the major NW-SE trending fault in U.K. Block 43/26, ("B" Structure wells).

(ii) Hamilton Brothers wells 43/26-1, 43/26-2 and 43/26-4 which are located to the south of the major NW-SE trending fault in U.K. Block 43/26, ("A" Structure wells).

(iii) Wells studied from locations outside UK Block 43/26, i.e. Amoco well 48/2-1, Amerada Hess 48/3-3 and Philips Petroleum 47/5-1.

Thus categories were constructed to check whether there is variation between clay populations both within U.K. Block 43/26, and also between wells located on U.K. Block 43/26 and wells from adjacent blocks.

A Students t test statistic was used firstly in order to test the null hypothesis "Samples from the Northern and Southern Structure of UK Block 43/26 are random samples from the same normal population" ( $H_0: U_1 = U_2$ ), after first checking to confirm normality within the distribution of data sets.

The Students test statistic ( $t$ ) was calculated using the equation.....

$$t = \frac{X_1 - X_2}{S_p * \text{SQRT} \left( \frac{1}{n_1} + \frac{1}{n_2} \right)}$$

where, X1 and X2 are the means of the two samples being studied, and.....

$$S_p^2 = \frac{(n_1 - 1) S_1^2 + (n_2 - 1) S_2^2}{n_1 + n_2 - 2}$$

$S_1^2$  and  $S_2^2$  represent the variance of the two samples,  $n_1$  and  $n_2$  represent the number of observations in each sample. The degrees of freedom associated with the "t" test were calculated using the equation:

$$\text{D.F.} = \left( \frac{S_1^2}{n_1} + \frac{S_2^2}{n_2} \right) / \left( \frac{S_1^4}{n_1^3} + \frac{S_2^4}{n_2^3} \right)$$

The values of t obtained (for n-2 degrees of freedom = 48) are as follows: "t" illite = 5.06; "t" chlorite = 0.61 and "t" kaolinite = 5.46. These values lead to rejection of the null hypothesis for illitic and kaolinitic clays at a 99% significance level; and imply significant difference between the clay populations for "A" and "B" structure sands in U.K. Block 43/26.

Clay mineral populations from wells outside U.K. Block 43/26, are similar to those from wells located

upon the "A" structure of U.K. Block 43/26. Again by use of a "t" test statistic, we may test the null hypothesis  $H_0: U_1 = U_2$  for the two populations.

The values of "t" obtained in this case ("t" illite = 0.69; "t" chlorite = 1.37 and "t" kaolinite = 1.09), lead to acceptance of the null hypothesis at a 99% significance level. They imply no significant difference between the clay population of wells located upon the "A" structure of UK Block 43/26 and wells located outside UK Block 43/26.

Brief investigation into clay species variations with particle size was accomplished by centrifuging clay suspensions for progressively longer times prior to precipitation upon porcelain discs for analysis. Very simply, diffractograms obtained from these samples indicate increasing intensity of 10A (Illite 001) peaks, and decreasing intensity of 7A (chlorite 002, kaolinite 001) peaks within progressively finer size fractions. This indicates that the illite content of the clay size fraction increases with decreasing particle size.

Variations in X-Ray diffractograms for clay mineral separates are summarised in Tables 3.4.10 - 3.4.12. Diffractograms indicate a variation in the composition of chloritic clays within wells studied, i.e.

Samples from wells 48/3-3, 48/2-1 and most samples from well 43/26-4 contain Mg chlorites, i.e. chlorites having odd order (001, 003) reflections of greater intensity than even order (002, 004) reflections.

An example of a typical diffractogram from one of these wells is shown in figure 3.4.1.

Samples from wells 47/5-1, 43/26-1, 43/26-2, 43/26-3 and 43/26-5 contain Fe chlorites which have even order (002, 004) reflections of greater intensity than odd order (001, 003) reflections. Examples of typical diffractograms from these wells are shown in figures 3.4.2 and 3.4.3.

The presence of two well defined reflections at around 7A distinguishes wells 43/26-3 and 43/26-5 from other wells studied. N.B. Two reflections at 7A are sometimes present in samples from well 43/26-1, the majority of samples from this well however provide diffractograms like those obtained from well 43/26-2.

The question thus arises are the two peaks at 7A in wells 43/26-3 and 43/26-5 representative of chlorite (002) / kaolinite (001) reflections at slightly different d spacings than those occurring in other wells studied, or do they reflect the presence of overlapping chlorite (002) / kaolinite (001) reflections (as seen in other wells) plus a new reflection (7.02A - 7.04A) indicative of an additional clay mineral phase. If an additional clay mineral phase is present, the position of the 7.02A - 7.04A reflection and its behaviour upon heating to 550°C might suggest that mineral is chamosite.

Fe chlorites and chamosite will dissolve in dilute hydrochloric acid solutions, but kaolinite should not (Brindley 1961). Investigations into the possible

presence of chamosite in wells 43/26-3 and 43/26-5 carried out using acid digestion (1.0% HCl) techniques on three samples proved inconclusive. This arises from the fact that kaolinite in samples from wells 43/26-3 and 43/26-5 appears unusual in that like chlorite it dissolves in weak hydrochloric acid. Results however did prove that the 7.15A - 7.18A peak is a chlorite (002) reflection since a reduced intensity peak remaining at this d spacing following acid digestion could not be removed from the diffractogram trace by subsequently heating the sample to 550°C.

Since the presence of a chamositic clay in samples studied from wells 43/26-3 and 43/26-5 can neither be proved or disproved, and because petrographic evidence indicates that kaolinite is especially abundant in these wells, the peaks at 7.04A - 7.05A are interpreted as disordered kaolinite (001) reflections.

No correlation between illite crystallinity and depth was noted for any wells studied. This contrasts with Lemn Sand data of *Arthur et Al* (1986), who plotted illite crystallinity data for block 49/28 against depth below base Chalk and top Triassic. Their data showed a positive correlation between crystallinity and depth below top Triassic for twelve study samples, and this was interpreted as indicating that the uplift which they suggest arrested illite development in block 49/28 took place after the end of the Triassic and before the onset of Maastrichtian chalk deposition. The application of this technique to the Lemn Sandstone of U.K. block 43/26



during the course of this study, has not produced any correlation between illite crystallinity and depth.

### 3.5 K-AR DATING OF AUTHIGENIC ILLITE SEPARATES.

Research by Lee (1984) and Lee et al (1985) suggests that the application of K/Ar age dating techniques to illitic clays may in some cases provide information about the timing of gas emplacement in Rotliegend sandstones. In particular he was able to document:

(a) Progressively younger K/Ar determined ages with decreasing illite particle size - suggesting that fine "hair-like" crystallites at the ends of illitic fibres constitute the latest formed illite.

(b) Progressively younger illite ages observed "down hole" within some Rotliegend sections. This suggests that illite growth (which Lee et al (1985) state is the last diagenetic event within the Permian sandstones of their study) is arrested by gas emplacement; and that younger ages are observed "down hole" as a result of downward migration of the gas-water contact.

For the purpose of this study it was decided to try and model late stage diagenesis in Hamilton Brothers 43/26 wells using the assumptions:

(i) Mean K/Ar dates obtained for fine grained separates from a particular well represent the mean age of formation of illite within that well.

(ii) Illite formation is arrested by gas "emplacement / migration".

It is important to note that in all samples studied illite is not the last diagenetic phase to have been precipitated. In "illitised" wells illite precipitation is followed by the precipitation of late quartz, and in wells where illite is only poorly developed the latest phase precipitated is commonly siderite. Thus assumption (ii) above does not imply that "gas emplacement" (at least in its early stages) completely arrests diagenesis. However, the assumption that gas emplacement arrests the formation of illite is considered valid on the basis of the diagenetic model presented in section 3.7 of this report. This model uses the "chemical" effects of early gas migration upon pore waters in order to explain the lack of illite, and the formation of siderite within gas producing "B" structure wells.

Ten clay separates from well 43/26-2 were prepared for analysis with average grain sizes of less than 0.5 microns (determined by S.E.M. analysis of separates). The data obtained is presented in Table 3.5.1. Dating was carried out commercially at Newcastle University, and the ten samples yield a mean age of 173my.

The data set is problematical. The  $K_2O$  values within mineral separates are very low, and are not typical of  $K_2O$  concentrations normally found within illitic clays (e.g. Lee (1984) documents  $K_2O$  values

ranging from 5.41 - 9.65% for illites within Rotliegend samples). Possible explanations for this discrepancy are that samples studied were impure, or that the illite has been altered. Kaolinite and chlorite were absent or present in only trace amounts (if present at all) in all samples studied, and since these clays do not contain K, they have no effect upon K/Ar age determinations.

The mean age for illite formation within well 43/26-2 (173my) compares very favourably with the results obtained by other researchers working both upon the North Ravenspurn prospect (British Petroleum), and also upon similar Rotliegend fields within this region of the Southern Permian Basin (e.g. Lee's determinations for Indefatigable and Leman Bank). It is therefore suggested the age of 173my is a basic constraint on the timing of gas emplacement for North Ravenspurn.

There does not appear to be any correlation between the K/Ar determined age of illite separates with depth.

### 3.6 FLUID INCLUSION STUDIES

Fluid inclusion studies involve the thermometric analysis of fluids which become trapped as inclusions within minerals during crystal growth (Sorby 1858). Differential contraction between the trapped fluid and the host mineral during cooling results in the formation of a vapour bubble within an inclusion. The temperature at which this vapour bubble disappears upon heating the

inclusion is known as the homogenisation temperature. (Th).

Temperatures of homogenisation may be regarded as trapping temperatures only under special circumstances. For example, if the inclusions trapped a boiling fluid (Roedder 1984). However, this case is rare and probably not applicable to inclusions within the Leman Sandstone. For inclusions which were not trapped as boiling assemblages the homogenisation temperature recorded must be "pressure corrected" to give a "true trapping temperature". Pressure corrections usually involve increasing the recorded temperature of homogenisation, and in order to apply them it is necessary to have obtained freezing data (salinity / density data) for inclusions.

Two fundamental problems are encountered in attempting fluid inclusions study upon authigenic phases within the Leman Sandstone:

(i) The scarcity of inclusions suitable for study, - inclusions are rare in dolomite and quartz phases. They are more abundant in sideritic phases, but relatively few of these appear suitable for study. i.e. many are irregular in shape, indicating they may have "necked down". Other inclusions studied did not give accurately reproducible results, a feature which is often true of cleavage orientated inclusions and probably indicative of leakage during measurement (Roedder 1984).

(ii) The size of inclusions available for study. Inclusions within authigenic phases are very small having

inclusion diameters in the order of 10 microns, and do not readily lend themselves to fluid inclusion measurements.

In this study, because of the small size of fluid inclusions, only determinations of temperature of homogenisation were carried out. Thus, with no freezing data and hence no pressure corrections, temperatures of homogenisation recorded can only be regarded as a minimum trapping temperatures for inclusions (Sorby 1858, Roedder 1984).

Fluid inclusions were observed in authigenic phases including ferroan dolomite, quartz and siderite. Inclusions most commonly occur as two phase liquid-vapour inclusions, with low vapour to liquid ratios. Measurement of homogenisation temperatures for primary inclusions within authigenic phases was carried out using a Linkham TH600 heating cooling stage. Homogenisation temperatures quoted in this report occur in the aqueous liquid phase. The temperatures of homogenisation obtained from inclusions within phases studied are presented in Table 3.6.1 and illustrated graphically in Figure 3.6.1.

The data obtained shows significant difference between temperatures of homogenisation for inclusions in siderite and quartz cements (Students "t" test statistic = 3.61) but no significant difference between homogenisation temperatures obtained for quartz and dolomite cements (Students "t" test statistic = 1.21).

However, due to the small number of dolomite inclusions studied, the apparent lack of any difference in homogenisation temperatures for quartz and dolomite should be viewed with caution.

If the temperature of homogenisation for mineral phases are compared with Horizon Temperature V Time plots and Burial History plots, then dolomite and quartz cement formed during the late Triassic following the main phase of basin subsidence; and sideritic cements formed during the middle-late Jurassic.

### 3.7 WHOLE ROCK GEOCHEMICAL ANALYSIS USING X-RAY FLUORESCENCE SPECTROSCOPY.

X-ray fluorescence is an analytical technique involving the bombardment of a prepared sample with primary X-rays, and the analysis of secondary "fluorescent" radiation which is emitted from that sample. Multiwavelength fluorescent radiation produced by the sample is composed of sets of individual wavelengths characteristic of elements present. Identification of component wavelengths of fluorescent radiation allows qualitative identification of elements. The intensity of the radiation is proportional to concentration, and by comparing intensities to those of international standards of known composition a quantitative analysis can be obtained.

X-ray analysis was carried out using a Phillips PW1400 wavelength dispersive X-ray fluorescence spectrometer. Samples were presented for analysis as

pressed powder briquettes. Analysis for eleven major elements were carried out following routine machine calibration using selected international standards and internal Permo-Triassic "red-bed" standards, the elemental composition of which had been determined in previous studies (Holmes et al 1983). Selection of international standards of similar composition to unknown samples minimised errors due to mass absorption effects.

All specimen and standard powder samples were "ignited" at 1000°C for one minute prior to being pressed into briquettes for analysis. This reduced the volatile content of samples, allowing better analytical totals to be obtained. However, the ignition process was unsuccessful in fully reducing the volatile content of specimens studied, and elemental abundances quoted in this text have been normalised to 100% (a normalisation factor of 1.06 being most common).

A measuring program was constructed to analyse for Si, Al, Fe, Ca, Mg, K, Na, Mn, Ti, P, and S. Calibration lines used in setting up this measuring program indicate an acceptable degree of accuracy and reproducibility for all elements analysed except for sodium and sulphur (lighter elements the fluorescence radiation of which may be absorbed by heavier elements present; an interelement "matrix" effect). Data presented for these elements must be viewed with caution. To provide an indication of the accuracy of results, six high silica samples of known composition which were not

included in the calibration were analysed. The samples included quartz porphyries, mica shist, quartz aplite, syenite and shale. The mean difference between actual and observed elemental concentrations for these samples is included in Appendix Fourteen.

Geochemical data were obtained for 117 samples, 81 of which were from wells located upon the southern "A" structure, and 36 of which were from wells located upon the northern "B" structure within UK block 43/26. The data are summarised in tables 3.7.1 to 3.7.4.

The comparison of data sets from different structures within U.K. block 43/26 is considered valid because:

A) Sediments from the same facies, but located upon different structures, have similar mean grain sizes (fine-medium grained). Thus compositional variation arising as a result of differences in sediment grain size may be considered minimal.

B) There is no evidence to suggest the existence of any compositional variation arising as a result of differences in framework clast composition between sediments from similar facies located upon different structures.

Geochemical data (mean elemental abundances) for aeolian and fluvial facies sandstones from the southern "A" structure were compared with aeolian and fluvial data from the northern "B" structure of UK block 43/26, using the Students "t" test statistic. The test statistic was used in order to test the null hypothesis "samples



collected from the "A" and "B" structures within North Ravenspurh are random samples from the same normal population ( $H_0: U_1 = U_2$ ).

The Students "t" test statistic was calculated using the equation:

$$t = \frac{\bar{x}_1 - \bar{x}_2}{Sp * \sqrt{\left(\frac{1}{n_1} + \frac{1}{n_2}\right)}}$$

where  $\bar{x}_1$  and  $\bar{x}_2$  are the means of the two samples being studied, and,

$$SP^2 = \frac{(n_1 - 1)S_1^2 + (n_2 - 1)S_2^2}{n_1 + n_2 - 2}$$

The mean elemental abundances and Students "t" test statistics observed are quoted in tables 3.7.5 to 3.7.6. Rejection of the null hypothesis at probabilities of less than 0.05% illustrates a significant difference between the Ca, Mg and K contents of aeolian facies sediments, and in the Ca and Mg content of fluvial facies sediments for the "A" and "B" structures.

N.B. Students "t" tests were carried out using the equation:

$$\frac{S_1^2}{n_1} + \frac{S_2^2}{n_2} \quad / \quad \frac{S_1^4}{n_1^3} + \frac{S_2^4}{n_2^3}$$

in order to estimate the degrees of freedom for the data sets in question (Williams 1983).

Further statistical analysis were obtained by constructing multi-element correlation matrices for "A" and "B" structure aeolian and fluvial sandstones. The correlation matrices produced are tabulated in tables 3.7.7 to 3.7.10. The upper portion of these tables contain the results of the null hypothesis "no correlation exists between sets of elements" ( $H_0: R = 0$ ). The results of this "t" test are expressed in terms of an acceptance or rejection of the null hypothesis at probabilities of less than 0.01% (99% significance). The "t" test statistic was calculated using the equation:

$$t = r / \sqrt{\frac{(n - 2)}{1 - r^2}}$$

The observed difference in the potassium content of "A" and "B" structure aeolian sandstones (i.e. the main gas reservoir units) is important because:

(i) The lower potassium content of "B" structure aeolian sandstones compliments semi-quantative x-ray diffraction data suggesting a lower degree of illitisation within the structure.

(ii) The lower potassium content of "B" structure aeolian sandstones compliments petrographic evidence which suggests greater development of secondary porosity within this structure (especially in well 43/26-5), i.e. any potassium fixed within detrital feldspars would be lost, as presumably these would disappear early during secondary porosity generation.

(iii) If potassium was not fixed within authigenic phases (i.e. illite) within "B" structure aeolian sandstones, then it must have been removed from these sediments in solution within porewaters expelled during gas emplacement.

It should be noted that differences in potassium content occur only between "A" and "B" structure aeolian sandstones (i.e. main reservoir intervals), and not between "A" and "B" structure fluvial sandstones. Also, for Al versus K correlations, "B" structure sandstones display lower correlation coefficients than "A" structure sandstones.

The difference in Ca and Mg contents between both aeolian and fluvial data sets from the "A" and "B" structures of UK block 43/26 is less easily quantified because these elements are essential components of more than one diagenetic phase within the Leman Sandstone, e.g. dolomite ( $\text{CaMg}(\text{CO}_3)_2$ ), anhydrite ( $\text{CaSO}_4$ ) and chlorite ( $\text{FeMgAl}_2\text{Si}_2\text{O}_{10}(\text{OH})_2$ ). Variation is best explained in terms of differing dolomite contents for "A" and "B" structure sandstones since:

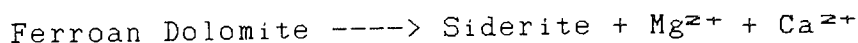
(i) It is not unreasonable to assume that variations in

the Mg and Ca content chloritic clay minerals will have only a minimal effect upon the bulk chemistry of the Leman Sandstone. Furthermore, X-ray diffraction analysis indicates there is no significant difference in the total chlorite content of "A" and "B" structure sands (see section 3.4).

(ii) Anhydrite is present in only very minor quantities in all specimens studied. There is no appreciable difference in the anhydrite content of sands from the "A" and "B" structures.

(iii) In wells 43/26-5 and 43/26-3 late stage sideritic cements may be seen forming at the expense of ferroan dolomite cements. This would be expected to be reflected in the whole rock geochemistry.

Thus, lower Mg and Ca contents for "B" structure sands may be interpreted as having arisen as a result of an overall reaction which may be summarised:



Since siderite is the last diagenetic phase to be precipitated, the  $\text{Mg}^{2+}$  and  $\text{Ca}^{2+}$  released as a result of this reaction are interpreted as being removed from the system, probably within pore waters leaving the reservoir units upon gas migration.

Lower Ca:Mg ratios exist with "B" structure sandstones than within "A" structure sandstones; and there is a correlation between increasing Fe content and Ca:Mg ratio. This correlation is not evident within "B"

structure wells.

A correlation between increasing Fe content and increasing Ca:Mg ratio for "A" structure sands (see figure 3.7.1) is easily explained because of the fact that Fe substitutes for Mg within ferroan dolomite lattices (Deer, Howie and Zussman 1968). The lack of a similar correlation within "B" structure sandstones probably arose because because Mg and Ca were lost from porewater systems as a result of gas emplacement following the above mentioned reaction involving the precipitation of siderite, i.e. when the Ca/Mg loss within "B" structure sandstones is balanced against Mg present within chloritic clays etc, (remember there is no difference in chloritic contents of "A" and "B" structure sands), then the Ca:Mg ratio is tipped in favour of Mg, and efectively decreased.

### 3.8 THE DIAGENESIS OF THE LEMAN SANDSTONE.

Paragenetic sequences for authigenic minerals within wells studied are shown in figures 3.8.1 to 3.8.3.

Early diagenesis includes the very early cementation of desert sediments by precipitation from near surface groundwater, and the mechanical infiltration of allogenic clays. Observations of Glennie *et al* (1978) and Kessler (1978) suggest that early diagenetic events in aeolian environments include cementation by gypsum and calcite. In particular Glennie

(1970) suggests that the source of gypsum cement may be the slow evaporation of groundwaters of Sabkha origin, which have seeped through dunes. Similarly, Kessler (1978) documented early calcite cementation of wadi sandstones in the Rotliegend facies of UK block 48/30.

Neither early gypsum or calcite are observed in the Rotliegend strata of the wells studied. However, it is believed that in the light of observations made by Glennie *et al* and Kessler (1978), their presence as early components in the diagenetic sequence is possible, and will be given consideration in the following arguments.

Any early gypsum cement would be expected to convert to anhydrite with increasing depth of burial. Glennie *et al* (1978) state that formation temperatures of 50°C or more result in gypsum crystals being converted to nodular anhydrite. Also the precipitation of early gypsum cements would have increased  $Mg^{2+}/Ca^{2+}$  ratio of porewaters resulting in the dolomitisation of early calcite cements to form non-ferroan dolomite relatively early in the diagenetic scheme.

Both the dehydration of gypsum to form anhydrite, and the dolomitisation of calcite are accompanied by a "volume loss", i.e. they are porosity enhancing transformations.

Both anhydrite and non-ferroan dolomite severely corrode and replace silicate clasts suggesting strongly alkaline conditions.

Anhydrite cements commonly replace non-ferroan dolomite cements indicating that non-ferroan dolomite formed prior to anhydrite. Very rarely, non-ferroan dolomite cements may be seen replacing anhydrite, suggesting that some minor dehydration of gypsum must have occurred prior to the formation of non-ferroan dolomite.

Thus, in the paragenetic sequences (figures 3.8.1 - 3.8.3) anhydrite formation is indicated as spanning the whole of an "Early diagenetic phase" and terminating with the formation of ferroan dolomite. Ferroan dolomite rhombs often corrode and replace earlier anhydrite cements.

Early diagenetic processes observed in wells studied also include the mechanical infiltration of allogenic clays, and an early phase of silica authigenesis.

The mechanical infiltration of allogenic clay really begins at deposition. These clays are recognised as forming iron stained pellicles which are continuous along grain contacts. Iron stained pellicles are rust red/brown coloured due to the presence of ferric iron ( $\text{Fe}^{3+}$ ) in the form of hematite ( $\text{Fe}_2\text{O}_3$ ). Red colouration originates as a result of the intrastratal dissolution of iron bearing silicates, and the incorporation of the iron released into the pellicular coatings. The fact that this occurs in oxidising/alkaline (high Eh/high pH) subsurface desert waters results in the iron occurring as

a ferric oxide (Walker 1967). Use of SEM reveals that allogenic clays occur as poorly crystalline/amorphous grain coatings or as "bridges" at grain contacts. Clay bridges typically have a "meniscus-like" form with concave margins and are of illitic composition.

Early silica authigenesis is believed to have taken place at shallow depths, relatively close to the desert sediment surface. Silica dissolved in desert ground waters is likely to be sourced from the dissolution of labile silicate clasts at shallow depths. Silica rich ground waters may be drawn upwards, and concentrated by evaporation occurring at the surface. This results in groundwaters becoming saturated with respect to silica, and small volumes of quartz are precipitated as poorly developed, incomplete overgrowths on detrital quartz clasts. In terms of a paragenesis, this process appears to occur after the mechanical infiltration of clays, and prior to the formation of non-ferroan dolomite. This model is similar to that proposed by Waugh (1970) to explain silica authigenesis in the Penrith Sandstone.

The suggestions of Glennie et al and Kessler (1978) clearly outline a possible method by which non-ferroan dolomite may form after a calcite precursor, and a schematic diagram can be constructed illustrating one possible way by which the processes characteristic of this "Early Diagenesis" may occur (see figure 3.8.4.). The ideas of Glennie and Kessler are obviously



attractive when trying to understand the complex diagenetic history of the wells studied, where no vestige of any calcite cement is observed whatsoever.

However, in view of the proposed sedimentological model, and the lack of any evidence of a precursor calcite cement, it is useful to consider the possibility of early non-ferroan dolomite forming as a primary precipitate. In particular, it is useful to consider the impact of fluvial "sheetflood" waters on the early diagenetic environment.

Very little evidence for the existence of channelised "wadi" systems has been observed in the wells studied. Instead, the majority of fluvial sands appear to represent quite large and probably laterally extensive sheet flood type events. *Glennie et al* (1978) and *Kessler* (1978) use the argument that waterflows through wadi sands for longer periods than it does over them, in order to allow calcite precipitation to occur to its maximum. In this respect, the use of wadi sands (sensu stricto) as possible sources of early calcite cement in wells studied is incorrect because they rarely exist.

Fluvial sands present were deposited rapidly from extensive sheetflood events, and are often characterised by poor sorting, water escape structures or a lack of depositional fabric.

An alternative model, which might explain the sequence of early diagenetic events in wells studied is shown in figure 3.8.5. This model utilises the presence of interdune/lake margin sabkhas, and the proximity of

sediments to a northerly located saline lake in order to source brines from which early gypsum precipitation occurs. Migration of these brines from sabkhas, into fluvial sheetflood and aeolian sediments (possibly by an evaporative pumping mechanism) allows precipitation of early gypsum in these facies.

Dehydration of gypsum to form the anhydrite observed in thin section may begin at the near surface, and will continue with burial (with an associated increase in porosity).

The increased abundance of anhydrite in fluvial sediments relative to aeolian sediments probably stems from the inherent lower depositional porosities of fluvial sediments, which give rise to greater capillarity through them.

Early gypsum precipitation results in high Mg:Ca ratios in groundwaters. However, these groundwaters are also of high salinity and precipitation of a dolomitic carbonate phase cannot occur (*Folk and Land 1975*), see figure 3.8.6). Precipitation of an early calcite cement phase is not invoked in the proposed model - instead, high salinity and the presence of  $\text{SO}_4^{2-}$  result in  $\text{Ca}^{2+}$  ions being incorporated into early gypsum cements.

Early silica precipitation occurred at the near surface by processes analagous to those described above, i.e. by the concentration of silica derived from labile clast dissolution.

The flushing of high salinity desert

groundwaters during fluvial sheet flood events will result in a sudden drop in salinity. However, the Mg:Ca ratio might be expected to remain high because of the low concentration of salts carried away by diluting waters (Folk and Land 1975). Thus the dilution of saline sabkha brines without appreciable variation in the Mg:Ca ratio, allows dolomite to precipitate. As the sheet flood wanes, (1) evaporation will increase salinity and (2) precipitation of dolomite will decrease the Mg:Ca ratio. Thus re-equilibration brings pore waters towards conditions under which dolomite cannot precipitate, and calcium sulphate can. This re-equilibration process may then be used to explain why in some thin sections anhydrite is observed both replacing and being replaced by non-ferroan dolomite. (The former case being the most common).

Sheetflood events may also provide part of the mechanism for early silica precipitation. Silica solubility is strongly dependent upon pH, (see figure 3.8.7) and a lowering of pH due to influx of the freshwater into near surface groundwaters will decrease silica solubility causing its precipitation.

The ability of sheet flood events to induce silica precipitation is clearly evidenced in wells studied by the presence of abundant silica cements, and silica cemented water escape structures within fluvial sands deposited as a result of rapid sheetflood processes. Thus, an alternative mechanism to explain the sequence of early diagenetic events observed in wells studied, might

involve the mixture of Mg rich hypersaline brines of sabkha origin, with fresh waters of sheetflood origin, in a near surface environment (see figure 3.8.5).

While this alternative model may be applicable in the cases studied, it does not exclude the possibility of the processes invoked by *Glennie et al* (1978) occurring outside the study area, e.g. to the south where more recognisably "channelised" wadi sands may be present, and the subsequent sequence of diagenetic events may be similar to those shown in figure 3.8.4.

This early stage of diagenesis characterised by silica, sulphate and non ferroan dolomite is recognisable in sediments from all facies within all wells studied, regardless of porosity / permeability relationships which might have been expected to impede the movement of fluids.

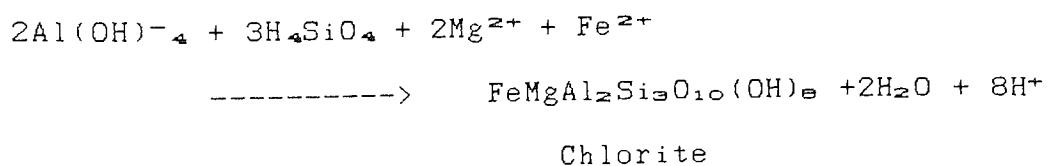
The next phase in the proposed diagenetic scheme for wells studied occurs at intermediate burial depths and is dominated by the formation of ferroan dolomite and chloritic type clays.

Increased  $[Fe^+]$  and  $[Mg^+]$  concentrations in pore fluids occur as a result of earlier dissolution of iron bearing silicates and leads to the formation of ferroan dolomite when burial brings the sediment into favourable pH conditions, i.e. high pH and low Eh (alkaline and reducing). The severity of replacement of silicate clasts by ferroan dolomite is less than that observed in the case of replacement by non ferroan dolomite;

indicating that ferroan dolomite precipitation took place under more "mildly alkaline" conditions. Dolomite replacement of silicate clasts (feldspar, lithic rock fragments etc.) contributes Si and Al to pore fluids.

Ferroan dolomite is seen to replace anhydrite in all specimens studied, and a gypsum  $\rightarrow$  anhydrite  $\rightarrow$  ferroan dolomite sequence of alteration is proposed.

Chlorite formation also occurs under conditions of low Eh and high pH, under conditions where ferric iron oxides are unstable. Thus iron and magnesium released by the alteration of haematite stained allogenic clays in an alkaline / reducing environment (together with any iron and magnesium released from the continued intrastratal replacement and dissolution of iron bearing silicates) are incorporated into chloritic clays. These clays are thought to have been formed at broadly the same time as, or slightly later than ferroan dolomite. Equation 3.1 illustrates the process of chlorite formation.



EQUATION 3.1

The development of chlorite appears directly responsible for the green colouration observed in the sediments of the facies types studied, and the particular "chlorite type" may vary in terms of Fe content both within and between individual wells. (see section 3.4)

In summary, diagenesis at intermediate burial depths is dominated by the formation of ferroan dolomite and "chloritisation", with associated loss of red sediment colouration. However, it should be noted that the formation of green "reduced" sediments is not evident in all facies. It is especially well developed in aeolian dune sands, less well developed in fluvial sandstones, and rarely developed within sabkha sequences. It is possible that variations in the degree of "chloritisation" observed between facies arise as a result of the initial porosity variations which exist between facies. Although sabkha facies sandstones contain abundant allogenic clays available for the process of chloritisation, their inherent low depositional porosity / permeability and abundant early cement prevents this occurring at intermediate burial depths. In fluvial sandstones the maintenance of some porosity at intermediate depths of burial, in spite of the development of early cements, allows the process of chloritisation to occur. In aeolian sandstones, much lower amounts of early cement and allogenic clay resulted in the preservation of porosity at both intermediate and deep burial depths, and an abundance of pore lining chlorite is seen.

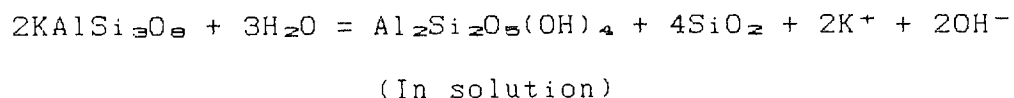
The remainder of the diagenetic processes (following chloritisation) which are invoked in the model are believed to have occurred during deep burial.

The formation of chlorite at intermediate burial

depths will have contributed  $H^+$  to pore waters (See equation 3.1), which drive pore solutions towards a more acid composition, and conditions favourable for:

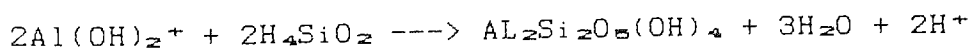
- (a) The dissolution of feldspar clasts and any labile rock fragments still present within sediments.
- (b) The removal of some carbonate cements to create secondary porosity.
- (c) The precipitation of kaolinite.

Grain dissolution involving feldspars may be thought of as being the direct cause of later kaolinite precipitation, i.e. alkali feldspar is unstable in the relatively acid conditions which follow chloritisation. A hydrolysis reaction using water as a weak acid is shown in equation 3.2.



EQUATION 3.2

Similarly we may consider an aluminium species derived from feldspar dissolution, and weak silicic acid.



EQUATION 3.3

The presence and type of aluminium species in solution is very dependent upon pH. Kaolinite is a characteristic mineral in near surface environments of "low pH", "high Eh", low alkali concentrations and intermediate  $H_4SiO_4$  activities (Hurst and Kunkle 1985). Kaolinite is also common within reducing environments,

especially where  $H_4SiO_4$  activities suitable for its stability have been maintained, and where aqueous iron has not concentrated in porewaters. Very generally, the activity of aluminium in porewaters increases with decreasing pH. (See Figure 3.8.8)

It should be noted that in the hydrolysis reaction (Equation 3.2), while the dissolution of feldspar occurs under relatively acid conditions, the reaction products are such that they drive pore waters towards a slightly more alkaline pH, under which the actual precipitation of kaolinite takes place.

Equation 3.3 describes a situation which is probably more analagous to what actually occurs at depth (pore fluids of "pure  $H_2O$ " would be very unlikely!) and it is important that reaction products in this case drive pore solutions towards a more acidic composition. Thus in order to increase the pH of the pore fluids enough to allow kaolinite to actually precipitate, some type of "neutralising" reaction is necessary, possibly involving acid pore fluids and carbonate cements (*Curtis and Spears 1971*).

Finally the different conditions necessary for the formation of chlorite and kaolinite are such that they rule out the possibility of their coeval formation, i.e. chlorite forms under conditions of high pH and low Eh (strongly alkaline and reducing), whilst kaolinite formation is favoured under conditions of much lower pH. Feldspar dissolution, and kaolinite formation introduce  $K^+$  into pore fluids, and when the  $K^+/H^+$  ratio is at its

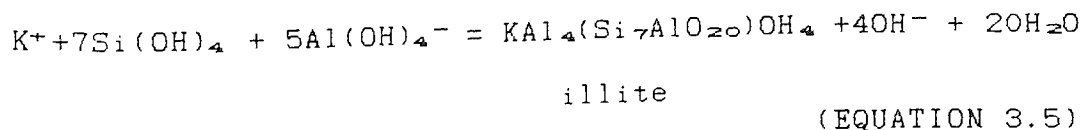
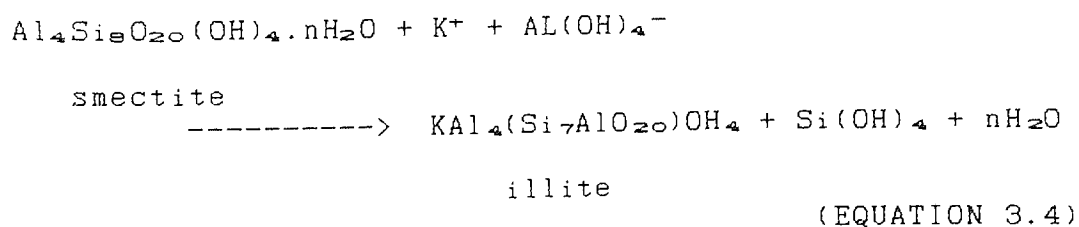


maximum illite is precipitated (Ali and Turner 1982). Illite formation in rotliegend sediments has been documented by Glennie et al (1978) and Rossel (1982) who recognise three mechanisms by which illite formation occurs:

- (i) The recrystallisation of allogenic components.
- (iii) The dissolution and alteration of framework grains.
- (iii) Kaolinite alteration under conditions of high {K+}.

Illite in the wells studied formed by recrystallisation of allogenic components, and precipitation from solutions enriched in K+ following intrastratal dissolution / replacement of framework clasts. No evidence to support the illitisation of kaolinite has been observed.

Equations describing these processes are as follows....



N.B. In Equations 3.4 and 3.5 (Macchi 1987) aluminium is represented as  $\text{Al}(\text{OH})_4^-$ . In equation 3.3, however, the aluminium species is  $\text{Al}(\text{OH})_2^+$ . This difference arises from the fact that aluminium is amphoteric and can

dissolve as both cations and anions depending upon pH. Illite formation is favoured by more alkaline porewaters than is kaolinite, and in Equation 3.5 aluminium species are interpreted as occurring as anions in mildly alkaline porewaters following neutralisation reactions.

In most wells studied, the final stage in the model proposed to explain the diagenetic sequence observed is commonly a late stage of silica precipitation. Late stage silica typically occurs as small euhedra some of which clearly enclose illite fibres and other earlier diagenetic components.

However, Hamilton Brothers wells 43/26-3 and 43/26-5 contain significant quantities of siderite which corrodes and replaces all earlier diagenetic phases. Siderite is absent or only poorly developed in other wells studied. Wells containing abundant siderite cement (43/26-3 and 43/26-5) are the best gas producing wells, and may also contain abundant ferroan dolomite which is often highly corroded and replaced by siderite. Wells 43/26-3 and 43/26-5 also contain significantly lower proportions of illite than other wells studied.

Siderite forms under a variety of pH conditions (most commonly under low pH) but only in pore waters of negative Eh, i.e. reducing environments. Figures 3.8.9 to 3.8.11 summarise conditions necessary for siderite formation. With these in mind it is significant to note that in all wells studied, the basic paragenetic sequence of events from deposition until the

precipitation of late quartz is fundamentally the same, with only minor differences in, for example, chlorite type, and ferroan dolomite, kaolinite and illite abundance.

The abundance of late siderite in good gas producing wells may be attributed to a phase of gas emplacement-related diagenesis, with siderite being precipitated from mobile acid pore waters which, because of their methane content, were of low Eh.

The presence of siderite replacing dolomitic cements would apparently indicate that siderite formed at the expense of at least some of the ferroan dolomite. If the ferroan dolomite acts as a source for some of the  $\text{CO}_3^{2-}$  and  $\text{Fe}^{2+}$  required for siderite formation, then  $\text{Ca}^{2+}$  and  $\text{Mg}^{+}$  from ferroan dolomite, coupled with  $\text{Si}^{+}$  and  $\text{Al}^{+}$  would be released as a result of siderite replacement of earlier mineral clasts and cements. If these ions are not involved in a late phase authigenic cement precipitation then they would be expected to be lost from the reservoir system during gas emplacement. This phenomenon may then be used to explain the presence of significantly lower Ca and Mg contents for "B" structure sandstones.

If siderite precipitation is facilitated by the introduction of low pH, low Eh pore waters into the reservoir during and prior to gas emplacement, then the abundance of sideritic cement in 43/26-3 and 43/26-5 might also be related to early emplacement of gas within these wells compared to other wells studied. This

possibility is supported by, and can explain the apparent lack of illite and abundance of kaolinite within wells 43/26-3 and 43/26-5. If the onset of gas "migration" occurs at or around chlorite precipitation stage in figures 3.8.1 to 3.8.3, then low pH/Eh Carboniferous derived porewaters might be used in the diagenetic model to explain the generation of secondary porosity in all wells studied (c.f. Schmidt et al 1977). However, if structural "seals" or "closures" existed for "B" structure sands at this time, then trapping of aggressive Carboniferous derived fluids would result in more extensive secondary enhancement of existing primary porosity for "B" structure sands. Under such conditions kaolinite would precipitate in abundance, but illite (the formation of which is favoured by higher pH and higher Eh conditions) would not precipitate (See Figures 3.8.12 to 3.8.14). Potassium not incorporated into authigenic phases within "B" structure wells would then effectively be lost from the reservoir system in porewaters expelled during the main phase of gas emplacement.

A similar diagenetic scheme has been described by Arthur et al (1986), who suggested that the occurrence of kaolinite in North Sea gas reservoirs may be controlled by the CO<sub>2</sub> content of fluids migrating from source rocks. Glennie et al (1978), also suggest that the loss of red colouration within North Sea Rotliegend sequences may be related to the production of CO<sub>2</sub> and acid formation

waters within underlying coal bearing strata.

### 3.9 CONCLUSIONS.

(i) Compositionally, sediments of the Leman Sandstone Formation consist of sublitharenites and orthoquartzitic sands.

The proposed diagenetic sequence for authigenic mineral phases present within these sediments is as follows:

EARLY SHALLOW BURIAL DEPTH - early quartz, early baryte, non ferroan dolomite, anhydrite.

INTERMEDIATE BURIAL DEPTH - ferroan dolomite, chlorite.

DEEP BURIAL - secondary porosity enhancement, kaolinite, late quartz, late siderite and baryte, illite.

(ii) Compositional variations exist both within individual facies traced across the North Ravenspurn anticline, and also between Leman Sandstone occurring upon U.K. block 43/26 and Leman Sandstone occurring on adjacent blocks.

Variations may be summarised thus:

"A" structure sandstones and sandstones from adjacent blocks are extremely illitised whereas "B" structure sandstones are not.

X-Ray analysis of the less than 2 micron "clay sized" sediment fractions within the Leman Sandstone indicate that chlorite mineralogy is variable. Wells 43/26-1, 43/26-2, 43/26-3, 43/26-5, and 47/5-1 contain

iron rich chlorites, but wells 43/26-4, 48/3-3 and 48/2-1 contain magnesium chlorites.

"B" structure wells contain significantly higher proportions of kaolinite and siderite than are found in "A" structure wells, and wells from outside UK Block 43/26.

(iii) Reservoir properties vary with facies. Aeolian dune sands form the best reservoir units, followed by fluvial and then sabkha sediments. Generally the sediments which displayed better depositional porosity / permeability characteristics form the best reservoir units.

(iv) Reservoir properties vary within individual facies across the North Ravenspurn Anticline. "B" structure reservoir units display better porosity / permeability characteristics than "A" structure reservoir units.

(v) Better reservoir quality within "B" structure sandstones arises because of more extensive secondary porosity development, and only minor development of illite within these sediments compared to "A" structure sandstones.

(vi) Comparison of data obtained during fluid inclusion studies and formation temperature time plots (CIGARS) indicate...

Dolomite and late quartz cements precipitated during the late Triassic (following the main phase of basin subsidence) under formation temperatures of

approximately 108°C.

Siderite cements formed during the middle - late Jurassic under formation temperatures of approximately 124.4°C.

(vii) K/Ar dating techniques indicate that illite precipitation within the Lemna Sandstone took place during the lower-middle Jurassic (approximately 173 my).

(viii) Geochemical modelling using X-Ray fluorescence spectroscopy reveals that "B" structure aeolian sandstones (main reservoir unit) contain significantly lower K, Ca, Mg, than "A" structure sandstones.

(ix) The differences observed in the geochemical composition of "A" and "B" structure sandstones may be readily explained using processes invoking earlier gas emplacement within "B" structure reservoir units, i.e. early trapping of aggressive Carboniferous derived fluids associated with the onset of gas emplacement results in:

(a) The development of larger volumes of secondary porosity within "B" structure sandstones than occurs in "A" structure sandstones.

(b) The establishment of porewater conditions within "B" structure sandstones, which were more suitable for precipitation of kaolinite than illite.

(c) Formation of siderite cements within the low Eh, low pH porewaters of "B" structure sandstones.

(d) Incipient illitisation within "B" structure sandstones due to the reservoir rapidly filling with gas.

(e) Within "B" structure wells, the  $K^+$  not incorporated into illitic clays was lost from the reservoir system (together with  $Mg^{2+}$  and  $Ca^{2+}$  released as a result of siderite replacement of dolomite) as gas emplacement forced porewaters out of the sediments.



## CHAPTER FOUR.

### THE STRATIGRAPHY AND SEDIMENTOLOGY OF THE PENRITH SANDSTONE.

#### 4.1 INTRODUCTION.

The Penrith Sandstone comprises a sequence of red Permian continental clastics which crop out in the Vale of Eden. The sequence rests unconformably upon reddened Carboniferous strata, and is overlain by an upper Permian "Zechstein" sequence consisting of continental clastics, evaporites and one intertidal / supratidal dolomite. The Penrith Sandstone contains sandy aeolian and fluvial deposits, together with coarse conglomerates and breccias. The main region of outcrop occurs on the western limb of the syncline between Kirkby Stephen and Armathwaite. The sequence may be up to 450m thick (Smith et al 1970).

The Permo - Triassic sequence within the Vale of Eden has been described previously by Versey (1939, 1960), Burgess (1965), Waugh (1970), Burgess and Wadge (1974), Burgess and Holliday (1979), and Macchi (1981). Permian sediments from the Vale of Eden are described in this thesis in order to outline the facies types which are present, and also in order to investigate the interaction between facies type, lithology and diagenesis.

#### 4.2 STRUCTURAL SETTING AND STRATIGRAPHY.

The Vale of Eden is a N.N.W. - S.S.E. trending basin bound to its northeast by the Pennine Fault and Alston Block, and to its southwest by the Lake District Massif. At its southern extremity the border is marked by the Dent Fault. In the north it opens into the Carlisle Plain which overlies the Carlisle basin. (See Figure 4.2.1 and 4.2.2).

The Permian basin was initiated following the Variscan earth movements that lead to uplift of the Lake District, and to folding and faulting along the Pennine line. At sometime during this period (late Carboniferous or early Permian) the Whin Sill was intruded into the sediments of the Alston Block to the east.

Compressional stresses associated with the Variscan resulted in strike-slip movement on the Pennine and Dent faults; subsequent east - west extension resulted in subsidence and basin formation in the Vale of Eden area (*Underhill et al 1988*). In general terms, the basin has the appearance of a half graben, with the thickest accumulation of sediment in the east, proximal to the footwall block. *Burgess and Holliday (1979)* suggest a down-throw of up to 500m in the vicinity of Roman Fell.

Following basin initiation, the western edge of the Alston Block formed an escarpment which remained an important palaeogeographical element from which coarse

detritus was derived throughout the Permian. The last earth movements to have effected the Vale of Eden are widely accepted as Tertiary in origin. Tertiary movements in the South of the Vale of Eden resulted in uplift and eastwards tilting of the Alston Block, and reactivation of older fault trends, typically in a down West direction, (Burgess and Holliday 1979). The stresses associated with these movements folded Permian strata within the Vale of Eden into an asymmetrical syncline parallel to the Pennine line. Effects these earth movements are observed in strata as young as Jurassic in the Carlisle Basin. Tertiary movements also resulted in uplift of the Lake District Dome. The Armathwaite Dyke, a tholeiitic intrusion extending for 80km across the northern Vale of Eden is also of Tertiary age. The Tertiary movements are analagous to the inversion of the Permian basins in the Southern North Sea; and Muirwood (1985) suggests that the Pennine boundary fault system may connect with the Dowsing and South Hewett fault systems of the Southern North Sea.

A summary of the Permo Triassic deposits present within the Vale of Eden is as follows:

The earliest Permian sediments include alluvial breccias (Brockrams) with aeolian and fluvial sands. (Penrith Series of Versey 1939, 1960).

Transgression of this continental sequence during the Zechstein lead to the deposition of a mudstone /

sandstone / evaporite sequence known as the Eden Shales. (Hilton Series of Versey 1960). Four evaporites are present within the Eden Shales (A B C and D beds), the lowest of which passes laterally into a sequence of fine sands, silts and muds known as the Hilton Plant Bed. The Hilton Plant Bed have been interpreted as fluvial sheetfloods deposited in a lake margin setting. Deposition of Lower and Upper Permian sequences was accompanied by the deposition of breccias at basin margins. The uppermost evaporite within the Eden Shales probably corresponds with the Upper Magnesian Limestone of Durham, and consists of tidal flat and algal mat dolomites (Burgess and Holliday 1979).

The base of the Triassic in the Vale of Eden is taken as occurring at the base of the St Bees Sandstone, (Arthurton and Wadge 1986). The St Bees Sandstone (Scythian) is the highest Triassic deposit occurring in the Vale of Eden. Further northwest, in the Carlisle Basin, the St Bees Sandstone is overlain by a further sequence of red continental sands, (the Kirklington Sandstone, of Anisian age) and red siltstones, mudstones and dolomitic limestones (the Stanwix Shales, Anisian - Norian). The Carlisle sedimentary basin fill also contains a dark shale / limestone sequence cropping out as an outlier to the West of Carlisle (See Figure 4.2.1), indicating that subsidence in the Carlisle area continued into the Jurassic.

#### 4.3 LITHOFACIES TYPES WITHIN THE PENRITH SANDSTONE AND ASSOCIATED SEDIMENTS.

Lower Permian strata in the Vale of Eden comprises a sequence of red quartzitic sandstones and limestone rich gravels.

The gravels include conglomerates and breccias, and are known locally as "Brockrams" and typically occur at the base of the Penrith Sandstone, or at basin margins. Two Brockram sequences are recognised (Burgess 1965): A lower "Penrith Brockram" which interfingers with the Penrith sandstones; and an upper "Stenkrith Brockram" which interfingers with Upper Permian Eden Shales. The Stenkrith Brockram is important because its development indicates that breccia deposition at basin margins took place throughout the Permian. Burgess (1965) states that in the south of the Eden Valley, the Stenkrith Brockram overlies strata of Verseys (1939) Hilton series (Eden Shales) in the region around Franks Bridge, Kirkby Stephen (Grid Ref. NY 775 090). However, to the South of Kirkby Stephen at Halfpenny House (Grid Ref. NY 769 671), the Stenkrith Brockram directly overlies the Penrith Brockram.

Four lithofacies types are recognised within the penrith sandstone and associated sediments. These are Aeolian sands, Fluvial sands, Conglomeratic Channel Fills, and Alluvial Fan Breccias.

(i) Aeolian facies are composed of fine - medium

grained, well sorted, well rounded sandstones. Cross stratification forms the main sedimentary structure in aeolian sands, and commonly occurs as large trough cross stratification sets, with less abundant planar cross stratification. Individual dune foresets are up to 50cm thick, and composed predominantly of grain flow laminations which may either coarsen or fine upwards. Individual cross sets of strata may be up to 8m thick.

There are also minimum interdune aeolian facies. Aeolian interdune sediments are composed of thinly laminated (cm scale) subcritically climbing translent strata, (wind ripple strata of Hunter 1977).

(ii) Fluvial Sand Facies comprise dark red / brown, fine to medium grained and poorly sorted sandstones. They are characterised by intraformational clay chips and scattered granules with much reworked aeolian sand. Internally they may show trough cross stratification, plane bedding, or may lack internal structure. Individual units fine upward, and may contain granule sized clasts at their bases. Thin red mudstone horizons (cm scale) may be present within fluvial sequences. Large quantities of highly rounded clasts, and a bimodal texture within fluvial sand indicates a reworked aeolian component.

(iii) Conglomeratic Channel Fill Facies occur interbedded with fluvial sands. They consist of poorly sorted pebble - boulder sized clasts set in a matrix of

poorly sorted, red, sand-grade detritus. Conglomerates may be composed of stacked fining upward sequences, or may lack internal structure. Conglomeratic units display clearly erosive bases.

(iv) Alluvial Fan Breccia Facies occur as laterally continuous "sheet-like" deposits bound by erosional bedding surfaces which occur on a 50cm - 3m spacing. Rarely, higher angled erosive bedding contacts define "channel-like" deposits which truncate sheetlike bedding planes.

Alluvial fan breccias are well cemented (calcite), clast-supported, and composed of poorly sorted, angular - rounded, limestone, chert and sandstone fragments. Individual units fine upward, and often display internal trough cross stratification, (festoon shaped scour and fills are common).

#### 4.4 LOCATION AND NATURE OF OUTCROPS STUDIED.

For the purpose of this study, outcrops of Penrith Sandstone and associated sediments are divided into two categories:

(i) Aeolian Penrith Sandstone cropping out in the region to the North of Penrith.

(ii) Mixed fluvial and aeolian sequences cropping out in the region between Appleby and Kirkby Stephen.

These categories allow the comparative study of silicified aeolian strata with un-silicified interbedded aeolian and fluvial strata. They enable an assesment of

the interaction between depositional environment and early diagenesis.

#### 4.4.1 AEOLIAN PENRITH SANDSTONE CROPPING OUT IN THE REGION NORTH OF PENRITH.

Aeolian sandstone sequences were studied at Cowraik Quarry, Stoneraise Quarry, and Lazonby Fell.

At Cowraik Quarry (Grid Ref. NY 542 310) to the northeast of Penrith, the Penrith Sandstone consists of red / brown, medium - coarse grained, well sorted sand which is exclusively aeolian in character. Exposures display large scale cross stratification, with individual sets occurring on a scale of 1m - 8m. Cross stratification defines broad shallow troughs, with minor "wedge-like" units being produced by the stacking / overlapping of coalescing troughs, indicating deposition by "barchanoid" or sinuous crested transverse bedforms. Foresets are dominated by grain flow laminae, and indicate deposition within a wind system blowing from the southeast.

The exposures at Cowraik may be divided into a series of lower and upper quarry workings. The lower workings comprise three faces excavated in unsilicified aeolian dune facies sandstone (see Plate 4.1). However, the most easterly of the lower workings displays a metre of red, flat bedded, medium - fine grained sands with a bimodal size distribution and wind rippled texture (subcritically climbing translantent strata of Hunter



1977, and Fryberger et al 1977). These sands are interpreted as representing interdune deposits, and are separated from overlying aeolian dune deposits by a flat erosive bounding surface (first order). The quarry workings at this location also display north - south trending veins and joints, bound on either side by a zone of yellow highly silicified sandstone up to 15cm wide.

The upper quarry workings comprise two main faces, both of which are excavated in silicified Penrith Sandstone and exhibit large scale trough cross stratification. Detrital quartz clasts display sharply defined crystalline faces, indicating that silica cement occurs in the form of well developed authigenic overgrowths. In particular, the western face of the upper quarry workings displays excellent examples of "wedge-like" fabrics produced by lateral pinchout of trough cross stratification sets. One unit at this location clearly shows foresets which become convex upward when traced up dip (see Plate 4.2). This unit appears to have a "dome" shaped cross section, the flanks of which are dominated by grainflow laminae which rapidly wedge out into further grainflow deposits when traced laterally. This unusual unit overlies a flat essentially planar bedding surface (first order?), which separates it from the steeply inclined foresets (composed of grainfall strata) of an underlying aeolian set. Collinson and Thompson (1982) describe convex upward cross stratification as occurring as a result of differing

rates of grainfall on different parts of a lee slope in barchanoid and dome shaped dunes. In addition to this, the diagrams presented by Mc Kee (1966) indicate that convex upward bedding fabrics occur in a variety of dune types, though typically towards the crests of aeolian bedforms. The unit displaying convex upward foresets at Cowraik Quarry is interpreted as representing a section through a "horn-like" projection which extends in a downwind direction, and occurs between the crescentic slip faces of sinous crested transverse bedforms.

Stoneraise Quarry (Grid Ref. NY 533 352) to the north of Penrith provides excellent three dimensional exposure of silicified Penrith Sandstone. The quarry comprises a single pit, the main face of which extends for some 50m and is typically 10m high, and provides a section through a single aeolian cross stratification set. Foresets within this set are curved, approximately parallel, and stacked to display a trough shaped cross section (See Plate 4.3). Foresets are concave upward, and their dip direction varies from  $290^{\circ}$  to  $350^{\circ}$ , defining a "scoop - like" form. Foresets are inclined at angles of up to  $28^{\circ}$ , and dip in the axis of the "scoop-like" trough is toward  $318^{\circ}$ .

The cross stratification set which dominates exposure at Stoneraise Quarry displays the "scoop-like", concave upward morphology of a "crescentic slipface" found upon barchan or transverse barchanoid dunes. (c.f. Macchi and Waugh 1984). Minor features present within

this cross stratification set include wind ripples, which are exposed upon the surfaces of some foresets and were formed by winds which blew across the slip face of the dune.

The cross stratification set which dominates exposure in Stoneraise quarry overlies a convex upward bounding surface separating it from a poorly exposed lower unit of cross stratified sand.

At Lazonby Fell (Grid Ref. NY 517 384) to the North of Penrith, the Penrith Sandstone is typically highly silicified, and forms a partially exposed "pavement" over much of the high ground. The region is one in which an abundance of small quarries provide exposures of well cemented, red - brown, medium - coarse grained, trough cross stratified sandstone. The sands contain abundant grainflow lamination, and foresets occur on spacings of up to 2.0m.

#### 4.4.2 MIXED FLUVIAL AND AEOLIAN SEQUENCES CROPPING OUT IN THE REGION BETWEEN APPLEBY AND KIRKBY STEPHEN.

Mixed fluvial and aeolian sequences in the region between Appleby and Kirkby Stephen were studied at George Gill, River Belah Bridge and Scar, Hilton Beck, Burrels Quarry, and Stenkrith Beck.

At George Gill (Grid Ref. NY 718 189), a series of small rock faces form the sides of a glacial valley and provide exposure of both silicified aeolian sands, and

non-silicified fluvial sands interbedded with conglomeratic breccias.

Silicified aeolian sands crop out in crags to the north and south of George Gill at Grid Ref. NY 719 188. Exposures on the northern side of the valley at this location consist of approximately 5m of red, medium - coarse grained, cross stratified aeolian sands. Individual sets of strata may be up to 3m thick, and are separated by distinctly curved (concave upward) non-parallel bounding surfaces. The angle of foreset lamination increases upward within individual sets, and foresets flatten out down dip to form "toesets". Aeolian sands are dominated by grainflow laminae composed of rounded, coarse - medium grained, spherical clasts. Grainflow laminae may exhibit inverse or normal grading.

Thin wind rippled dune base / interdune deposits also occur at the base of this exposure, and are overlain by a set of grainflow dominated strata of the type described above. An aeolian deflation lag (1cm - 2cm thick) containing tiny dreikanter (up to 8mm) occurs at the base of the wind rippled unit. Dreikanter rest directly upon an erosional bounding surface which truncates foreset lamination within the underlying set. Abundant North - South trending silica cemented fractures are present in this exposure.

Exposure on the southern side of George Gill (Grid Ref. NY 719 188) consists of 10m of moderately silicified cross stratified aeolian sand. Cross sets are separated by curved (concave upward), non-parallel erosional

bounding surfaces (see Plate 4.4). Strata are dominated by grainflow deposits, and foresets represent aeolian slipfaces deposited within an easterly prevailing wind. Macchi and Waugh (1984) describe set bounding surfaces as representing the eroded stoss slopes of underlying dunes, indicating dunes to have a climbing morphology.

At Grid Ref. NY 718 187, 200m downstream from the above exposures, a sequence of red / brown sands and breccias crop out in the steep valley side. The Penrith Sandstone at this location is poorly cemented and contains abundant brown mudstone clasts. The sands are less well sorted than aeolian sediments to the north, and are interpreted as being fluvial in origin. The presence of highly rounded clasts within fluvial sands is indicative of their containing a reworked aeolian component. Small scale tabular cross stratification is present within fluvial sands, and sets of strata (up to 1m) contain planar foresets. Fluvial sands are separated from overlying aeolian strata by a grassy break in slope, which when traced laterally suggests the presence of a flat tabular base (first order bounding surface) to the aeolian sand unit. The position of the break in slope suggests that the base of the aeolian sand body dips gently eastward, and when restored to the horizontal, Macchi and Waugh's (1984) interpretation of a climbing morphology to aeolian bedforms is apparently still valid.

Two brockrams are present near the base of the

fluvial section in George Gill. The lower brockram (see Plate 4.5) is at least 3m thick, and is separated from an upper brockram by up to 2m of fluvial sand. The brockrams are clast supported, and composed of angular - subrounded clasts 0.5cm - 15cm in diameter. The upper brockram has an erosional base, and when traced eastward incises down through fluvial sands into the lower brockram.

The upper brockram at George Gill reportedly contains quartz dolerite clasts of "Whin Sill type" (Dunham 1932), and is of stratigraphical importance. Brockrams at George Gill represent conglomeratic channel fills. A simple stratigraphic section for George Gill is shown in figure 4.4.1

The Penrith Sandstone exposed in sections at River Belah Bridge (Grid Ref. NY 7945 1205) and River Belah Scar (Grid Ref. NY 7936 1210) consists of soft, red, predominantly fluvial sand interbedded with conglomerate.

Fluvial sands are medium - coarse grained, poorly sorted, contain abundant intraformational clay flakes, and may fine upward from a thin granular base. Poor sorting, an abundance of highly spherical clasts and a bimodal texture is indicative of reworking of aeolian sand.

Fluvial sands display low angle trough cross amination - planar lamination (mm - cm scale), or may lack internal structure. Individual beds are bound by slightly erosional bedding surfaces, and may be capped by

thin red / brown mudstones. Trough cross stratification is only poorly developed within fluvial sands at River Belah Scar, but is visible in one fluvial sand wedge between two conglomerate horizons in the upper portion of a face in the center of the exposure (i.e the sand above the conglomerate in Plate 4.6).

Conglomerates exposed in the River Belah sections are up to 2.5m thick, and consist of poorly sorted dolomitised limestone clasts set in a fine grained sandy matrix. Conglomerates have highly erosive bases, and are often steeply incised into underlying fluvial sands, (see Plate 4.6). Conglomerates may wedge out laterally. Internally, conglomerates may consist of stacked sequences of horizontally stratified fining upward units, or may lack internal structure. Parallel alignment of some clasts is evident, and *Macchi and Waugh* (1984) have reported imbrication indicating flow towards the southwest.

The steep, often highly erosive lower bounding surfaces of conglomerates suggest that they represent coarse grained channel fills, and a fluvial wadi setting has been proposed (*Macchi* 1981). Structureless fluvial sands may be indicative of rapid deposition from ephemeral floodwaters with subsequent loss of any internal structure; or may indicate deposition within a fluvial regime where energy was too high to allow the development of tractional bedforms. *Macchi and Waugh* (1984) have suggested that a change in clast orientation from horizontal at the base of units to sub-vertical

near the top of units may be produced by syndepositional de-watering.

Aeolian sands are recognised at only one location, some 20m north of River Belah Bridge, where 2m of cross stratified aeolian sandstone overly 2m of fluvial sand and conglomerate. Aeolian sands are red, poorly cemented, and composed of highly rounded clasts displaying a distinctly bimodal texture. The angle of aeolian foresets increases upward from near horizontal to angles of  $25^{\circ}$  within the single set of strata exposed, and the downwind shingling of duneforms by the processes of incision and overlap is evident. The asymptotic bases of aeolian foresets overly a thin (10cm) fine grained Brockram which contains reworked dreikanter, and overlies 80cm of plane bedded fluvial sand. The base of the sequence at this location consists of a metre of conglomerate. Aeolian foresets indicate deposition from an easterly wind.

A thick sequence of strata similar to that exposed in the River Belah crops out in Hilton Beck (Grid Ref. NY 7151 2037 - NY 7195 2055). Here foresets within soft aeolian sands consistently show deposition from an easterly wind. Fluvial strata dominate sections at Hilton Beck, and consist of thick units of soft, red, medium sand with scattered pebbles and chocolate coloured mud clasts. Individual beds are up to 3m thick and display little internal structure. Silicified joints are common, and are bound by bright yellow silicified zones



up to 20cm wide. Thin discontinuous brockrams occur as "channel-like" conglomerates as described at River Belah.

At Burrells Quarry Grid Ref. NY 677 180, to the south of Appleby, the lower of the Permian brockrams (The Penrith Brockram) described by Burgess (1965) is exposed. Brockrams at this location are fundamentally different to those exposed at River Belah, George Gill and Hilton Beck. They are clast supported breccias composed predominantly of angular - sub rounded calcitic limestone clasts, and are tightly cemented by calcite. They do not occur associated with red fluvial and aeolian sands.

Breccias are poorly sorted, up to 80cm thick, and typically fine upward from cobble grade material to granule grade material (or less commonly sand). (see Plate 4.7). They display a wide variety of internal structure.

Individual beds display a "sheet-like" morphology, and are bound by erosional bedding surfaces (see Plate 4.7). Internally beds display parallel lamination, low angle cross stratification, or distinct trough cross stratification with "festoon-like" scour and fill. Trough sets indicate flow to the northeast.

The strata at Burrells Quarry are interpreted as a sequence of alluvial fan breccias. They are clearly the product of episodic waning flows, and the braided distributory sheetflood mechanism of Bull (1977) appears their most likely mode of deposition. Highly rounded spherical, sand-grade clasts within alluvial fan breccias

suggests they contain reworked windblown detritus.

Stenkrith Beck (Grid Ref. NY 7730 0735) is the type locality for the Stenkrith Brockram, the highest of the Permian brockrams. The Stenkrith Brockram wedges out northwest into the Eden Shales and Belah Dolomite, and is overlain by the St Bees Sandstone. The Stenkrith Brockram occurs at a stratigraphically higher position than the Penrith Sandstone, and is important because its presence implies that considerable relief was maintained at basin margins throughout the Upper Permian, allowing continued deposition of coarse detritus within alluvial fan settings.

At Stenkrith Beck, brockrams form a sequence of poorly sorted, clast supported, limestone-rich breccias (see Plate 4.8) which occur in "sheet-like" units bound by erosional bedding surfaces. Limestone clasts are angular - subrounded, fossiliferous and calcitic. Individual units fine upward from coarse pebble grade material to gravel, and are up to 50cm thick. The sequence is tightly cemented by calcite.

Internally, brockrams display plane bedding, low angle and trough cross stratification. They appear to have been deposited under similar conditions to the alluvial fan breccias at Burrells Quarry. Cross stratification and pebble imbrication indicate northward transport.

#### 4.5 SEDIMENTOLOGICAL MODEL.

The well established model explaining facies variations within the Lower Permian strata of the Vale of Eden is one in which aeolian sands, fluvial sands (and associated conglomerates) and alluvial fan breccias were deposited in an arid basin setting (Waugh 1970). The aeolian Penrith Sandstones are interpreted as the "distal" equivalent of marginal alluvial facies (Macchi 1981, Steele 1981).

Alluvial strata (e.g. the Penrith Brockram) accumulated as fans of coarse grained detritus at basin margin locations, with the dominant depositional mechanism being that of "braided distributory sheetfloods" as described by Bull (1972, 1977).

Interbedded fluvial sand and conglomerate seen at River Belah, Hilton Beck and George Gill indicate deposition within a system of shallow fluvial channels. Macchi (1981) suggests flash floods flowing off the Pennine margin reworked windblown sand and deposited it within wide, shallow ephemeral channels (wadi's) similar to those found in lowland areas of modern day semi-arid regions. Conglomeratic brockrams are interpreted as channel base deposits within a northwesterly flowing ephemeral fluvial system (Macchi 1981), in which the main type of detritus is reworked aeolian sand. The predominance of low angle - plane laminated, or structureless sand is indicative of deposition within

upper flow regimes. The presence of curled clay flakes within fluvial sands indicates that ephemeral flows reworked earlier fluvial deposits. Curled clay flakes represent desiccated mudstone horizons formed by low stage deposition of fines. To the northwest, away from basin margins, alluvial fan breccias and fluvial strata give way to predominantly aeolian sediments.

Aeolian Penrith Sandstone is dominated by simple large scale trough cross stratification sets, with unimodal dip directions. Waugh (1970) interpreted the aeolian sands as representing a system of barchan dunes deposited within an easterly prevailing wind. However, barchan dunes form on hard desert surfaces with sparse supplies of sand (Cooke and Warren 1973, Glennie 1987), and the migration of sinuous crested transverse bedforms (as suggested by Steele 1983) is more likely to explain bedding characteristics observed within the Penrith Sandstone which developed within a "sand sea". Mader and Yardley (1984) also suggest that the predominance of trough and tabular planar cross sets documents simple migration of sinuous crested and/or straight crested transverse dunes.

Interdune deposits are generally not well developed in exposures studied, and are represented only by first order diastems. Mader and Yardley (1984) however, report that thicker more abundant sheet-sands occur in the lower portion of the Penrith Sandstone, and suggest that their rarity in higher parts of the sequence may reflect the transition from a marginal to a more

central erg facies (c.f. Kocurek 1981, Clemmensen and Abrahamsen 1983).

The interaction between fluvial and aeolian environments is clearly exhibited in basin margin facies, where fluvial systems reworked aeolian sand. Macchi (1981) suggests that fluvial events within the Penrith Sandstone increased in frequency with time, until an ephemeral system was established which dissected the aeolian complex, eventually burying it.

The main contrasts between the Penrith Sandstone and other Lower Permian strata studied may be summarised as follows:

Facies types present within the Penrith Sandstone Formation differ from those of the Leman Sandstone Formation of the North Ravenspurtn region (Chapters Two and Three) in that:

(a) Sabkha facies sediments have not been observed within the Penrith Sandstone.

(b) The development of alluvial fan breccias is much more important within the Penrith Sandstone than in the Leman Sandstone.

(c) Fluvial sandstones within the Penrith Sandstone are generally thicker than those observed in the Leman Sandstone of North Ravenspurtn, and appear to represent ephemeral channel fills rather than sheetfloods.

Rotliegend strata within the Vale Of Eden are very similar to Rotliegend strata in the Worcester Basin (see Chapters Six and Seven), and similar basin origins are

proposed. In the Worcester basin however, fluvial sediments are rare, and when present appear to represent sheetloods rather than channel fill sands. Also, alluvial fans bordering the Worcester Basin are dominated by clastic and volcanic detritus, rather than carbonate clasts.

#### 4.6 CONCLUSIONS.

(i) The Penrith Sandstone formation consists of aeolian sands, fluvial sands and conglomerates, and alluvial fan breccias.

(ii) Aeolian sediments consist of aeolian dune sands composed of grainfall and grainflow strata, with minor interdune facies composed of subcritically climbing "wind rippled" strata. Aeolian dunes are interpreted as sinuous crested transverse bedforms deposited within an easterly prevailing wind system. Aeolian sands are frequently highly silicified.

(iii) Fluvial strata consist of fluvial channel sands (apparently containing a reworked aeolian component) and coarse channel fill conglomerates.

(iv) Alluvial strata consist of coarse carbonate rich breccias deposited by braided distributory sheetfloods at basin margins.

## CHAPTER FIVE

### 5 THE PETROLOGY AND DIAGENESIS OF THE PENRITH SANDSTONE AND ASSOCIATED SEDIMENTS.

#### 5.1 THE PETROLOGY OF AEOLIAN AND FLUVIAL SANDS.

Using the sedimentological model presented in chapter four, variations in the petrology and diagenesis of different sedimentary facies have been studied, and are modelled in the following chapter.

##### 5.1.1 DETRITAL MINERALOGY.

###### 5.1.1.1 Quartz.

The Penrith sandstone is composed predominantly of subrounded - well rounded clasts of quartz (49% - 72% on average). Quartz clasts with simple non-undulatory extinction are the dominant quartz clast type and commonly form 52% - 91% of the total quartz. Polycrystalline quartz grains having more than three crystal units per grain form 7% - 32% of quartz present, whilst undulatory quartz and quartz grains composed of 2 or 3 crystal units per grain are both present in quantities less than 10%.

The inferred quartz source area using the four variable quartz diagrams of *Basu et al* (1975) is one of middle - high rank metamorphic rocks.

Polycrystalline quartz grains may show recrystallised metamorphic textures, or "sutured" and

"graphic" boundaries between constituent crystal units. Detrital quartz clasts may contain abundant rutile needles, mica, or green chloritic inclusions.

#### 5.1.1.2 Feldspar.

Feldspar is common within the Penrith Sandstone, and occurs as alkali feldspar clasts constituting 1% to 7.5% of total rock constituents. Plagioclase feldspars are very rare within the Penrith Sandstone.

#### 5.1.1.3 Lithic Rock Fragments.

Lithic rock fragments within the Penrith Sandstone include:

##### (a) Sedimentary Rock Fragments.

Sedimentary rock fragments are the most common lithic clasts within the Penrith Sandstone. They typically occur as fine grained quartzitic sandstone clasts, often with abundant iron oxide cements. Fine grained siltstone / shale clasts are common within fluvial sandstones, as are small detrital micas. Sandstone clasts typically exhibit well developed quartz cements, and minor intraclastic porosity.

Chert clasts are common in fluvial and aeolian sandstones, and evidence points to their having a sedimentary origin, i.e. spicules and chalcedonised coral fragments. Chert clasts form less than 1% of the total rock volume, and in some specimens are the most common lithic fragments after sandstone clasts.



(b) Metamorphic Rock Fragments.

Metamorphic rock fragments are rare within the Penrith Sandstone. When present they appear to be the low grade metamorphic equivalent of the sandstone clasts described above. They also occur as totally recrystallised clasts composed predominantly of parallel aligned, equigranular, elongate quartz crystals with mica present along schistose lamination.

(c) Igneous Rock Fragments.

Both acid (rhyolitic) and basic lithologies are present.

Rhyolitic fragments are leucocratic and consist of fine grained quartz and feldspar intergrowths. Spherulitic textures are common.

Basic rock fragments are fine grained, dark coloured and rich in opaque minerals. They display very little determinable mineralogy apart from quartz and feldspar.

"Granitic" rock fragments may also be present, and are composed of quartz and feldspar (sometimes displaying graphic intergrowth) with minor amounts of mica.

5.1.1.4 Allogenic Clay.

Allogenic clays within the Penrith Sandstone form pellicular coatings or "meniscus" bridges between clasts (visible using S.E.M.). They are most abundant, and best developed within fluvial sands and unsilicified

aeolian sands. Allogenic clays are composed of poorly crystalline illite / smectite.

The remaining detrital clastic constituents within the Penrith Sandstone may include mica clasts (in fluvial lithologies), heavy minerals (Zircon and tourmaline) and detrital opaques.

### 5.1.2 AUTHIGENIC MINERALOGY - AEOLIAN AND FLUVIAL SANDS.

#### 5.1.2.1 Quartz.

Authigenic quartz is common within certain aeolian sands (see Plate 5.1), but its development is by no means widespread throughout the Penrith Sandstone. *Burgess and Holliday* (1979), and *Waugh* (1970) indicate that silicified sands occur towards the top of the aeolian sequence, away from basin margins.

Where developed, authigenic silica typically forms optically continuous overgrowths upon detrital quartz grains. Detailed descriptions of quartz overgrowths have been given by *Waugh* (1970), who recognised three distinct types of overgrowth:

(a) Simple overgrowths consisting of single crystal units upon unstrained quartz clasts.

(b) Overgrowths having undulatory extinction, and occurring upon strained quartz clasts which exhibit undulatory extinction.

(c) Polycrystalline overgrowths, occurring upon polycrystalline quartz clasts. In this case each crystal unit within the overgrowth is in optical continuity with

its host unit within the detrital clast.

Quartz overgrowths are rare within sands containing calcite cements. Where observed, they are only very poorly developed and are typically enclosed within areas of poikilotopic calcite.

Late stage silica cements are frequently observed in sediments immediately adjacent to fracture systems within both silicified and non-silicified sandstones. This indicates the formation of some silica cement is facilitated by the migration of silica bearing fluids through post depositional fracture systems.

#### 5.1.2.2 Authigenic Feldspar.

Authigenic alkali feldspar is common within both silicified and non-silicified aeolian and fluvial sands.

Authigenic alkali feldspar typically occurs as "sawtooth" overgrowths upon detrital clasts. Complete overgrowths are less common. Thick, well developed overgrowths are frequently observed, but rarely completely enclose detrital clasts. Authigenic feldspar overgrowths clearly pre-date authigenic quartz overgrowths, which sometimes partly enclose or envelop them. (See Plates 5.2 and 5.3).

#### 5.1.2.3 Illite / Smectite Clays.

Illitic / smectitic clays occur as grain coatings and pore linings best developed in non-silicified aeolian and fluvial sands. Pellicular coatings are thick and dark brown coloured in non-silicified aeolian and fluvial

sands, but "thinner" and pale yellow / brown in silicified lithologies.

Grain coating / pore lining authigenic clays consist of irregular platelettes orientated perpendicular to grain surfaces, and often display poorly developed boxwork textures. These clays in part represent recrystallised allogenic clays, as well as wholly authigenic clay.

Some yellow / brown (Fe stained) authigenic clays within silicified sandstones clearly postdate quartz overgrowths (See Plate 5.4), and are interpreted as forming relatively late during diagenesis.

#### 5.1.2.4 Dolomite.

Dolomitic "cements" have been observed only in silicified aeolian sandstones from Stoneraise Quarry (See Plate 5.5). Dolomite forms small cement rhombs (approx 0.03 mm) which are enclosed within authigenic quartz overgrowths, and which therefore pre-date silica authigenesis. Although dolomitic cements have only been observed within quartz overgrowths at Stoneraise Quarry, their widespread presence within aeolian sands is indicated by the presence of abundant rhombic dissolution voids within quartz overgrowths (see plate 5.6). These features have also been documented by Waugh (1970).

Dolomitic cements have not been observed within unsilicified Penrith Sandstones. Their presence within unsilicified sandstones cannot be inferred because of the lack of authigenic quartz cements, and hence of

diagnostic dolomoulds.

#### 5.1.2.5 Calcite.

Calcitic cements occur within unsilicified aeolian and fluvial sandstones. They have not been observed within silicified lithologies.

Calcitic cements occur as zoned rhombs (0.2 mm) which most commonly have a ferroan core and non-ferroan margin. Cement crystals frequently display irregular margins indicative of some calcite dissolution, and often occur in close association with one another, forming small, scattered nodules of calcite. Larger calcite crystals may exhibit poikilotopic textures (see Plate 5.7) and corrode silicate clasts, (especially clasts with poorly developed pellicular coatings).

#### 5.1.2.6 Kaolinite.

Kaolinite is common within silicified and unsilicified Penrith Sandstone.

In unsilicified sands kaolinite is sometimes present as flakes enclosed within poikilotopic calcitic cement, (see Plate 5.8), and also as kaolinitic porefills which apparently postdate calcitic cements and porosity enhancement. In silicified aeolian sandstones kaolinitic clays form coarse grained porefills. Kaolinite pseudomorphs (presumably after feldspar) are present within both silicified and unsilicified sands.

#### 5.1.2.7 Gypsum / anhydrite.

Gypsum and anhydrite cements have not been

observed in surface samples collected from the Penrith Sandstone. However, Burgess and Holliday (1974) document pervasive gypsum - anhydrite cement within the Penrith Sandstone of the Hilton Borehole. Waugh (1970) also reports gypsum to be present within borehole cores, stating that it occurs as single euhedral crystals filling pores or enclosing clasts. Waugh interprets the source of calcium and sulphate for gypsum formation as originating in the evaporite deposits of the overlying Eden shales.

### 5.1.3 QUANTITATIVE MINERALOGY - AEOLIAN AND FLUVIAL SANDS.

Quantitative analysis of aeolian and fluvial sands was achieved by simple point counts. Point counts of 250 points per thin section were carried out on sandstone specimens. Compositional data obtained was used in order to produce ternary compositional plots (Pettijon 1973), and four variable quartz provenance diagrams which Basu et al (1975) suggest are indicative of the rock types present within quartz source areas. See Figures 5.1.1 and 5.1.2.

In addition to compositional data gathering, point counting was used to provide an indication of sediment size and sorting. This was achieved by measuring the apparent long axis of every fifth grain encountered during the point count. Data obtained by point counting is summarised in figures 5.1.3 - 5.1.4.

Figure 5.1.3 illustrates that the Penrith

sandstone consists predominantly of moderately sorted sands, with moderate - close packing. No difference is observed between the packing of silicified and unsilicified sands, a factor which suggests that cementation took place following compaction within the Penrith Sandstone. This agrees with observations of Steele (1983), who suggested 20% compaction within aeolian sandstones prior to quartz cementation. Figure 5.1.4 also indicates that authigenic silica is poorly developed in sands containing minor amounts of carbonate cement.

Whole rock geochemical analysis of the Penrith sandstone was carried out using X-ray fluorescence spectroscopy. Results of geochemical analysis obtained are presented in table 5.1.1, and are discussed in Chapter Ten of this thesis.

#### 5.1.4 SEMI QUANTITATIVE X - RAY DIFFRACTION ANALYSIS OF THE "CLAY" SIZED SEDIMENT FRACTION WITHIN THE PENRITH SANDSTONE.

X-Ray diffraction analysis of eight sandstone specimens were carried out in order to establish the composition of the clay size fraction present within the Penrith Sandstone.

Samples were prepared and run using techniques outlined in section 3.4, and the relative percentages of clay minerals present were established using simple calculations outlined in Carver (1974). The results of

semi-quantitative clay analysis are presented in table 5.1.2.

Clay minerals are abundant in all non-silicified samples studied from the River Belah section, but are considerably less abundant in silicified aeolian sands from Cowraik Quarry and George Gill. Clay mineral samples from the Penrith Sandstone are summarised in table 5.1.3.

Analysis of X-Ray diffractograms indicate that illitic and smectitic clays dominate the clay mineral assemblage. The movement of illite (001) and (003) reflections in opposite directions upon glycolation is indicative of the intrastratification of illitic and smectitic minerals. The presence of a reflection between 10A and 17A in traces obtained from glycolated samples indicates that the interstratification is ordered to some degree (Shrodon 1980).

Tables have been produced by Reynolds (1984), which use the position of the 10A illite (001) reflection upon glycolation in order to estimate the composition of interlayered clays. Use of these tables suggests that an admixture with approximately 80% illitic and 20% smectitic layers is common within the clay fraction of the Penrith Sandstone.

The loss of a reflection at 7A upon heating samples to 550°C suggests that kaolinitic clays dominate over chloritic clays within the Penrith Sandstone.



5.2. THE PETROLOGY OF CONGLOMERATES AND BRECCIAS  
(BROCKRAM SEQUENCES).

Two types of Brockram exist: conglomeratic channel fills within mixed fluvial and aeolian sand sequences; and breccia deposits reflecting sheetflood processes occurring upon alluvial fans.

5.2.1 DETRITAL MINERALOGY - CONGLOMERATIC CHANNELS.

5.2.1.1 Quartz.

Detrital quartz is an important constituent within conglomeratic channel fills (up to 25% of the total clastic content within samples from River Belah sections, and up to 60% in samples from Hilton Beck).

Quartz clasts are well sorted and highly rounded, often displaying a distinctly bimodal size distribution; factors which indicate that much quartz represents reworked windblown sand (see Plate 5.13). Detrital quartz clasts are almost without exception free of quartz overgrowth.

5.2.1.2 Lithic rock fragments.

(a) Sedimentary rock fragments.

Carbonate clasts (Carboniferous limestone) form an important detrital constituent within conglomeratic channel fills.

Carbonate clasts form up to 80% of the total clast content within conglomerates at River Belah Bridge and River Belah Scar. Carbonate clasts at these locations are composed entirely of dolomitised limestone.

Dolomitisation of limestone clasts is interpreted as having occurred at sometime subsequent to their incorporation within channel fill conglomerates because they often occur as hollow "geode-like" structures which would not have survived fluvial transport.

Limestone clasts are also present within channel fill conglomerates at Hilton Beck. At this location clasts are composed both of recrystallised anhedral - euhedral calcite spar (non-ferroan), and also partially dolomitised limestone. No fossil allochems are present within these clasts, but quantities of clay, opaques, and fine grained microspar often define irregular forms which were originally skeletal grains. Chertified and partially chertified limestone clasts are also present.

Rock fragments composed of detrital silicate clasts occur as fine - medium grained sandstone clasts and shale fragments. Sandstone clasts are highly corroded, and display a high proportion of intraclastic porosity formed in particular by the removal of feldspar. Kaolinitic cements are common porefilling phases within areas of intraparticle porosity, and may form large pseudomorphs after whole clasts. Quartzitic sandstone clasts are an important constituent of Brockrams at Hilton Beck, where they form up to 34% of the total clast content.

Igneous rock fragments as described in section 5.1.1 may also be present in very minor quantities within conglomeratic channel fills, as may detrital

opaques.

#### 5.2.1.3 Feldspar

Detrital feldspars are rare within breccias forming conglomeratic channel fills. When present, they occur as alkali feldspar with no authigenic overgrowth.

#### 5.2.1.4 Allogenic clays.

Allogenic clays are common as poorly developed grain coatings within conglomeratic channel fills. They are also intimately associated with early calcite cements in Breccia samples from Hilton Beck. (See Section 5.2.3)

### 5.2.2. DETRITAL MINERALOGY - ALLUVIAL FAN BRECCIAS.

#### 5.2.2.1 Lithic rock fragments.

Carbonate clasts (Carboniferous limestone) are the most common detrital clast type present within alluvial fan breccias, forming up to 90% of the total clast content. Early dolomitisation of carbonate clasts is not observed (c.f. conglomeratic channel fills at River Belah).

Limestone clasts are typically packed biosparites, and allochems present include shell debris, crinoid ossicles, echinoid plates, corals and foraminifera. All allochems are recrystallised and composed of calcite spar or microspar. "Oyster - like" shell fragments and corals may be extensively chertified. Poorly washed biomicrite clasts containing peloids may also be present. Echinoid

plates up to 5mm across are common clastic constituents.

Quartzitic sandstone clasts may be present in small quantities (up to 6% of the total clast content) within the Brockrams at Stenkrith Beck and Burrells Quarry.

Igneous rock fragments as described in section 5.1.1 may also be present in very minor quantities within alluvial fan breccias.

#### 5.2.2.2 Quartz.

Detrital quartz occurs as well sorted, very well rounded clasts indicating a possible aeolian component within alluvial fan breccias. Quartz forms up to 41% of clastic constituents within alluvial fan breccias.

#### 5.2.2.3 Feldspar.

Detrital feldspar is not common within alluvial fan breccias.

#### 5.2.2.4 Allogenic clays.

Allogenic clays are common within alluvial fan breccias, where they form poorly developed early grain coatings.

### 5.2.3 AUTHIGENIC MINERALOGY - CONGLOMERATIC CHANNELS AND ALLUVIAL FAN BRECCIAS.

#### 5.2.3.1 Calcitic Cements.

Calcite cements are present in both conglomeratic channel fills and alluvial fan breccias.

Calcite most commonly occurs as zoned crystals

which coarsen away from pore margins and totally occlude porosity.

Cements at River Belah and Hilton Beck most commonly display zonation of crystals from ferroan cores to non-ferroan margins.

At Stenkrith Beck zoned cements most commonly have non-ferroan cores and ferroan margins, and show an overall trend from small non-ferroan calcite rhombs at pore margins to coarse porefilling ferroan calcite.

Calcite cements within Brockrams from Burrells Quarry may show either ferroan to non-ferroan, or non-ferroan to ferroan zonation, but most commonly occur either as blocky, entirely ferroan or non ferroan calcite crystals. Ferroan calcite cements are common in fine grained sediments adjacent to detrital iron oxide clasts, and commonly severely corrode silicate clasts. (See Plate 5.9)

Multiple zonation of larger calcite crystals occurs in all Brockrams, and up to five compositional zones have been observed in coarse cements. Zonation of calcite cement crystals is clearly indicated by cathodoluminescence techniques (See Plate 5.10). Iron oxides are also present within some of the largest porefilling calcite crystals, and typically occur as roughly euhedral rhombic zones "mimicking" crystal outlines, or as small scattered blebs (See Plate 5.11).

Calcite cements are interpreted as meteoric phreatic cement on the basis of criteria cited by Longman

(1980), i.e. the presence of abundant equant calcite crystals with interlocking textures which coarsen towards the center of pores; and post depositional syntaxial overgrowth of calcite on echinoderm fragments. Syntaxial overgrowths are of irregular thickness (they may thicken towards pore centers), and often clearly encompass well rounded detrital quartz clasts of aeolian origin (See Plate 5.12.). This evidence suggests that at least some of the calcite forming syntaxial overgrowths on echinoderm fragments was actually precipitated following their incorporation into Brockram sequences. *Evamy and Shearman* (1965) have described overgrowths upon echinoderm fragments, and suggest that they form most readily in freshwater diagenetic environments.

The ferroan nature of much sparite cement also supports the suggestion of *Evamy* (1969) and *Richter and Fuchtbauer* (1978), that many ferroan calcites precipitate within low Eh meteoric phreatic zones.

In addition to meteoric phreatic cement, channel fill conglomerates from Hilton Beck contain calcite cements which display textures indicative of precipitation within a freshwater vadose environment (see Plates 5.13 and 5.14).

Vadose zone cements are composed predominantly of non-ferroan calcite, and occur most commonly as fine grained equant crystals which irregularly or partially coat grains, and display pendant / pillar and meniscus textures. Their distribution within conglomeratic channel fills is patchy, reflecting the presence of both

air and water within pore spaces. These observations compare favourably with criteria cited by Longman (1980) for the recognition of vadose zone carbonate cements.

Vadose zone cements appear "dirty", and have quantities of clay associated with them. Their development occurred without significant occlusion of porosity. Early cements with textures indicative of precipitation within vadose environments do not appear to have been important within conglomeratic channel fills or alluvial fan breccias from other locations.

#### 5.2.3.2 Gypsum.

Gypsum cements were observed only within alluvial fan breccias from Stenkrith Beck, and occur as "lozenge" shaped crystals which clearly pre-date porefilling calcitic cements (see Plates 5.15 and 5.16) which enclose them.

Gypsum cement crystals are by no means common within the alluvial fan breccias from Stenkrith Beck, and many crystals show extensive dissolution to form areas of mouldic porosity bound within iron oxide / clay coatings. This apparently indicates that iron oxide precipitation postdates gypsum precipitation.

#### 5.2.3.3 Authigenic Clays.

Illitic / smectitic clays are present as poorly crystalline pore linings within the fine grained fraction of Brockrams at River Belah and Hilton Beck, and as alteration products associated with the replacement /

dissolution of detrital sandstone clasts.

Kaolinitic clays occur as pseudomorphs after sedimentary rock fragments, or as porefilling phases infilling large secondary pores within rock fragments.

### 5.3 DIAGENESIS.

#### 5.3.1 DIAGENESIS WITHIN BROCKRAM CHANNELS - RIVER BELAH AND HILTON BECK.

A paragenetic sequence established for authigenic mineral phases within the channel fill conglomerates of River Belah and Hilton Beck is shown in figure 5.3.1.

Early processes occurring within channel conglomerates at River Belah include the mechanical infiltration of allogenic clays, and dolomitisation of limestone clasts. Early dolomitisation of limestone clasts probably occurs due to the evaporative concentration of near surface groundwater shortly after sediment deposition. The early replacement / dissolution of labile silicate clasts within channel conglomerates was also initiated at this time.

Early pore occlusion within Brockram channels at Hilton Beck began with the infiltration of allogenic clays, and the precipitation of vadose zone carbonate cements within the relatively open framework of the conglomeratic channel fill. Dolomitisation of carbonate clasts does not appear to have been important at this location. Carbonate cements are recognised as having formed within the vadose zone on the basis of criteria



cited by Longman (1980), and are composed predominantly of non-ferroan calcite. Precipitation of meniscus calcite cement takes place from residual ephemeral waters within conglomeratic channel sediments in the shallow subsurface.

The precipitation of vadose zone cement was accompanied by the infiltration of allogenic clays, which were subsequently stained red by the precipitation of grain coating iron oxides in an alkaline oxidising environment. The margins of meniscus cements may have thin iron oxide coatings.

Dolomitisation of limestone clasts at River Belah, and precipitation of vadose zone carbonate cements within Brockram channel fills at Hilton Beck, is followed by the precipitation of phreatic calcite cement. These cements consist of interlocking equant calcite crystals which coarsen towards pore centers and occlude virtually all existing pore space. Individual cement crystals are commonly zoned, the typical sequence of zoning being one in which crystals exhibit ferroan calcite cores and non-ferroan calcite margins. Large cement crystals displaying multiple zonation indicate that calcite was precipitated from groundwaters of fluctuating iron content, or fluctuating Eh.

If calcite cements precipitated from groundwaters of fluctuating iron content, zonation may occur merely as a result of the depletion of the iron content of pore waters by its incorporation into the ferroan calcite

lattice. Hence the majority of zoned crystals observed show a simple transition from ferroan calcite cores to non-ferroan calcite margins. The multiple zonation of calcite cements could arise as a result of the continued replacement / dissolution of iron bearing rock fragments, thus increasing the iron content of pore waters and driving solutions back towards concentrations where iron is incorporated into the calcite lattice.

If zonation within phreatic calcite cements occurs as a result of fluctuating Eh within porewaters, then changes which take place might involve..... (i) The seasonal influx of high Eh, oxygenated meteoric groundwaters into a subsurface groundwater system of low Eh during periods of ephemeral rainfall; or (ii) the episodic uplift of sediments into zones of oxygenated groundwater conditions.

The presence of iron oxides (haematite) forming continuous "euhedral" zones in coarse porefilling calcite crystals (mainly non-ferroan), illustrates the episodic nature of calcite growth, with iron oxide precipitation alternating with the precipitation of calcite. The precipitation of phreatic calcite cements is accompanied by the dissolution / replacement of silicate clasts, a process which provides a source of iron for authigenic iron oxides. Some kaolinite pseudomorphs observed within these sediments may form at this stage.

The source of  $\text{CaCO}_3$  for calcite cement is assumed to be the abundant carbonate rocks within source areas, and early intrastratal solution of carbonate clasts.

5.3.2 DIAGENESIS WITHIN ALLUVIAL FAN BRECCIAS OF  
STENKRITH BECK AND BURRELS QUARRY.

A paragenetic sequence established for authigenic minerals within the Brockrams of Stenkrith Beck and Burrells Quarry is shown in figure 5.3.2.

Early processes occurring within alluvial fan breccias begin with the infiltration of allogenic clays at deposition, and precipitation of evaporite minerals (gypsum) from saline near surface waters.

Gypsum cements occur as early, partly pore occluding crystals which post-date allogenic clay coatings, but which are clearly earlier than calcitic cements which enclose and partially replace them (see Plates 5.15 and 5.16)

Early precipitation of gypsum within these Brockrams might be expected to increase the Mg / Ca ratio of near surface groundwaters, and cause dolomitisation of carbonate clasts. (c.f. River Belah Section). The fact that this does not occur is probably because calcitic carbonates form an extremely high proportion of the clast content within alluvial fan breccias. High calcitic clast content within breccias may mean that groundwaters flowing through them were always saturated with respect to calcium, and precipitation of minor amounts of gypsum had little effect upon Mg / Ca ratios. (c.f. River Belah sections where lithic clasts may form up to 30% of the total clastic constituents).

Unlike the Brockrams at Hilton Beck, the Stenkrith and Burrells Quarry brockrams show very little evidence of early vadose zone cementation. This difference appears to arise as a result of differing depositional characteristics between the above mentioned Brockrams. The Brockrams at Hilton Beck form as channel fill conglomerates within a fine grained fluvial sequence; while the coarse breccias at Stenkrith Beck and Burrells Quarry were deposited as sheetfloods upon an alluvial fan. The Stenkrith and Burrells quarry breccias are more poorly sorted than conglomeratic channel fills, which must have had a relatively open framework to facilitate the precipitation of carbonate cements with pendant / meniscus textures. It is proposed that the lack of an open structure within alluvial fan breccias deposited by sheetfloods accounts for poor development of cement structures which may be attributed to vadose zone cementation.

Rare cements which may be attributed to vadose zone cementation are observed only in coarse grained breccia samples at Stenkrith, and appear to occur within areas that must originally have formed large primary pores.

The infiltration of early allogenic clays, and the precipitation of early evaporite minerals is followed by the precipitation of authigenic clays (illite / smectite), and the precipitation of zoned porefilling calcite cements. Calcitic cements are typically zoned.

with non-ferroan calcite cores, and ferroan calcite margins. Calcite cements replace silicate clasts, and the presence of iron oxides forming continuous "zones" within larger crystals suggests that calcite precipitation was broadly contemporaneous with the formation of authigenic iron oxides. Some calcite cements precipitated at this stage during diagenesis occur as syntaxial overgrowths on echinoderm fragments.

### 5.3.3 DIAGENESIS WITHIN THE PENRITH SANDSTONE (S.S.)

Paragenetic sequences for authigenic phases within both silicified aeolian sandstone sequences, and non-silicified aeolian and fluvial sandstone sequences are shown in figures 5.3.3 and 5.3.4.

Early processes which occur within both fluvial and aeolian sandstones begin with the mechanical infiltration of allogenic clay, and the onset of early, near surface dissolution of labile silicate clasts (c.f. Walker 1978). Iron released as a result of early clast dissolution is incorporated into iron oxide stained pellicular coatings.

In the silicified aeolian sands of Lazonby Fell, Stoneraise, George Gill, and Cowraik Quarry, these early processes are accompanied by the precipitation of dolomitic cements. Dolomite cements occur as tiny, discrete rhombs which are now most frequently represented as dolomoulds (See Plate 5.6) within later silica cement, (also documented by Waugh 1970).

Dolomitic cements have not been observed within unsilicified aeolian and fluvial sands. However, since the principle evidence for their existence at silicified localities is the presence of dolomoulds within silica cements, their presence within unsilicified sands cannot be ruled out.

The source of calcium and magnesium for early dolomite cement might be related to the basinward migration of  $\text{CaCO}_3$  rich brines from marginal alluvial fan settings. Dolomitic carbonates might be favoured as a result of evaporative concentration of brines, possibly aided by the precipitation of early gypsum.

Continued intrastratal dissolution of labile silicate clasts with early burial results in the continued precipitation of iron oxides, and the formation of illite / smectite authigenic clays as early grain coatings / pore linings within fluvial and aeolian sandstones.

Clay authigenesis is followed by the precipitation of authigenic feldspar as syntaxial overgrowths upon alkali feldspar clasts. Illitic clays are interpreted as having been precipitated under conditions of highest  $\text{K}^+ / \text{H}^+$  ratios within porewaters following the intrastratal solution of detrital silicates. Feldspar is precipitated following a lowering of this ratio as a result of the precipitation of authigenic clays. (Ali and Turner 1982).

The next important pore filling phase within the

Penrith Sandstone occurs as calcitic cements, which are only present in unsilicified fluvial and aeolian sands, e.g. River Belah and Hilton Beck. At Cowraik, Lazonby Fell, George Gill and Stoneraise, feldspar authigenesis within aeolian sands is followed by a phase of silica precipitation.

Calcite cements are zoned (ferroan core to non-ferroan margin), and may be poikilotopic. They clearly post-date authigenic feldspar, and in some cases can be seen to enclose flakes of authigenic kaolinite. These observations compare favourably with Waugh's (1979) interpretation of diagenetic processes within British Permo - Triassic sandstones, i.e. that porewaters would be enriched in Ca, Si, and  $\text{CO}_3^{2-}$  following the precipitation of illitic clay and authigenic feldspar. Any alumina still present within porewaters is likely to precipitate with silica as kaolinitic clays, whilst  $\text{Ca}^{2+}$  and  $\text{CO}_3^{2-}$  are then incorporated into calcitic cements.

Calcitic cements clearly replace some silicate clasts, and their precipitation may be allied to the formation of secondary porosity if calcite is subsequently removed.

Zonation of calcitic cement probably reflects the depletion of  $\text{Fe}^{2+}$  with continued calcite precipitation within reducing subsurface groundwaters.

The absence of calcitic cement within silicified sandstones of Cowraik, Lazonby Fell, Stoneraise and George Gill, does not necessarily imply that they were never precipitated as an authigenic phase within

these sands. Two alternatives are possible:

(i) Calcitic cements were derived ultimately by the basinward migration of carbonate rich porewaters which derived their  $\text{Ca}^{2+}$  and  $\text{CO}_3^{2-}$  from limestone rich alluvial fan breccias. Carbonate cements were restricted to marginal alluvial fans and the interbedded fluvial and aeolian strata at basin margins, where groundwaters maintained a high carbonate content. Away from basin margins, the carbonate content of porewater is depleted as a result of calcite precipitation in basin margin facies. This leads to a phase of silica and kaolinite authigenesis within porewaters depleted in  $\text{K}^+$ ,  $\text{Al}^+$ , and carbonate; but enriched in silica derived from the dissolution / replacement of silicate clasts by carbonate cements in sediments at basin margins, (see Figure 5.3.5). If the mechanism of brine migration from basin margin to basin center is evaporative pumping (which is likely in an arid basin where evaporation exceeds precipitation), then it can explain the distribution of silica cements as indicated by Burgess and Holliday (1979) and Waugh (1979), i.e. towards the top of the Penrith Sandstone formation away from basin margins. The restriction of cements to locations near the top of the Penrith Sandstone probably occurs because porewaters could not become sufficiently evolved to allow silica precipitation to take place until relatively late during the deposition of the Penrith Sandstone. i.e. When large quantities of carbonate rich sediment had



accumulated at basin margin locations, and sufficient silicate clast dissolution / replacement had taken place within these sediments to allow silica concentration within basinward aeolian sediments.

(ii) Calcitic cements are derived ultimately by the basinward migration of carbonate rich porewaters which derived their  $\text{Ca}^{2+}$  and  $\text{CO}_3^{2-}$  from carbonate rich marginal alluvial fan breccias. Calcite was deposited throughout the basin of deposition, but subsequently removed from sands which were subject to a later phase of silica authigenesis.

In the above model, the paragenetic sequence of authigenic minerals within the Penrith Sandstone (Figure 5.3.5) is explained by the evolution of porewater systems within sands to precipitate all authigenic phases.

However, the location of silicified sandstones broadly coincides with Namurian / Lower Coal Measures subcrops. This is important because the formation of both silica and kaolinite could in theory be related to processes similar to those evoked by *Schmidt and McDonald* (1977) for the generation of acid pore water systems (and secondary porosity) during burial diagenesis. i.e. It might be related to the lowering of the pH of porewaters following thermal maturation within underlying Carboniferous sediments upon burial. (See Figure 5.3.6). If this was the case, then the introduction of  $\text{CO}_2$  (derived by de-carboxylation of organic matter) into the porewater system of the Penrith

Sandstone under conditions of maximum burial would produce a decrease in their pH, and facilitate the precipitation of silica and kaolinite. It would also produce secondary porosity as a result of neutralisation reactions between porewaters and carbonate cement. The distribution of silica cements might be explained by precipitation within units having the highest porosities and hence fluid mobility (i.e. aeolian sands); and by the ponding or trapping of Carboniferous derived fluids beneath the Eden Shales.

The "final" minerals observed to have formed within the Penrith Sandstone include.....

(a) Late stage kaolinitic clays infilling secondary pores in both silicified and non-silicified sands. They are best developed within silicified sands and may be produced by the methods outlined in models above, or by uplift of the Penrith Sandstone into a zone of freshwater diagenesis.

(b) Late stage clays / fe oxides which are observed coating well developed silica overgrowths within some silicified sandstones (see Plate 5.4). When studied using S.E.M. with Edax, clays produce traces indicative of illite and iron oxide.

The diagenetic models outlined above provide two alternative mechanisms for silica authigenesis within the Penrith Sandstone, both of which are different to models previously described by Waugh (1970). Waugh suggested

that silica cement formed early during diagenesis, as a result of surface or near surface evaporation of desert dews or silica rich brines brought to the surface as a result of capillary action. Silica is unstable relative to these alkaline groundwaters, and dust formed as a result of grain abrasion in the desert environment is dissolved.

Steele (1981) outlined a number of fundamental flaws in Waugh's model:

- (i) Extensive development of quartz overgrowth within the Penrith Sandstone is virtually unique.
- (ii) Silicified sandstones are not well documented at surface localities in modern aeolian sequences.
- (iii) No silcrete textures are present to indicate syndepositional cementation.
- (iv) If siliceous dust was being dissolved in desert dews, then more evidence of framework clast dissolution should be evident.

The lack of silcrete textures suggests that overgrowths formed under somewhat deeper conditions than Waugh (1970) envisaged. Steele (1983) suggests that quartz overgrowths are the product of diagenesis at depth, and that the variability of silica cement within the Penrith Sandstone is due to cement inhibition by clay pellicles. Steele (1983) was unable to recognise any "credible intraformational source of silica, or compelling extraformational source of silica" for overgrowths within the Penrith Sandstone. The models proposed in this report provide a credible source of

silica, and two alternative mechanisms by which it may precipitate.

#### 5.4 CONCLUSIONS.

(i) The Penrith Sandstone comprises a mixed sequence of aeolian sands, fluvial sands, fluvial conglomerates and alluvial fan breccias.

(ii) Sandy aeolian and fluvial deposits consist of mature orthoquartzitic sands, sublitharenites, or subarkoses. Fluvial conglomerates and alluvial fan breccias are composed predominantly of carbonate clasts with minor amounts of quartz, sandstone and chert clasts.

(iii) Diagenetic processes occurring within aeolian and fluvial Penrith Sandstone are directly related to diagenetic processes occurring within marginal alluvial fan breccias and conglomerates, i.e. diagenesis is largely facies dependent.

(iv) Diagenesis within marginal alluvial fan breccias and conglomerates is dominated by carbonate precipitation. A paragenetic sequence consisting of haematite, gypsum, ferroan calcite, non-ferroan calcite, illite / smectite, and kaolinite is proposed.

(v) A paragenetic sequence consisting of haematite, illitic / smectitic clays, feldspar (minor), calcite and kaolinite, exists for non-silicified fluvial and aeolian sands occupying basin margin locations.

(vi) A paragenetic sequence consisting of early dolomite, haematite, illitic / smectitic clays, feldspar and quartz (major) exists for silicified aeolian sands occupying "basinward" settings.

(vii) Different diagenetic histories within the Penrith Sandstone and associated sediments may be explained by the depletion of  $\text{CO}_3^{2-}$  and enrichment of silica within basinward migrating formation waters. These processes occur largely as a result of the precipitation of carbonate and replacement of silicates within marginal alluvial deposits.

(viii) An alternative model which could explain the distribution of silica cements within the Penrith Sandstone utilises the fact that areas of silicified sandstone broadly coincide with areas of Namurian / Lower Coal Measures subcrop, while unsilicified sandstones broadly coincide with areas of Carboniferous Limestone subcrop. This may indicate that thermal maturation of organic matter within Carboniferous clastic sequences is responsible for a phase of "low pH diagenesis" and silica precipitation within the porous aeolian sediments overlying them.

## CHAPTER SIX.

### 6.0 THE SEDIMENTOLOGY AND STRATIGRAPHY OF THE BRIDGNORTH SANDSTONE.

#### 6.1 INTRODUCTION.

The Lower Permian sediments of the Bridgnorth Sandstone Formation were deposited in the Worcester, Stafford and Knowle basins, (terminology after *Chadwick* 1985). These are fault bounded "graben - like" structures whose boundary faults exhibit a north - south "Malvernoid" Trend.

The Bridgnorth Sandstone Formation comprises a continental red bed sequence which is almost entirely aeolian in character, with minor alluvial sediments being present only at the base of the formation at basin margins.

#### 6.2 STRUCTURAL SETTING.

The Worcester, Stafford and Knowle sedimentary basins (See Figure 6.2.1) are fault bounded grabens with north - south trending boundary faults. Basin initiation occurred in extended continental lithosphere following the cessation of late Carboniferous (Variscan) earth movements. In the case of the Worcester and Knowle basins, Permian sediments occupy the sites of former Variscan highs - the Worcestershire Horst and the Mercian Uplands of *Wills* (1956).

The Worcester Basin is an approximately

symmetrical graben bounded to its west by a western boundary fault ( East Malverns Fault Axis), and in its east by an eastern boundary fault and the Vale Of Moreton Axis. *Chadwick* (1985) has suggested that boundary faults formed as a result of the extensional reactivation of pre-existing structures which may have represented a Palaeozoic positive flower structure. The Worcester Basin was formed as a result of the negative inversion of this structure during late Palaeozoic / Early Mesozoic extension. Seismic data (*Chadwick* 1985) indicates basinward thickening of the Bridgnorth Sandstone and Sherwood Sandstone Formations across marginal normal faults, indicating major fault controls on sedimentation.

The Worcester basin is floored by Carboniferous strata, Lower Palaeozoic strata, and Precambrian basement containing north - south "Malvernoid" structural elements; it opens northward into the Stafford basin, and northeastwards into the Knowle basin.

The Stafford basin is bound to its west by the Wenlock Horst in the north, and Enville fault in the south. Eastwards it is bound by the South Staffordshire Horst Block, which gives way south and east into the Knowle basin. It is floored largely by strata of Carboniferous age.

### 6.3 THE STRATIGRAPHY OF THE BRIDGNORTH SANDSTONE.

The Bridgnorth Sandstone has at different times been referred to as the Lower Bunter Sandstone, Lower

Mottled Sandstone, and Dune Sandstone. The terms "Lower Mottled" and "Lower Bunter" were applied at a time when the Bridgnorth Sandstone was believed to be of Lower Triassic age. Wills (1948) first applied the term "Dune Sandstone" to the beds; and the present nomenclature (also first applied by Wills), is that suggested in the British Geological Society Special Report No. 5, (Smith et al 1972) which provides a correlation of Permian rocks in the British Isles.

The Bridgnorth Sandstone Formation may be divided into:

(i) A basal sequence of red continental breccias.

Breccias are known variously as the Abberley Breccias (Southwest Staffordshire and Western Worcestershire), the Clent Breccias (Western portion of the South Staffordshire Coalfield), the Nechells Breccia (Eastern portion of the South Staffordshire Coalfield), the Kenilworth Breccia (Warwickshire), and the Haffield Breccia (Malvern region). All breccias form the basal part of the Permian basin fill, and are considered to be broadly contemporaneous. The occurrence of breccias is somewhat restricted to basin margin locations,

(ii) An upper sequence dominated by aeolian sand (the Bridgnorth Sandstone sensus stricto). Aeolian sands are replaced in areas of the South Staffordshire Coalfield by a further sequence of breccias directly overlying Carboniferous strata, and are overlain by conglomerates of the Kidderminster Formation (Boulton 1933, Wills



1936, *Smith et al* 1974). These "Higher Permian Breccias" are known variously as the Quartzite Breccia, the Barr Beacon Beds, the Hopwas Breccia and the High Habberley Breccia. In South Derbyshire parts of the Moira Breccia show the same relationship. (*Hains and Horton* 1969).

*William Wickham King* (1893) suggested that breccia deposits were probably similar to superficial deposits found along the margins of desert plains in central Persia (described by *Blandford* 1873). Subsequent studies by *King* (1923), *Boulton* (1933), *Shotton* (1937) and *Wills* (1948, 1956) all support an alluvial origin for these breccia deposits.

According to present convention the base of the Permian System in the West Midlands is taken to occur at the base of the Clent Breccias and their equivalents; and the top of the Permian System is taken to be at the base of the Kidderminster Formation which unconformably overlies the Bridgnorth Sandstone Formation. A Permo - Triassic stratigraphy applicable to the region of study is shown in figure 6.3.1. (*Smith et al* 1972).

#### 6.4 THE SEDIMENTOLOGY OF THE BRIDGNORTH SANDSTONE FORMATION - LOCATION AND NATURE OF OUTCROPS.

##### 6.4.1 THE PERMIAN BRECCIAS.

##### 6.4.1.1 Basal Permian Breccias.

In the region to the south of Enville, a roadside exposure approximately 200m southwest of The Lydiates

(Grid Ref. SO 8210 8350) displays red aeolian sandstones which are located near the base of the Bridgnorth Sandstone unit. When this outcrop is followed southwest along the road for a further 100m, underlying basal Permian breccias crop out in the roadside. Breccia beds at this location are clast supported, with a wide variety of angular, poorly sorted clasts ranging from less than 1 cm up to 12 cm in length. Clasts are set in a red / brown poorly consolidated muddy matrix. Breccia beds at this location actually occur at the crest of a small southwesterly trending ridge, a feature noted by *Whitehead and Pocock* (1925), who pointed out that breccia outcrops in the region tend to form areas of higher relief. *Whitehead and Pocock* also document the presence of more than one breccia horizon towards the base of the Bridgnorth Sandstone in this region. These breccias are known locally as the Enville Breccias, and the presence of a number of breccias in this region suggests the interdigitation of aeolian facies sandstones with marginal alluvial fan breccias.

Further exposures of basal Permian breccia (The Clent Breccia) may be observed at Sling Gravel Pits (Grid Ref. SO 9460 7810) in the Clent Hills. Breccias at this location are poorly sorted, poorly consolidated sediments containing mainly angular clasts up to 30 cm diameter. Clast types include volcanics, quartzite, chert, and rare limestone clasts. Breccias are for the most part clast supported, with angular clasts being set in a red /

brown mudstone or sandy mudstone matrix. Exposures within the gravel pits are overgrown, and much of the pit appears to have been levelled with the consequence that little evidence as to the nature of bedding within the breccias, may be detected.

At Stagborough Hill, to the west of Stourport and the River Severn, Clent Breccia reportedly overlies Upper Coal Measures (Keele and Highley Beds, *Mitchel et al* 1961). Exposure is poor, but a stream section at Grid Ref. SO 7905 7730 provides small outcrops of red breccia, in which a variety of angular, pebble grade clasts are set within a red, fine grained, muddy matrix. Breccias are clast supported, and clast types present include dark grey / green volcanic clasts, chert and fine grained quartzite clasts.

Three Hundred metres south of this stream section, a heavily overgrown quarry provides small exposures of the same breccia. No bedding is determinable at this location (due to the poor nature of the exposure), but *Mitchel et al* (1961) have reported massive breccias dipping  $70^{\circ}$  to the southeast. *Mitchel et al* also document a section (no longer visible) some 180m south of this quarry, showing massive breccia dipping  $45^{\circ}$  towards the east; apparently overlain by Bridgnorth Sandstone.

At Church Hill (Grid Ref. 7105 7310) a disused gravel pit provides a number of small breccia exposures. Clent Breccias at this location consist of angular pebble grade clasts (1 - 2 cm diameter) set in a red muddy

matrix. Breccias are clast supported and display little evidence of bedding. Clast types present include light coloured volcanic clasts, quartzites, limestones and cherts. Exposure at present is poor, but *Mitchel et al* (1961) report that one face within the gravel pit displayed 38 feet of loose breccia dipping 20° to the northeast, and that the breccia rests upon Upper Carboniferous Highly Beds.

At Osebury Rock (Grid Ref. SO 7380 5560) Permian breccias known locally as the Haffield Breccia crop out in precipitous sections overlooking the River Teme. Breccias are overlain by a mixed sequence of red, fine - medium grained fluvial and aeolian sandstones of uncertain age.

The sands at this location have been described as "normal Bunter sandstones" by *Earp and Hains* (1971), and their contact with the underlying Haffield Breccia is reported to be conformable. (N.B. No exposure of the actual contact was located during the course of this study). It is likely that the fluvial and aeolian sands overlying the Haffield Breccia in the vicinity of Osebury Rock can be attributed to the Wildmoor Sandstone Formation, which *Smith and Burgess* (1984) describe as probably being of fluvial origin. However, the precise stratigraphic position of these sands may remain in some doubt since:

- (a) The area appears structurally complex.
- (b) Analysis of the Bridgnorth Sandstone Formation in

core available from the Kempsey Borehole has revealed the presence of some strata which (by analogy with North Sea core material) may be fluvial in origin.

The Haffield Breccia contains subrounded - angular, gravel - boulder grade clasts up to 80 cm in diameter. The majority of clasts are pebble grade and are arranged in "sheet-like" fining upward units 30cm to 1m thick. Metamorphic, volcanic, and sedimentary clasts are present, set within a fine grained, red / brown, sand - mud grade matrix. Breccias are clast supported. Thin (0.5cm - 1cm) red / brown mud silt grade sediments may cap fining upward units. Fining upward units typically show internal structure in the form of trough cross stratification. Pronounced scouring of pre-existing bedforms by successive breccia units is evident, and some breccias are clearly "channel-like" fills.

Haffield breccias crop out in roadside exposures at Grid Ref. SO 7361 5536 where they apparently pass upward into a sequence of red fluvial and aeolian sands; and at Grid Ref. SO 7375 5514, immediately to the east of Knightwick Station, where they are faulted against a sequence of red fluvial and aeolian sandstones.

Breccias at Osebury Rock are interpreted as sediment deposited as sheets by ephemeral flows (sheetflood events) upon marginal alluvial fans. (c.f. Bull 1977).

#### 6.4.1.2 Higher Permian Breccias.

A number of breccias within the English Midlands

are considered to post date the "Clent" breccia, and be broadly contemporaneous with the Bridgnorth Sandstone.

One such breccia horizon crops out in road cuttings at High Habberley to the west of Kidderminster. "High Habberley Breccias" overly the Bridgnorth Sandstone, and are themselves unconformably overlain by the basal conglomerates of the Kidderminster Formation. In reality however, breccias probably interfinger with the Bridgnorth Sandstone.

Good sections of High Habberley Breccia visible in a road cut at Grid Ref. SO 8100 7590, (on the eastern end of the Kidderminster - Bewdley road), show the breccia to be poorly sorted, coarse grained, polymictic, and clast supported. It contains both angular and rounded clasts up to 10cm in diameter. Cross bedding is clearly visible within breccias, and individual sets fine upwards from pebble grade material into fine gravel. (See Plate 6.1). Bedding foresets are inclined at angles of up to  $20^{\circ}$  and are frequently tangential to underlying bedding planes. Shallow "trough - like" scours may also be detected towards the upper portions of some beds. These structured, cross bedded breccias composed of fining upward units are interpreted as being indicative of fluvial deposition occurring upon a marginal alluvial fan.

At High Habberley, a road cut on the Bewdley - Wolverley road (Grid Ref. SO 8080 7700) displays a short section of Bridgnorth Sandstone overlain by 15m or more

of High Habberley Breccia. The Bridgnorth Sandstone at this location is composed of red, well sorted aeolian sand. The High Habberley Breccia consists of dark red - brown, angular, pebble-gravel grade material. Exposure is poor, but breccia units immediately overlying the aeolian sands appear to fine upwards from poorly sorted, clast supported, pebble grade breccia into well sorted gravel grade material. This fining upward trend is apparently repeated throughout the exposure. No cross stratification was observed within the breccias at this location, though this may be due to the overgrown nature of exposures.

At Barr Beacon (Grid Ref. SO 0588 9644) excellent exposures of the Barr Beacon Beds are visible in westerly facing quarries.

The Barr Beacon Beds at this location consist predominantly of red, coarse - medium sandstones with thin gravel - pebble grade breccia horizons. Individual beds have a tabular or "sheet-like" geometry, and invariably fine upwards. Fining upward units typically have a pebble - gravel grade base composed predominantly of angular, "varnished" quartzite clasts passing up into coarse - medium sands, often containing highly rounded clasts. Large brown mudstone clasts and scattered granules are common within sandy units.

Internally, sheet-like sandstone units exhibit cross stratification (often steeply inclined and consisting of concave upward foreset lamination at angles of up to 25° or more) in which trough cross laminated

"scours" are frequently recognised. Plane bedded and structureless sands are also present, but are less common. In addition to occurring as "scour" fills bound within sheet-like sand-bodies, trough cross stratification sets may be observed occurring as larger erosional scours which cut into, and truncate sheet-like sand-bodies.

Sheet-like fining upward units often show an upward transition from an angular pebble grade lag, through a thin sequence of structureless sands (up to 10 cm) having a "wavy" or "undulatory" upper surface, into cross laminated sands with high angled foresets. Other fining upward cycles show a direct transition from an angular pebble grade base into well sorted cross laminated sands, (see lithological log provided in Appendix Nine).

Plane bedded, sheet-like fining upward units occur in medium - fine grained sandstones. Fine grained, plane bedded fining upward units are typically capped by thin (1 cm thick) red mudstone horizons, which may contain desiccation cracks.

Sheet-like fining upward units are interpreted as representing ephemeral sheetfloods upon the distal portions of marginal alluvial fans. Deposits are clearly the product of episodic waning flow regimes. Structureless sands seen towards the base of some fining upward units probably reflect either rapid deposition and subsequent dewatering of sediment with loss of internal



structure, or deposition within a flow regime too high for the development of tractional bedforms. Thin red mudstone horizons at the top of fine grained, plane bedded units reflect the low stage settling out of fine mud grade material on the surface of sheetflood deposits. Desiccation of mudstone horizons is indicative of the drying out of sheetflood surfaces between individual sheetflood events.

Trough cross stratification which is effectively bound within sheet-like fining upward sand-bodies reflect processes of scour and fill accompanying the deposition of individual sheetflood units.

Trough cross stratification sets which erode and truncate earlier sheetflood deposits (see Plate 6.2) often contain thin (1 cm thick) red mudstone horizons which clearly "line" or "drape" erosional scours. These thin mudstone bands reflect the low stage settling of fines within erosional ephemeral channels. The scale of this trough cross stratification might suggest a more "proximal" fan setting than trough cross stratification which is bound within sheetflood units. The presence of highly rounded quartz clasts within better sorted horizons is indicative of the presence of a reworked aeolian component within sands (*Shotton 1937*).

A short section through part of the sequence visible at Barr Beacon Quarries is shown in Appendix Nine.

Marly breccia beds containing small quartz and sandstone pebbles have been described from canal cuttings

at Hamstead (Grid Ref. SO 0533 9300), by Whitehead 1925. Exposure of the Hopwas Breccia within these canal cuttings is heavily overgrown, but small areas of fine red / brown silty sandstone and fine gravelly breccia can be found in steep faces some 5 or 6 metres above a Carboniferous sequence of red fluvial sands and conglomerates. The breccia horizons are interpreted by the Geological Survey as the Hopwas Breccias, and are overlain by pebbly sands and conglomerates of the Kidderminster Formation. Whitehead (1925) reports 6 metres of Hopwas Breccia at this location. The Hopwas Breccia is believed to be broadly contemporaneous with strata observed at Barr Beacon.

#### 6.4.2 THE BRIDGNORTH SANDSTONE (Sensu Stricto).

Four main areas of Bridgnorth Sandstone outcrop occur within the English Midlands. (see Figure 6.4.1), These are:

- (i) A belt occurring along the River Severn beginning at Dudmaston Hall (Grid Ref. SO 7500 8900) in the south, and extending northwards along the Severn Valley through Quatford (Grid Ref. SO 7400 9120), Bridgnorth (Grid Ref. SO 7150 9330) and Shifnal (Grid Ref. SJ 7500 0780).
- (ii) A belt extending southward along the Abbots Castle Hill escarpment from Hill End (Grid Ref SO 8230 9450) to Kinver (Grid Ref. SO 8420 8360).
- (iii) An area to the West of Kidderminster which extends Southwards from the Habberley Valley in the north, to

Mount Pleasant (Grid Ref. SO 8000 7380) in the south.

(iv) An area immediately to the southeast of Wem.

Subsurface data was obtained from the B.G.S Kempsey no.1 and Netherton no.1 boreholes, located within the Worcester basin.

Throughout the region of study the Bridgnorth Sandstone is red coloured (brick red - reddish brown) and weathers to an orange / dark brown colour, often with pale irregular "mottling". The sands are fine - medium grained, quartzitic, virtually entirely aeolian in character, and poorly cemented.

#### 6.4.2.1 THE REGION AROUND BRIDGNORTH.

The region around Bridgnorth provides by far the most spectacular exposures of the Bridgnorth Sandstone in the English Midlands. Much of the exposure occurs as high, steep cliff faces. This is surprising considering its friable nature and poor cementation. However, exposures forming the highest and most pronounced features are invariably capped by conglomerates of the Kidderminster Formation, and it appears to be this association which has led to preservation of the sandstone as cliffs. (Also seen at Kinver Edge and along the Abbots Castle Hill escarpment).

Precipitous sections are visible at Jacobs Ladder (Grid Ref. SO 7235 9400) and Pendlestone Rock (Grid Ref. SO 7240 9396), where over 50 metres of large scale

trough cross bedded Bridgnorth Sandstone are overlain by Kidderminster Conglomerate. The sandstones are red, fine - medium grained, moderately sorted and well rounded, and in areas contain abundant grain flow laminae.

Southeast of Jacobs Ladder, the Permo - Triassic unconformity is well exposed in road cuttings along the A454 Wolverhampton road north of the Hermitage (Grid Ref. SO 7680 9360); and also in a quarry at Queens Parlor (Grid Ref. SO 7670 9330).

At the Hermitage, red, trough-cross bedded aeolian sands are overlain by the Kidderminster Conglomerate. The Sands contain abundant grainflow lamination, and in areas apparently opposing foreset dip directions are produced by the vertical stacking and overlapping of large shallow trough cross-stratification units. The sub-Triassic depositional surface at this location is "step - like" in its nature, clearly indicating that aeolian Permian sediments were well indurated prior to the deposition of the Kidderminster Conglomerate.

In the town of Bridgnorth, aeolian sands are exposed in cliffs forming the south and eastern sides of Castle Hill. Gardens at the eastern side of Castle Hill (Grid Ref. SO 7180 9315) provide an excellent example of large scale aeolian cross stratification. The most prominent feature displayed in this exposure is a very large (second order) bounding surface separating two cosets of strata which show apparently opposing dip directions. The bounding surface appears to be a very

large almost planar structure, and clearly truncates foreset lamination within the strata beneath it. The resulting cross stratification at the northern end of this exposure displays a "herring - bone" type pattern, in which beds show marked flattening of dip at the toe of foreset lamination. Downwind shingling of dune forms by overlap and incision is clearly evident, and the apparently counterdipping foreset directions observed between sets of strata (see Plate 6.3) are generated by the overlapping of very large scale trough cross stratification sets (estimated width up to 500m). When cross stratification within the lower coset of strata is traced southward for 100m along this cliff face, unidirectional foresets give way to apparently counterdipping wedge - like fabrics generated by the overlapping of smaller shallow trough cross stratification sets, (See Plate 6.4).

At Quatford, two miles south of Bridgnorth, excellent exposures of Bridgnorth Sandstone occur in road cuttings along the A442 Bridgnorth - Kidderminster road. The best exposures occur near a petrol station at Grid Ref. SO 7582 9048 and displays examples of "wedge - like" fabrics generated by the overlapping and vertical stacking of trough cross stratification sets (described by Mader and Yardley 1985). A sketch of part of this exposure illustrating the presence of counter-dipping wedge-like fabrics is included in Figure 6.4.3. The figure also includes a palaeocurrent rose (after Shotton

1937), which clearly indicates deposition within an easterly wind system, and shows opposing foreset directions to be an apparent phenomenon.

A smaller roadside section at Chappel Lane in the village of Quatford (Grid Ref. SO 7400 9120) has 8m of red, trough cross bedded aeolian sands overlying a sequence of uniformly dipping aeolian sandstones 5.5 m thick. The lower portion of this exposure comprises a single dune set (at least 5.5 m thick) which contain no internal erosion surfaces are evident.

At Gags Hill (Grid Ref. SO 7555 9058) aeolian sands are visible in three metres of exposure at the entrance to a small cave. The main feature of the sandstone at this location is the presence of a very well cemented horizon at the base of the exposed section, contain a network of rusty brown, positive weathering veinlets. The beds overlying this abnormally well cemented layer are of "typical" aeolian Bridgnorth Sandstone, but contain large numbers of positive weathering, buff / white, nodules composed of carbonate cement. Baryte cements are also present at this location.

#### 6.4.2.2 OUTCROP IN THE REGION AROUND ENVILLE AND KINVER.

Small exposures of Bridgnorth Sandstone occur to the North of Enville along the Abbots Castle Hill escarpment. The best of these is at Tinkers Hill (Grid

Ref. SO 8230 9450), where the Claverly - Seisdon road crosses the escarpment. Here, trough cross stratified beds from near the top of the Bridgnorth Sandstone are exposed in a small cutting, but contact with the overlying Kidderminster conglomerate is no longer visible.

Small exposures of trough cross bedded aeolian sand are found around the town of Kinver, but the most extensive exposure displaying the thickest sections are found to the southwest along the Kinver Edge escarpment.

At Holy Austin Rock (Grid Ref. SO 8350 8360) on the northern end of the escarpment, a series of cliff exposures are carved into a number of "rock houses". Exposure is excellent, and the block - like nature of the excavations allows a three dimensional view of the internal structure of the sandstones, (see Plate 6.5). Over 60m of red, poorly cemented, cross stratified sandstone is exposed at the Holy Austin Rock section, and in steep hillsides to the immediate south. Sands are typically fine - medium grained, and contain abundant grainflow laminations which may be up to 10 cm thick. Grainflow laminae may show normal or reverse grading.

Trough cross bedding dominates exposure at Holy Austin Rock, and apparently opposing foreset directions are generated by vertical stacking and overlapping of trough cross stratification sets. Erosional "scours" infilled by trough cross stratification sets testify to dune modification by processes of blowout and fill (Mader

and Yardley 1985), and result in the production of interset diastems (second order bounding surfaces) which are strongly concave upward, and which to a certain extent preserve relief.

A rare example of an interdune sheetsand is visible within the higher exposures at Holy Austin Rock. (See Plate 6.6). Interdune deposits consist of 1.8m red, fine grained, parallel laminated / wind rippled sandstone. Plane bedded strata (mm scale) at this location pass up into low angle subcritically climbing translantent strata formed by the migration of wind ripples under conditions of net sedimentation. In climbing translantent strata, each continuous laminae records the passing of a ripple (Hunter 1977, Fryberger et al 1979). The plane bed lamination at this location appears very similar to that described in ancient interdune environments by Clemmensen and Abrahamsen (1983). These sands pass upward into 2.8 m of fine - medium grained cross bedded aeolian sandstone, in which the dip angle of foreset lamination increases upwards throughout the unit.

The base of the wind rippled, sheet-like sandstone is marked by a flat planar surface (by definition a first order bounding surface) below which some 14 m of cross bedded aeolian sandstones crop out. Cross bedded sands underlying the interdune deposit occur in sets up to 4m thick and contain abundant grainflow laminae.

Further large scale aeolian cross stratification is visible in westerly facing cliffs to the south of Holy



Austin Rock. In particular, exposures at Nannys Rock (Grid Ref. SO 8300 8270) and Vales Rock (Grid Ref. SO 8280 8210) display large scale, shallow trough cross stratification sets up to 5m thick, and containing abundant grainflow laminae.

#### 6.4.2.3 THE REGION AROUND KIDDERMINSTER, BEWDLEY AND HIGH HABBERLEY.

At High Habberley, a road cut on the Bewdley - Wolverley road (Grid Ref. SO 8080 7700) displays a short section of trough cross stratified Bridgnorth Sandstone overlain by beds of the High Habberley breccia.

Roadcuttings at Grid Ref. SO 8005 7595 on the Kidderminster - Bewdley road display excellent sections of aeolian Bridgnorth Sandstone. The most notable feature at this location is a pronounced, (slightly convex upward) slightly climbing, bounding surface separating a lower sequence of grainfall dominated deposits from an upper set in which foreset laminae pass downward into asymptotic grainflow dominated strata. (see Plate 6.7). The downwind shingling of dunes with associated overlap and incision of bedforms is clearly evident within the upper set at the west of this exposure. Palaeowind directions at this location indicate westerly aeolian transport.

Bridgnorth Sandstone also crops out within the Devils Spittlefull Nature Reserve, immediatly to the south of the West Midlands Safari Park. The best

exposure occurs at a hill capped by sandstone crags known as The Devils Spittlefull (Grid Ref. SO 8075 7470). In particular the cliffs at the southwest end of the Spittlefull display an 11.5 m thick section of trough cross stratified aeolian sandstone, dominated by grain fall deposits.

#### 6.4.2.4 THE REGION IMMEDIATELY SOUTH OF WEM.

This region comprises the portion of the Cheshire basin that is occupied by the South Staffordshire Coalfield, and lies just to the north of the Wrekin. Aeolian sands occurring below the Kidderminster Conglomerates in this region are known as the Collyhurst or Kinnerton sandstones. They represent a northern extension of the aeolian Bridgnorth Sandstones, and in this report are referred to as the Bridgnorth Sandstone to avoid confusion with nomenclature.

Exposure is very limited, but a number of interesting localities exist.

The best exposure occurs in a road cut at Rock Hall, Preston Brockhurst (Grid Ref. SJ 5400 2505). At this location, the normally red aeolian sandstone contain areas of buff / yellow sand, occurring as very large irregular blotches, discontinuous "patchy" areas apparently following cross lamination, or as small scale mottling. Yellow regions appear to have been formed as a result of the leaching of red iron oxides from the beds, and sometimes smaller leached areas are bounded by a thin

dark rusty zone where iron oxides have been concentrated

Sedimentary structures are well developed within the aeolian sandstones at Rock Hall. Important is the presence of a thin 1.5 m (maximum) fine grained, yellow, plane bedded sandstone which extends through much of the length of the exposure. (See Plate 6.8). This sand unit contains thin wind ripple lamination, has a flat planar base, and clearly truncates pre-existing aeolian bedforms, (See Plate 6.8). Cross bedded aeolian sandstones overlying the plane bedded sandstone are dominated by grainflow laminations, and foresets typically pass into asymptotic "toe-sets" continuous over distances of up to 10m.

The plane bedded sandstone outcropping at Rock Hall is interpreted as an interdune sheet-sand, and its base is thus considered to be a first order bounding surface. Aeolian sediments immediately overlying plane bedded sandstones are clearly representative of dune base deposition; and the downwind shingling of aeolian bedforms accompanied by the processes of incision and overlap is evident.

Baryte cement nodules are common in both red and yellow areas of sand but appear to be restricted to porous dune facies sandstones, and to coarser areas of grainflow laminae within dune base deposits. Nodular baryte cements appear especially abundant within grain-flow laminae in fine - medium grained aeolian sandstones immediately below fine grained interdune deposits. This may be indicative of the ponding

of upwardly mobile diagenetic fluids at porosity/permeability gradients or barriers. Cu and Ba mineralisation occurs along faults in the vicinity of Preston Brockhurst, and baryte mineralisation within aeolian sands may be contemporary with this. Mineralisation has been interpreted as Tertiary in age (Poole and Whiteman 1966).

Small exposures of trough cross stratified Bridgnorth Sandstone occur at Rock Cottage (Grid Ref. SJ 6260 2120); and at the entrance to Potford Farm (Grid Ref. SJ 6400 2220). At Potford Farm a small exposure of fine - medium grained red sandstone shows evidence of dune modification in the form of shallow trough cross stratification sets infilling erosional scours within pre-existing aeolian bedforms.

#### 6.4.4.5 SUBSURFACE DATA.

The Bridgnorth sandstone was studied in the subsurface using core material from the British Geological Survey Kempsey no.1 borehole (Grid Ref. SO 8609 4933), and cuttings from the Netherton no.1 borehole (Grid Ref. SO 9982 4138).

The Bridgnorth Sandstone reaches a thickness of 3077 ft in the Kempsey borehole, and the cored interval studied (4485 ft - 7562 ft) comprises a mixed sequence of red fluvial and aeolian sandstones. A lithological log for the cored section studied is shown in Figure 6.4.4. Aeolian strata consist of red, moderately well

cemented, fine - medium grained, well sorted, clean sandstones. Cross stratification is present within aeolian sandstones, and foreset inclination typically increases upward (to angles of  $25^{\circ}$ ) within cross sets. "Tongue - like" grainflow laminae composed of well rounded, medium sized grains are present in parts of the sequence.

White carbonate cement nodules are common within aeolian sands (up to 1.0cm in diameter). The largest nodules occur within grainflow laminae. Carbonate cement nodules are the subsurface equivalent of "mottling" seen in the Bridgnorth Sandstone at surface outcrop.

Fluvial strata recognised, consist of red, fine - medium grained sandstones. Both structured and structureless fluvial sands are present.

Structured fluvial sands are distinguished from their aeolian counterparts by the predominance of low angle cross stratification sets, thin red clay rich laminae (sub mm scale) draping cross lamination, and the presence of tiny mica flakes. Structured fluvial sediments are interpreted as fluvial sheetfloods.

Structureless fluvial sands are moderately well cemented. Bimodal texture and well rounded clasts within structureless fluvial sands may be indicative of the fluvial reworking of aeolian deposits. Similarly, the presence of structureless sands which grade downward into sands which are apparently of aeolian origin, and which are overlain by wavy bedded fluvial sandstones is

probably indicative of the reworking of aeolian sands by ephemeral flows.

Bridgnorth sandstone in the Kempsey borehole lies unconformably upon Lower Palaeozoic / Precambrian volcanoclastic sandstones, tuffs and agglomerates. The basal portion of the Bridgnorth Sandstone Formation consists solely of fine grained, red, well sorted sandstones: no breccia horizons are present.

Cuttings (taken at 10 ft borehole intervals) from the Netherton Borehole (10 miles southeast of Kempsey no.1) also indicate a sharp transition between dark, fine grained Lower Palaeozoic strata and red Permian sands. The absence of basal Permian breccias in boreholes contrasts markedly with the occurrence of breccia at Osebury Rock some 10 miles to the northwest of the Kempsey site.

Further information as to the nature of the relationship between Permian Breccias and the Bridgnorth Sandstone exists in the form of written stratigraphic descriptions for exploratory water borings carried out in the region of study between 1880 and 1930.

In particular, *Richardson* (1928, 1930) provides lithological descriptions of strata encountered in a number of exploratory water borings, while *Whitehead* and *Pocock* (1947) provide tabulated data including formation thicknesses for numerous boreholes. These data have been summarised in figures 6.4.5, 6.4.6, 6.4.7, and Appendix Ten.

Few grid references are available for these

boreholes, but locations as given by the Geological Survey (*Whitehead and Pocock 1946*) are duplicated in Appendix Fifteen.

East - west correlations of strata present below the Kidderminster Conglomerates (Appendix Ten and figures 6.4.5 and 6.4.6) illustrate the increasing importance of breccia deposits towards basin margin locations.

Line 1 in Figure 6.4.5 illustrates the presence of the Barr Beacon Beds directly beneath the Conglomerates of the Kidderminster Formation at the eastern margin of the South Staffordshire Basin (Barr Beacon). At Bridgnorth, in more westerly, basinward locations, the aeolian Bridgnorth Sandstone replaces coarser alluvial sediments beneath the Permo - Triassic unconformity. A similar relationship is inferred in line 2 of Figure 6.4.5, where aeolian Bridgnorth Sandstone underlies Kidderminster Conglomerates at Wordsley, but are replaced by Hopwas beds in the Hamstead district. (N.B. at Kingswinford Workhouse, Kidderminster Conglomerates are reported to be in faulted contact with the Clent Breccia).

Line 3 in Figure 6.4.6 (see also Appendix Ten) illustrates the presence of a thick sequence of Clent Breccia beneath the Kidderminster Conglomerates in a boring at Nechells in Birmingham. When traced westwards the breccia passes into aeolian Bridgnorth Sandstone. Lithological logs have been reconstructed from borehole data published (*Richardson 1928, 1930*) for borings at

Nechells Gas Works and Stourbridge G.W.R. Goods station, both of which penetrated the Clent Breccias. (See Appendices Eleven and Twelve)

In Line 4 in Figure 6.4.6, breccias present below the Kidderminster Conglomerates in the Burcote and Romsley borings give way to aeolian sand when traced west to Kidderminster. The upper portion of these aeolian sands are replaced by thin breccias at High Habberley. A lithological log for the boring at Burcote Pumping Station has been reconstructed from borehole descriptions (Richardson 1928) and is illustrated in Appendix Thirteen.

Line 5 in figure 6.4.7 is a northwest - southeast correlation for the Worcester Basin, compiled using borehole data from Kempsey (Grid Ref. SO 8609 4933), Netherton (Grid Ref. SO 9982 4138), and Sherborne (Grid Ref. SP 1565 1396). The section illustrates the presence of a thick basal Permian breccia at surface outcrop (at Osebury Rock), and the absence of any breccia horizons within boreholes. This indicates breccias are restricted to basin margin locations. The Sherborne Borehole in the southeast of the Worcester Basin, contain Kidderminster Conglomerates which directly overly Carboniferous strata.

## 6.5 SEDIMENTOLOGICAL MODEL.

The poorly sorted coarse detritus of the Clent Breccias and their equivalents are interpreted as having



been deposited upon alluvial fans in basin margin locations. The principle mechanism of deposition recognised is fluvial (represented by structured fining upward units), and deposits are recognised as having accumulated as a result of ephemeral sheetfloods across the fan surface.

Bull (1977) described most water lain alluvial sediment in the alluvial fan environment as consisting of sheets of sand, silt and gravel deposited by a network of braided distributory channels. These sheets of sediment are deposited by ephemeral surges which spread out from the end of a fan. Shallow distributory channels formed are rapidly filled with sediment, and then shift a short distance, repeatedly dividing and rejoining.

It is believed that well structured sheet-like breccias exposed at Osebury Rock, and the sand and gravel detritus of the Barr Beacon Beds represent deposits of this type.

In the case of Barr Beacon Beds, the fine grain size observed within the sediments may be indicative of deposition within a more distal fan environment. Also, the presence of well sorted spherical quartz grains within sands at this location indicates the fluvial reworking of aeolian detritus, and suggests a close proximity to the main dune field. Poorly sorted breccia horizons with high matrix contents may represent debris flow deposits. If this is the case then they are likely to have formed where source conditions provided an abundance of fine detritus and steep slopes (*Blackwelder*

1928, Bull 1964), where moveable sediment volume is high compared to the volume of available water (Wasson 1977).

Cross stratification within aeolian Bridgnorth Sandstone indicates deposition within an easterly prevailing wind. Bounding surfaces recognised at outcrop consist mainly of trough shaped second order surfaces reflecting the migration of dunes between or across draa's, with third and fourth order surfaces representing the reactivation and modification of aeolian slipfaces. The predominance of simple large scale trough cross stratification sets is interpreted as being indicative of the migration of sinuous crested transverse dune forms. "Wedge-like" fabrics observed are generated by the vertical stacking and overlapping of trough cross stratification, or trough and planar cross stratification sets. Interdune deposits are rare within the Bridgnorth Sandstone, and this is probably indicative of aeolian deposition within a sand saturated environment. Aeolian strata are interpreted as representing the deposits of transverse dunes rather than barchans, because the latter tend to form on hard desert surfaces with sparse sand supply (Cooke and Warren 1973, Glennie 1987). Transverse dunes reportedly form in moderate to strong unimodal wind regimes (Mader and Yardley 1984).

Steele (1983) also suggests that cross stratification sets within the Bridgnorth Sandstone reflect the migration of transverse dunes over tranverse draa. Steele envisaged these bed forms as efficient sand

trapping features, which grew quickly at the upwind erg margin and subsequently migrated across it in equilibrium. Subsequent work by Mader and Yardley (1985) is in agreement with the views of Steele.

Both climate and sand supply are important factors in governing whether dunes accumulate in a basin, or whether deflation takes place. Climate also controls fluvial discharge, and hence fluvial erosion / reworking of aeolian dunes (Clemmensen and Abrahamsen 1983). The scarcity of fluvial deposits within the Bridgnorth Sandstone may indicate that transverse bedforms were able to develop relatively unhindered by erosive fluvial activity and attain great heights, producing very large scale trough cross stratification sets. The only evidence of fluvial reworking of aeolian sands is observed in alluvial basin margin facies at Barr Beacon, and in core material from the Worcester Basin. However, relatively poor exposure of the Bridgnorth Sandstone in the Worcester basin, and the lack of exposure of Permian sediments within a ten mile wide tract of land between Bridgnorth and Barr Beacon prevents evaluation of the true extent to which fluvial systems developed towards basin margins.

## 6.6 CONCLUSIONS.

(i) The Bridgnorth Sandstone Formation comprises an almost entirely aeolian sequence deposited in the Worcester, Stafford and Knowle Basins.

(ii) Aeolian dunes are interpreted as sinuous crested transverse bedforms deposited within an easterly prevailing wind.

(iii) Minor alluvial sediments occur at basin margins. Alluvial strata comprises both coarse, angular, clast supported detritus e.g. the Clent breccia and its equivalents; and also sand - gravel grade detritus as observed at Barr Beacon. Alluvial strata were deposited predominantly by sheetflood processes upon marginal alluvial fans. The fluvial reworking of aeolian detritus occurred in these marginal settings, but poor exposure prevents evaluation of the extent to which fluvial systems may have developed.

(iv) The predominance of aeolian strata and lack of interdune facies within the study area would apparently indicate that dunes accumulated within a sand saturated system.

(v) The scoured and eroded nature of the Permo-Triassic unconformity in the region of study suggests that the aeolian Bridgnorth Sandstone was already well indurated prior to the deposition of the Kidderminster Conglomerates.

## CHAPTER SEVEN

### THE PETROLOGY AND DIAGENESIS OF THE BRIDGNORTH SANDSTONE.

The petrology and diagenesis of the Bridgnorth Sandstone are described here in order to provide a comparative study with the petrology and diagenesis in other Lower Permian formations studied; and to evaluate the processes which influence diagenesis in these formations.

#### 7.1 DETRITAL MINERALOGY.

##### 7.1.1 Quartz.

The Bridgnorth Sandstone is composed predominantly of subrounded - well rounded quartz grains (46% - 66% on average). Quartz grains with simple non-undulatory extinction are the dominant quartz type present forming up to 60% of the total quartz. Polycrystalline grains having more than three crystal units per grain are present in much lesser quantities (11% - 34%), whilst strongly undulose quartz grains and grains composed of 2 - 3 crystal units form less than 10% of quartz grains present.

The inferred quartz provenance determined using four variable quartz type diagrams of *Basu et al* (1975) is one of middle - high grade metamorphic rocks. Vermicular chlorite inclusions are common within some grains and may be indicative of a hydrothermal origin for some quartz (*Folk* 1974).

### 7.1.2 Feldspar.

Feldspar may form up to 12% of the Bridgnorth Sandstone, and occurs as corroded alkali feldspar clasts which may have well developed authigenic overgrowths. Plagioclase feldspar is extremely rare, and its presence is indicated only by vague remnants of corroded grains showing polysynthetic twinning.

### 7.1.3 Rock Fragments.

Lithic fragments present within the Bridgnorth Sandstone are varied. Sedimentary, igneous and metamorphic lithologies are present.

Sedimentary rock fragments are common, and occur mainly as fine grained, well sorted sandstone clasts which are slightly micaceous, highly compacted and contain large quantities of opaque iron oxides.

Metamorphic clasts are the most common lithic fragments after those of sedimentary origin, and appear to be the low grade metamorphic equivalent of detrital sandstone clasts.

Igneous rock fragments present occur most commonly as either rhyolitic or basic types. Rhyolitic fragments are light coloured and consist of fine quartz and feldspar intergrowths, often with spherulitic textures. Basic rock fragments are dark coloured (they contain abundant opaques) and fine grained with little determinable mineralogy.

Granitic rock fragments are not common. When present they occur as coarse grained, light coloured

clasts consisting of quartz and feldspar with minor amounts of mica. They may show graphic intergrowth textures between quartz and feldspar.

Chert clasts may also be present, and occur as large well rounded grains heavily stained by iron oxides. "Spicule-like" forms are sometimes present within chert clasts, indicating a probable sedimentary origin.

#### 7.1.4 Heavy minerals and detrital opaques.

The principle detrital opaque mineral present is haematite, which occurs as small rounded clasts. Occasionally "spindle-like" ilmenite exsolution lamellae are present within detrital haematite, and typically display a cross hatched or "cloth-like" texture when observed in reflected light.

Martite grains are also common within samples studied; martitization being a process involving the oxidation and replacement of magnetite by haematite along (111) cleavage directions. (Craig and Vaughan 1981)

Some grains present show rhythmically banded haematite and silicate. Turner and Ixer (1977) and Turner, Ixer and Waugh (1978) described similar grains in the Triassic St Bees Sandstone, and concluded that the texture may be indicative of a low temperature hydrothermal origin.

Rutile / anatase ( $\text{TiO}_2$ ) is also present as a detrital component, and occurs as large rounded leucoxene grains. Zircon and tourmaline are also present.

In terms of a provenance for the Bridgnorth

Sandstone, it is suggested that much of the detritus was derived from sandstones, meta-sediments and volcanics of Palaeozoic / Precambrian age, which formed upland areas (e.g. The Malvern Axis) adjacent to basin margins.

## 7.2 AUTHIGENIC MINERALOGY.

### 7.2.1 Feldspar.

Authigenic alkali feldspar is very common as overgrowths upon detrital clasts within the Bridgnorth Sandstone. Overgrowths occur chiefly as "saw-tooth" forms on the margins of clasts (See Plate 7.1 and 7.2). Occasionally they occur where feldspar occurs at the margins of composite grains such as sandstone rock fragments. Less commonly authigenic feldspar occurs as porefilling crystals exhibiting "adularia habit" and preferred orientation.

The use of S.E.M. reveals that tiny authigenic feldspar crystals with adularia habit often occur growing within crystallographically orientated solution pits within detrital alkali feldspars. (See Plate 7.3).

Electron microprobe analysis of feldspar overgrowths reveals them to be composed of K, Al, and Si, whilst host clasts commonly contain minor amounts of Na (See Table 7.2.1). The high degree of chemical purity exhibited by these overgrowths has been documented previously by Waugh (1978), and the data presented in figure 7.2.1 compares very closely with Waugh's results.



### 7.2.2 Quartz.

Authigenic quartz is present in only very minor quantities within the Bridgnorth Sandstone. It occurs mainly as ragged, very poorly developed overgrowths on detrital grains. Rarely it occurs as tiny euhedra which are best observed within samples from the Kempsey Borehole, and frequently occur upon quartz clasts with incomplete pellicular coatings. In terms of a paragenesis, authigenic quartz appears to post-date authigenic feldspar and authigenic illite / smectite.

### 7.2.3 Illite / Smectite Clays.

Clays of illite / smectite composition commonly occur as small, very poorly crystalline, irregular flakes tangentially coating grain surfaces. Clays of this type form red (haematite stained) pellicles around detrital clasts. S.E.M. analysis reveals that these illitic clays form "meniscus bridges" between clasts, the bridges being composed of twisted amalgamations of illitic fibres and flakes. Tangentially orientated grain coating clays are interpreted as being allogenic.

Illite / smectite clays also occur as authigenic grain coatings / pore linings (see Plate 7.4). They are composed of poorly crystalline platelettes orientated perpendicular to grain surfaces, and commonly exhibit a poorly developed "boxworked" texture. Clays of this type are best developed within subsurface samples collected from the Kempsey Borehole, and are interpreted as authigenic clays formed partly by the recrystallisation

of allogenic grain coatings.

In terms of a paragenetic sequence, most illitic clays appear to have formed prior to authigenic feldspar and quartz. However, some clays clearly coat authigenic feldspar crystals, indicating that some illitic material was formed following feldspar authigenesis.

#### 7.2.4 Kaolinite.

Kaolinite is common within the Bridgnorth Sandstone (see Plate 7.5). Kaolinite occurs as pseudomorphs bound within haematite stained pellicles, and as porefilling cements within oversized pores. In terms of a paragenesis the bulk of kaolinite forms earlier than diagenetic calcite, but post-dates feldspar dissolution and authigenesis. The presence of "un-deformed" kaolinite pseudomorphs "floating" within secondary pores suggests that pseudomorphs formed following compaction of the Bridgnorth Sandstone. Some kaolinite may post-date authigenic calcite.

#### 7.2.5 Carbonate Cements.

Carbonate cements within the Bridgnorth Sandstone occur as both non-ferroan calcite and dolomite. Carbonate cements are exceedingly rare at surface outcrop, but are abundant in samples from the Kempsey Borehole.

Carbonate cements within samples from the Kempsey Borehole consist predominantly of non-ferroan calcite, although minor volumes of non-ferroan dolomite are also present in some samples. Cements occur as discrete

euohedral rhombs, or as larger, anhedral, poikilotopic nodules. In some samples dolomite replaces an earlier phase of anhydrite.

In rare carbonate cemented samples collected from surface outcrop, both non-ferroan calcite and non-ferroan dolomite are present. Ferroan calcite is rare, and when present is found as a replacement phase occurring within thick opaque grain coatings. Dolomite within these samples forms after calcite (see Plate 7.6), and cement textures are often poikilotopic.

Cold cathodoluminescence microscopic analysis of surface specimens of Bidgnorth Sandstone reveals the presence of minute areas of orange luminescing carbonate which are not detected using conventional petrographic techniques. Luminescent centers occur mainly as isolated "specks" within areas of porefilling clay / haematite, in otherwise carbonate free samples. Less commonly they are pervasive throughout clays, where they may occur as slightly larger crystals.

In terms of a paragenesis, carbonate cements post-date authigenic feldspar, quartz, illite / smectite, and some kaolinitic clay.

#### 7.2.6 Anhydrite.

Anhydrite is rare, and has been observed only in a few samples from the Kempsey Borehole, where it occurs as small, irregular areas of cement largely replaced by dolomitic carbonate.

### 7.2.7 Baryte.

Baryte cements are observed both in surface outcrop and in samples from the Kempsey Borehole.

Baryte in samples from the Kempsey Borehole is extremely rare. When present it occurs associated with anhydrite cements, infilling small areas of primary porosity.

Baryte within samples collected from surface outcrop appears to be a relatively late phase, occurring as euhedral "lath-like" crystals which extend across oversized secondary pores and often completely encompass clastic constituents (see Plate 7.7). Late baryte cements within aeolian sands cropping out at Rock Hall are probably related to Cu and Ba mineralisation present along nearby faults.

## 7.3 QUANTITATIVE PETROLOGY.

Quantitative analysis of the Bridgnorth Sandstone was accomplished by simple point counts, X-ray diffraction analysis of clay sized sediment fractions, and whole rock geochemical analysis using X-ray fluorescence spectroscopy.

### 7.3.1 ANALYSIS OF POINT COUNT DATA OBTAINED FOR THE BRIDGNORTH SANDSTONE.

Counts of 250 points per thin section were carried out on representative specimens collected from both surface outcrop and the Kempsey Borehole.

Compositional data obtained during point counting were used in order to produce ternary compositional plots (Pettijon 1973), and also four variable quartz type diagrams which Basu et al (1973) suggest are indicative of rock types present within source areas (see Figures 7.3.1 - 7.3.4). Point count data was also used in order to provide an indication of sediment size and sorting, and results obtained are summarised in Figure 7.3.5.

Figure 7.3.5 indicates that the Bridgnorth Sandstone is composed of fine - medium grained sands which are typically moderately - moderately well sorted, and show moderate - close packing. Surface samples display looser packing, and better sorting and porosity than samples collected from the Kempsey Borehole. Looser packing within surface samples may indicate that they have never been buried as deep as samples from the Kempsey Borehole, or may simply be an artifact of surface weathering and clast dissolution.

Approximate estimates of compaction may be obtained from point count data by assuming initial porosities of 39% for wind ripple strata, and 45% for sand flow laminae (Hunter 1977). Estimates of compaction for near surface samples of aeolian Bridgnorth Sandstone are 14% - 24%, and estimates of compaction for subsurface samples of Bridgnorth Sandstone are 29% - 40%.

Surface samples apparently contain higher proportions of both porosity and authigenic feldspar than subsurface samples. Much of the porosity within surface

samples is secondary in origin, and calcite cements are absent - presumably because they have been leached out as a result of surface weathering.

Grain coating clays of illite / smectite composition are abundant in samples from the Kempsey Borehole, but are poorly developed in surface samples. Weathering processes may account for the removal of grain coating clays, and also increased kaolinite content within surface samples.

### 7.3.2 SEMI QUANTITATIVE X-RAY DIFFRACTION ANALYSIS OF THE CLAY SIZED SEDIMENT FRACTION WITHIN THE BRIDGNORTH SANDSTONE.

X-ray diffraction analysis of ten surface samples and five subsurface samples were carried out in order to establish the composition of the clay sized sediment fraction within the Brignorth Sandstone.

Samples were prepared and run using techniques outlined in section 3.4. Relative percentages of clay minerals present were estimated using simple calculations outlined in Carver (1974), and are presented in tables 7.3.1 and 7.3.2.

X-ray diffractograms of clay mineral separates from the Bridgnorth Sandstone are summarised in table 7.3.3. Analysis of X-ray diffractograms indicate that illitic and smectitic clays dominate the clay mineral assemblage. The movement of illite (001) and (002) peaks in opposite directions upon glycolation of samples is

indicative of the interstratification of illite and smectite. A reflection between 12A and 17A in diffractograms from glycolated samples indicates that this interstratification is ordered to some degree, and the tables of Reynolds (1984) suggest an admixture with 80% - 90% illitic layers. The loss of a reflection at 7A upon heating samples to 550°C indicates that kaolinitic clays dominate over chlorite.

### 7.3.3 WHOLE ROCK GEOCHEMICAL ANALYSIS OF THE BRIDGNORTH SANDSTONE USING X-RAY FLUORESCENCE SPECTROSCOPY.

Results of whole rock geochemical analysis of the Bridgnorth Sandstone are presented in table 7.3.4.

A comparison of aeolian samples collected from the Kempsey Borehole with aeolian sands collected from surface outcrop is included in table 7.3.5.

Geochemical data compares favourably with point count data, i.e. samples collected from surface outcrop have higher Si and K contents, but lower Al, Fe, Ca, Mg, Mn and Ti contents than subsurface samples.

The absence of carbonate cements within surface samples can explain their lower Ca, Mg, and Mn content compared to subsurface samples. Also, a lower percentage of iron stained clays (illite / smectite) within surface samples contributes to their lower Al, Fe, Ca and Mg content. S.E.M. study reveals most surface samples consist of "polished" quartz clasts with only poorly

developed grain coating clays, whereas subsurface samples contain abundant grain coating and pore lining clays.

#### 7.4 THE DIAGENESIS OF THE BRIDGNORTH SANDSTONE.

A paragenetic sequence for authigenic mineral phases within the Bridgnorth Sandstone has been constructed using both surface and subsurface samples, and is illustrated in Figure 7.4.1

Diagenesis commences at deposition by processes similar to those described by Walker *et al* (1978). The mechanical infiltration of allogenic clays which contribute to grain coatings, and early dissolution / replacement of labile silicate clasts (minerals low in the stability tables of Goldich 1938) in near surface high Eh, high pH groundwaters. Elements released as a result of these dissolution and replacement reactions include Fe, Al, Si, Ca, Mg, K etc (Walker *et al* 1978). Continued intrastratal hydrolysis of silicates with burial will result in the dissolution of minerals such as alkali feldspar, which occur higher in Goldich's (1938) stability table (see Plate 7.8).

Following the infiltration of clays, the earliest pore-filling authigenic phases identified within the Bridgnorth Sandstone are anhydrite and baryte. These have only been recognised within borehole samples, and are by no means common. It is suggested that they precipitated from evaporative waters close to the sediment surface, and their cation source may also be



related to early intrastratal dissolution of silicates.

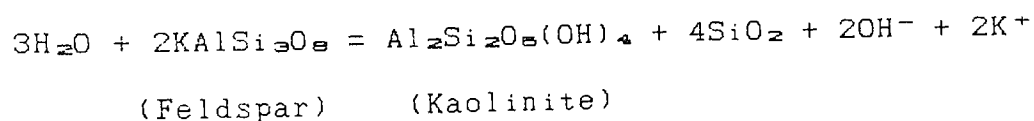
K, Al, and Si released as a result of intrastratal clast dissolution are incorporated into authigenic clays of "illitic" composition. These clays are actually largely of illite / smectite composition, and typically form poorly crystalline grain coatings / pore linings, often with a poorly developed "boxwork" texture. They may in part represent the recrystallisation of allogenic grain coating clays in early K rich porewaters.

The Fe released as a result of clast dissolution / replacement in near surface high Eh, high pH groundwater is precipitated as a "pigment" within pellicular grain coatings. This "reddening process" stains both allogenic and authigenic grain coating and pore lining illite / smectite clay. Walker (1967) proposed that the initial iron mineral which formed within grain coating clays was a ferric hydrate "precursor" which converted to haematite upon aging.

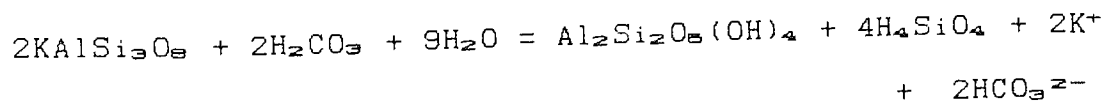
Following the precipitation of illitic clays under an initially high  $K^+/H^+$  ratio, interstitial solutions were depleted in K, Al, and Si. Lowering of the  $K^+/H^+$  ratio of porewaters following illite precipitation leads to the formation of alkali feldspar (Ali and Turner 1982) which precipitates as optically continuous overgrowths upon detrital clasts (see also the combination diagram in Figure 3.8.12). The source of  $K^+$  for feldspar authigenesis is assumed to be the dissolution of labile clasts and detrital feldspars.

That some dissolution of detrital feldspar had occurred prior to feldspar authigenesis is clearly evidenced by the presence of authigenic feldspar crystals growing within dissolution voids, or from crystallographically orientated solution pits in detrital clasts (see Plate 7.3).

Continued depletion of  $K^+$  concentrations within intrastratal solutions occurs as a result of feldspar authigenesis, and leads to a phase of kaolinite precipitation. Kaolinite occurs as both porefilling cements and also as pseudomorphing phases after alkali feldspar. The latter is clearly evidenced by the presence of kaolinite pseudomorphs with poorly developed alkali feldspar overgrowths. The hydrolysis of feldspar and formation of kaolinite may be summarised by the use of simple reactions of the type indicated below:



EQUATION 7.1



EQUATION 7.2

Authigenic silica (which is only poorly developed within the Bridgnorth Sandstone) is interpreted as having precipitated following the authigenesis of "illitic" clay, feldspar and kaolinite. When porewaters were

sufficiently depleted with respect to  $K^+$  and  $Al^{3+}$ , and relatively enriched in Ca, Mg, and Si.

Silica authigenesis is followed by the precipitation of carbonate cements (predominantly calcitic) following depletion of porewaters with respect to silica, and hence enrichment relative to Mg, Ca and bicarbonate. Calcium was derived ultimately from labile silicate clast dissolution, and bicarbonate present within solutions is probably derived as a result of both the dissolution of calcitic cements within sandstone rock fragments, and meteoric input into groundwater systems. The dolomitisation of calcitic cements occurred at some stage during diagenesis, possibly as a result of increased Mg/Ca ratios within porewaters following initial calcite precipitation.

Calcitic cements are one of the latest authigenic phases to precipitate, and this is evidenced by their "enclosing" both kaolinitic clays, and feldspar clasts with authigenic overgrowths. However, some authigenic minerals present (especially in surface outcrop) clearly post-date the precipitation of carbonate cements. These phases include late stage kaolinite, illite / smectite, iron oxides and baryte.

Late kaolinite, illite / smectite and iron oxides are interpreted as having formed following uplift of the Bridgnorth Sandstone into a zone of freshwater diagenesis, i.e. they are the product of surface weathering. Where observed at Preston Brockhurst, late baryte cements occur in sediments adjacent to mineralised

faults.

Labile silicate dissolution and kaolinitisation of feldspars are important porosity enhancing processes within the Bridgnorth Sandstone. The large extent to which secondary porosity is developed in surface outcrop is aided by the removal of carbonate cements. The characteristic pale "mottles" observed within the Bridgnorth Sandstone appear to occur at the site of former carbonate cement nodules.

#### 7.5 CONCLUSIONS - CHAPTER SEVEN.

(i) Aeolian sediments consist of sublitharenites and subarkoses. The proposed diagenetic sequence for authigenic minerals within these sediments is: early anhydrite / baryte, illite / smectite clays, haematite, feldspar, kaolinite, quartz, and carbonate.

A late stage of clay / iron oxide diagenesis recognised within surface sediments occurred upon uplift of the Bridgnorth Sandstone into a zone of subaerial weathering.

(ii) Authigenic illite and smectite dominate clay mineral assemblages within aeolian facies sandstones. Interstratification of illite / smectite is observed, and an admixture with 80% illitic layers is common.

(iii) The "scoured", and erosional nature of the Permo - Triassic unconformity within the region of study reveals that considerable induration of the Bridgnorth

Sandstone occurred during the Permian, prior to the deposition of the Kidderminster formation.

(iv) The model proposed to explain the sequence of authigenic minerals within the Bridgnorth Sandstone involves the evolution of porewater systems with burial in order to precipitate ionic species derived from early labile silicate clast dissolution / replacement. The dissolution and replacement of labile silicate clasts resulted in the creation of enhanced or secondary pores within the Bridgnorth Sandstone.

(v) Aeolian sands were subject to moderate amounts of compaction during burial, but this is only evidenced in borehole samples. The estimated compaction within subsurface samples of Bridgnorth Sandstone is 29% - 40%. In samples collected from surface outcrop, continued clast dissolution under surface conditions has lead to enhanced secondary porosity development, and an artificially loose "packing". Estimates of compaction within surface samples of Bridgnorth Sandstone are 14%-24%.

(vi) Whole rock geochemical analysis of the Bridgnorth Sandstone reveals that surface samples are depleted with respect to Al, Fe, Ca, Mg, Mn, and Ti, when compared with subsurface samples. This reflects the removal of carbonate cements, grain coating clays, and any unstable clasts still present under conditions of surface weathering. It suggests that extreme care needs to be

exercised when evaluating diagenesis in samples collected from surface outcrop, especially in porous strata such as aeolian dunes.

## CHAPTER EIGHT.

### THE SEDIMENTOLOGY AND STRATIGRAPHY OF THE HOPEMAN SANDSTONE.

#### 8.1 INTRODUCTION.

The Hopeman Sandstones are a sequence of drab continental sediments cropping out along the southern margin of the Moray Firth coast between Burghead and Covesea Skerries. Sandstones comprise chiefly of aeolian deposits, although minor fluvial horizons are present. The sands contain large scale soft sediment deformation structures, and have also yielded reptilian faunas. The maximum thickness of the Hopeman Sandstone determined in the I.G.S. borehole at Clarkey Hill is 60m.

#### 8.2 STRUCTURAL SETTING.

The Hopeman Sandstones were deposited in a marginal setting to the Moray Firth Basin, an approximately northeast - southwest trending structure probably initiated during the early Permian, and floored by Old Red Sandstone and Carboniferous sediments. (Glennie 1982).

The limits of the Moray Firth Basin are broadly defined by the Helmsdale and Great Glen Faults in the west, the northeast extremity of the Grampian Spur in the east, the Grampian Highlands in the south, and the Caithness Ridge and Wick fault zone in the north.

Deep seismic data (Chesher and Lawson 1983)

indicates that the Mesozoic basin depocenter lay somewhere to the south of the Great Glen Fault, and attained a depth of at least 3000m.

The basin margins are fault controlled. All Mesozoic strata within the Moray Firth Basin have been affected by faulting, the faults commonly being parallel or sub-parallel to the trends of the basin margins.

Important periods of fault activity recognised by Chesher and Lawson (1983) include: Post base Permo/Triassic - Pre lower Jurassic faulting, lower - middle Jurassic faulting, and lower Cretaceous faulting.

Major faults such as the Great Glen Fault zone were active throughout the Mesozoic, and may represent reactivation of earlier zones of weakness.

A sketch map illustrating the location of the study area and major structural elements is shown in figure 8.2.1.

### 8.3 STRATIGRAPHY.

The Hopeman Sandstones occur at the base of the Permo - Triassic sequence along the Southern Moray Firth coastline. They are overlain by (and may be partly coeval with) the Burghead Sandstone Formation - a "Triassic" fluvial sequence. The Burghead Beds are overlain by and partly coeval with the Lossiemouth Sandstone, a predominantly aeolian sequence with minor fluvial horizons. The Lossiemouth Sandstone passes upward into a conglomeratic horizon known locally as the



" Sago Pudding Sandstone", which in turn passes upwards into, a silcretised / calcretised horizon known as the Stotfield Cherty Rock.

The stratigraphic age of the Hopeman Sandstone cropping out along the Moray Firth coastline and its relationship with similar sandstones found inland at Quarry Wood (also known as Cutties Hillock, Grid Ref. NJ 1850 6380) has been the subject of intense debate for many years. Age dating of the sands has been accomplished using reptilian remains and trace fossils. A major problem in correlation arises because to date only inland exposures have yielded reptile remains, whilst coastal exposures have only revealed reptile tracks.

Walker (1973) regarded the sandstones at Cutties Hillock to be of Upper Permian - Lower Triassic age. Peacock (1968) and Williams (1974) regarded the inland exposures and coastal exposures as time equivalents, and divided inland exposures around Quarry Wood into two zones:

(i) A lower unit consisting of pebbly based sheetflood deposits which lie unconformably upon the Old Red Sandstone, and show evidence of being fluvially reworked aeolian deposits.

(ii) An upper unit of approximately 30m cross bedded sandstone which Williams (1974) interpreted as fossil barchan dunes.

Warrington *et al* (1980) provide a classification of the Permo - Triassic rocks of Elgin which is shown in figure 8.3.1. Warrington recognised the Hopeman

Sandstone as being late Permian - Lower Triassic (Scythian) in age.

Glennie and Buller (1983) divided the Hopeman Sandstone Formation into two units: a lower unit, the upper portion of which contains large scale deformation structures; and an upper undeformed unit which they interpret as the equivalent of the sandstone cropping out at Quarry Wood.

Glennie and Buller (1983) attributed the large scale deformation structures present within the upper portion of their Lower Hopeman Sandstone unit to the escape of air/water from transverse aeolian dunes following the catastrophic flooding of the Moray Firth Basin by the Zechstein Sea. In this way they were able to suggest a correlation between the deformation structures in the Hopeman sandstone and those in the Weisslegend of northwestern Europe and the North Sea. This implies the Lower Hopeman Sandstone unit is Permian in age, whilst the Hopeman Sandstones which overlie deformed sands are Late Permian - Early Triassic in age.

Palaeontological studies (Benton and Walker 1985) indicate that reptile tracks within the Hopeman Sandstone cropping out along the Moray Firth coast resemble mid - late Permian dicynodont tracks elsewhere in the United Kingdom. Remains from inland locations include dicynodonts (Geikia and Gordonina) and a pareiasaur (Elginia), which indicate a date in the late Permian near the Triassic boundary. Benton and Walker

(1985) clearly distinguish between the Hopeman Sandstones, cropping out at coastal localities and those at inland locations, and recognise sandstones found at inland locations as forming a separate formation - The Cutties Hillock Formation.

In more recent work, (Clemmensen 1986) it has been suggested that the Hopeman Sandstone represents the deposits of "crescentic, reversing, or star dunes". Clemmensen suggests that Hopeman palaeowind directions results are similar to those found in lower Triassic reversing dunes in East Greenland, and that this indicates that both the dunes in east Greenland and northeast Scotland were affected by a global Triassic wind system rather than a local Permian wind system.

The debate continues...

#### 8.4 SEDIMENTOLOGY - LOCATION AND NATURE OF OUTCROPS.

The Permo - Triassic succession is exposed in a continuous coastal section between Burghead (Grid Ref. NJ 1100 6900) and Covesea (Grid Ref. NJ 1850 7100).

Cliff and wave cut platforms to the west of Burghead harbour are composed of Triassic Burghead Beds. These consist of stacked sequences of fine - medium grained, cross bedded (low angle planar or trough sets with sandy "bar - like" bedforms are present), fluvial sediments deposited in sandy braided ephemeral channels. Beds are typically highly silicified, and may contain nodular fluorite cement.

The Burghead Beds extend eastwards along the wave cut platform from Burghead harbour to Masonshaugh Quarries (Grid Ref. NJ 1298 6910), where they are down faulted against Hopeman Sandstones to the north. The fault (which trends W.N.W. - E.S.E.) is exposed in a recess at the east of the quarry. North and east of the fault, sandstones of aeolian character outcrop, and data of *Glennie and Buller* (1983) indicate that these sediments are in fact "Upper Hopeman Sandstone".

The sandstones at this location are rusty brown weathering, fine - medium grained, well sorted, and display cross bedding in which the angle of inclination of foresets increases upward (to 25°) within individual sets of strata. The sands have a bimodal texture composed of well rounded clasts. Bedding foresets dip towards 270°. Grainflow and grainfall laminae are recognised in some sediments. Trace fossils in the form of small (3cm - 4cm) regularly spaced reptile imprints may also be found at this location. Sands adjacent to the fault, are highly silicified, but become more friable when traced away from the fault zone. An abundance of mineralised veins parallel to the strike of this fault, and broadly coincident with the trend of the basin margin are visible in both the Burghead Beds and Hopeman Sandstone cropping out in the foreshore around Masonshaugh Quarries.

Excellent exposure of aeolian sandstone (Upper Hopeman Sandstone according to *Glennie and Buller* 1982)

occurs in cliffs and wave cut platforms between Masonshaugh Quarry and Greenbrae Quarry (Grid Ref. NJ 1380 6925). Limited outcrop also occurs in disused railway cuttings south of coastal sections. East of Greenbrae Quarry the aeolian sandstones contain abundant deformation structures and have been described as "Lower Hopeman" by *Glennie and Buller* (1982).

The coastal section provides spectacular outcrops of aeolian sandstone. In particular, cliffs between Masonshaugh Quarry and Cumingston caves. (Grid Ref. NJ 1270 6920) display aeolian sands in which the direction of foreset dip is continuously consistent with those observed at Masonshaugh Quarry, i.e. towards 270°. Foresets are typically 10cm - 20cm thick, and set boundaries occur on spacings of up to 10 meters or more. Foreset laminations within sets are approximately parallel, giving rise to planar cross stratification units, and aeolian strata are dominated by grainfall laminae. Uniform foreset dip direction over large distances and lack of opposing cross sets within these sandstones is probably indicative of the migration of large, relatively straight crested transverse dunes, with little interruption by modification events.

At Roddach Bow (Grid Ref. NJ 1365 6920) some 550m northeast of Masonshaugh Quarry, the first evidence of cross bedding with opposing dune foreset directions occurs within the aeolian sands cropping out along this coastal section. Sediments at this location are

moderately well cemented, fine - medium grained, well sorted sands comprised of small scale (typically 1m -3m) trough cross bedded dune sets, displaying "wedge-like" fabrics. (See Plate 8.1)

"Wedge-like" fabrics with opposing foreset directions may be generated within sequences of transverse aeolian dunes by either:

(i) Dune modification under directionally fluctuating or reversing winds;

(ii) The superimposition of large shallow trough sets, in which case the opposing foreset directions are an apparent phenomenon. "Wedge-like" fabrics with opposing foreset directions are also characteristic features within longitudinal or seif dunes, and *Williams* (1974) interperated part of the aeolian Hopeman sequence as seif-like dune forms. However, the lateral pinch-out of trough sets in two directions, and an almost consistant direction of infilling of trough forms (c.f. *Mader and Yardley* 1985) would suggest that the fabric observed at Roddach Bow is not that of a longitudinally orientated bedform.

"Wedge-like" fabrics with counterdipping foreset laminae observed at Roddach Bow probably arise as a result of the superimposition of small scale trough cross stratification sets on the lee side of transverse dunes.

Sediments at Rodach Bow contain baryte and carbonate cements. Baryte cements are present as "rosette" like aggregates (2.5cm in diameter) of baryte laths. Carbonate cements form "meniscus - like" pillars

between dune bedded foresets.

The aeolian sands at Roddach Bow also contain sediment structures the origin of which are uncertain. The features occur as "groove-like" casts on the base of a slab of overhanging rock at a cave entrance. (Grid Ref. NJ 1365 9620). (See Figure 8.2) The grooves (1cm-2cm wide, and up to 30cm long) are preserved as positive features visible upon the base of the slab, on the planar surface of an inclined dune foreset, a region in which sedimentary structures have low preservation potential. The grooves may represent the tail resting traces of some type of small reptile. However, if this were the case it is perhaps a little unusual that there are no footprints preserved in the same slab.

Alternatively, the features may represent parts of "avalanche scars" preserved on the slip face of a dune, features similar to those described in the Lyons Sandstone by Walker and Harms (1972).

East of Hopeman, between Hopeman harbour (Grid Ref. NJ 1460 6994) and Covesea Skerries (Grid Ref. NJ 2020 7135) the coastal section provides excellent exposures of predominantly aeolian sediments containing large scale deformation structures, (Lower Hopeman Sandstone of Glennie and Buller 1983).

Lower Hopeman aeolian deposits consist of yellow - grey (rusty brown weathering), fine - medium grained, well sorted sands. They are poorly cemented and composed of well rounded clasts. Grainfall and

grainflow deposits are recognised, although the latter are not prolific. The sands display large scale cross bedding, often with opposing foreset directions. Generally foreset directions along the Covesea coast indicate deposition within an approximately north-easterly prevailing wind system. Aeolian sandstones cropping out below the eastern wall of Hopeman harbour (Grid Ref. NJ 1460 6994) and in the foreshore to the north of Hopeman Lodge and Bremou Well (Grid Ref. NJ 1515 7010) contain abundant nodules of baryte cement.

Soft sediment deformation structures along this coastline are spectacular. They consist primarily of large "dish" structures separated by fluid escape columns or sheets, overturned bedding, and complexly deformed bedding. Dish structures occur on a variety of scales, and may range from less than one meter to tens of meters in diameter. (See plate 8.3).

Deformation structures are believed to have formed by liquefaction as a result of the evacuation of trapped air pockets from sand dunes following inundation of the Permian dune field by the Zechstein transgression. (Glennie and Buller 1983). Associated features include sandstone dykes, and totally structureless sands which are often tightly packed and apparently well cemented. These "tight" sands probably formed by consolidation and re-packing of dune sands following air/water escape.

At Grid Ref. NJ 1550 7030, in the foreshore to the north of Hopeman golf course, a rare example of a fluvial



sand is present interbedded with deformed aeolian sandstones.

The fluvial sediments consist of 2m - 3m of medium and fine grained sandstones, the base of which contain 9 pebbles, mudflakes, and lithified sandstone clasts. Well rounded clasts and a bimodal texture within fluvial sands indicates they contain a reworked aeolian component. Lithified sandstone clasts are not lithologically different to Hopeman sands, and are indicative of early diagenetic processes binding sediment and allowing its transportation as a coherent clast. Individual units may fine upward from a pebble "lag" at their base, or may be internally structureless. Ripple forms indicating flow towards 340° are present upon bedding surfaces some 15cm above the base of the fluvial sediments. Reptile footprints are also present at this location (see Plate 8.4). Fluvial sediments were probably deposited as sheetfloods.

*Glennie and Buller (1983)* have interpreted some shallow water ripples and streaming lineations within sands along this coastline as having formed in sub-aqueous environments associated with the Zechstein transgression. They suggest that some structureless sands which are overlain by shallow water ripples were deposited from sand volcanoes or fissures, and oozed out over adjacent "saucer-like" deformation structures.

East of Hopeman, the steep cliffs around Clashach and Covesea Quarries provide spectacular exposures of

large scale dunes.

Cliff sections at Covesea Quarries contain further evidence of soft sediment deformation within the aeolian sand sequences. Here deformed aeolian sands overly uniformly southward dipping sandstones, interpreted by *Glennie and Buller* (1983) as representing a transverse dune deposit. Similar transverse dune deposits are visible in the cliffs backing coves to the east of Covesea Quarries, where the large scale of the aeolian cross bedding is clearly evident, e.g. at Grid Ref. NJ 1718 7038, some 350m East of Covesea Quarries, very large scale trough cross bedding is evidenced by the presence of a major curved bounding surface (second order) separating two sets of strata (see Plate 8.5.). Counter-dipping foreset directions between lower and upper sets at location 1 in Plate 8.5 are only apparent; as evidenced by the presence of coincident foreset dip directions for lower and upper sets at location 2. Generation of apparently counter-dipping fabrics occurs as a result of the superimposition of the upwind and downwind (or left and right sides) of very large shallow trough sets.

At Clashach Quarry (Grid Ref. NJ 1630 7020), friable yellow dune sands show large scale trough cross bedding often displaying "wedge-like" fabrics with opposing foreset directions, (see Plates 8.6 and 8.7) Opposing foresets dip towards  $264^{\circ}$  and  $165^{\circ}$ . Comparison of Plates 8.6 and 8.7 with Plate 8.5. (coastal section

east of Covesea) might lead to the conclusion that counter-dipping wedges visible at Clashach quarries are an apparent phenomenon produced by the overlapping of large shallow trough sets. At Clashach however, opposing foreset directions within superimposed dune sets appear to be laterally consistent, a feature which might not be expected in the case of superimposed troughs (unless very large), and may reflect dune modification under a fluctuating wind regime. Sands around Clashach Quarries are dominated by grainfall laminae.

Exposures adjacent to a small cave within Clashach Quarry, (Grid Ref. NJ 1600 7012) contain abundant carbonate cements, which occur as vertical "pillars" or "sheet-like" bodies orientated parallel to the place of dune foresets (see Plate 8.8.). This cement morphology may be indicative of ponding of mineralising fluids at permeability barriers / gradients occurring at bedding planes.

#### 8.5 SEDIMENTOLOGICAL MODEL.

The proposed model for the Hopeman Sandstone is one in which large transverse dunes were deposited in a basin margin setting, subject to minor fluvial influence. A transverse dune system deposited within a north-easterly prevailing wind system (first proposed by *Glennie and Buller* 1983) is favoured over the star dune model of *Clemmensen* (1988) on the basis of field observation, i.e. the presence mainly of large scale

dunes with uniform foreset dip direction traceable over quite large distances. Studies of recent star dunes (Nielsen and Kocurek 1987, McKee 1979, 1982, Fryberger and Dean 1979, and Lancaster 1983) indicate that star dunes form under wind regimes with three or more wind directions.

Clemmensen (1988) presents a scenario for the Hopeman Sandstone in which "complex star dunes alternate with star dune corridors which contain fields of smaller reversing dunes, interdune flats, or (rare) ephemeral streams". Some star dunes are interpreted by Clemmensen as being stationary, whilst others were laterally migrating, (stationary bedforms gradually being replaced by laterally migrating bedforms with time). Clemmensen (1988) recognises two types of aeolian deposit within the Hopeman Sandstone:

(i) Deposits composed of small to giant scale trough cross stratification sets, frequently containing sand-flow strata, and representing dune slipface and associated lee side deposits.

(ii) Counter-dipping, wedge shaped, large scale or giant scale sets dominated by wind rippled and sand-fall strata.

Nielsen and Kocurek (1987) studying star dunes in the Dumont Dune Field (California), noted that star dune deposits consist predominantly of low to moderate angle wind ripple laminae separated by gently inclined truncation surfaces. Slip face preservation is likely within star dunes if the dune was stationary and

vertically accreting, but not if the slip faces migrated back and forth across the dune. Slip face deposits would be unlikely to be preserved in migrating star dunes even under high angles of climb. *Nielson and Kocureck* also note that stationary vertically accreting star dunes give rise to lenses of dune strata (with abundant opposing sets) separated by interdune deposits; whereas star dunes that migrate should form "sheet-like" deposits separated vertically and laterally by interdune deposits. Neither case appears to be applicable to the Hopeman Sandstone Formation where interdune deposits are rare; a feature which indicates dune accumulation within a sand saturated wind system. (c.f. The Bridgnorth Sandstone)

Truly opposing foreset dip directions, where observed in the Hopeman Sandstone reflect processes of dune modification and merging by alternating erosional and depositional bedforms under a fluctuating wind regime. In addition to these, apparently counter dipping foreset directions arise as a result of the superimposition of large shallow trough sets - a feature which again reflects modification under the alternating activity of erosional and depositional bedforms.

The origin of deformation structures within the Hopeman Sandstone is problematical. *McKee* (1945) used the sliding or slumping of small masses of sand on aeolian slip faces under local overloading (e.g. animals or rainfall) in order to explain small scale deformation structures within the Coconino Sandstone. Whilst this mechanism might be useful in explaining some small scale

structures within the Hopeman Sandstone (e.g. possible avalanche scars at Roddach Bow), it probably occurs on too small a scale to explain large deformation structures within the Hopeman Sandstone.

The association of fluid escape features and sandstone dykes with deformed aeolian sequences indicates that deformation took place in the presence of water. Rapid fluctuations in the ground water table have been suggested by *Doe and Dott* (1980) in order to explain deformation structures within aeolian sand sequences of the Navajo Sandstone, and should be considered as a possible origin for deformation structures within the Hopeman Sandstone. However, deformation resulting from water table fluctuations would be centered in the lower portions of dunes, and unlike the deformation features observed within the Hopeman Sandstone, would be unlikely to extend upwards to the top of dunes (*Glennie and Buller* 1983). Also, the formation of very large scale deformation structures within the subsurface by this mechanism is considered unlikely, although such processes could arguably account for the presence of some smaller deformation features.

*Peacock* (1966) suggested that large scale deformation structures within the Hopeman Sandstone may be produced as a result of liquefaction and undercutting of slip faces by floodwaters associated with heavy rainfall. Recent work by *Frostick et al* (1988) also suggests that slumping on the flanks of large dunes after

heavy rainfall is the most likely mode of formation of deformation structures. *Frostick et al* utilise the presence of "well developed if minor" river channels that cut into the base of dunes in order to trigger erosion. They also state that the lack of marine sediments and "wholesale wave erosion" of poorly consolidated sand points toward an origin somewhat different to that proposed by *Glennie and Buller* (1983) for deformation structures.

*Glennie and Buller* (1983) attribute the large scale deformation structures present within the upper portion of their Lower Hopeman Sandstone unit to the escape of air/water from transverse aeolian dunes following the catastrophic flooding of the Moray Firth Basin by the Zechstein Sea. They suggest a correlation between deformation structures observed along the Moray Coast with similar structures in Poland (*Jerzykiewicz et al* 1976), and in offshore North Sea wells.

*Glennie and Buller* further use this hypothesis to explain drab colouration within the Hopeman Sandstone. The Hopeman Sandstones were above the water table at the time of Zechstein floods, and are therefore not red coloured because they never encountered oxidising subsurface desert waters. *Glennie and Buller* attribute the lack of marine "Zechstein" strata along the Moray Coast to its extreme basin margin position. They also suggest an extremely rapid geological transgression in order to explain the lack of peneplanation of the Rotliegend dune field, and presence of only shallow water

sedimentary structures overlying deformed aeolian units.

The model of Glennie and Buller (1983) provides a viable mechanism by which such large scale soft sediment deformation is likely to occur at the same stratigraphic level in the Hopeman Sandstone. The slumping of aeolian dunes due to heavy rainfall / fluvial reworking (Frostick et al 1988) is considered doubtful because fluvial horizons are rare, and their influence on the development of aeolian bedforms would be expected to be relatively minor. Furthermore, if deformation occurred by the undercutting of slipfaces (with rotational slip) by floodwaters, then the contacts between deformed and undeformed strata might be expected to be more steep than are observed in the Hopeman Sandstone (Peacock 1966). Clemmensen (1988), and Frostick et al (1988) suggest that deformation structures are not found at the same stratigraphic level, but are instead scattered throughout the sequence. However, this is difficult to prove because of the limited exposure. If correct though, it is still difficult to envisage deformation features such as large scale recumbent folds etc, forming by slumping during periods of heavy rainfall, or by subsurface mechanisms related to the expulsion of air / water as a result of compactional processes.

## 8.6 CONCLUSIONS.

(i) The Hopeman Sandstone comprises a drab, predominantly aeolian sand-body with only very minor



fluvial horizons. Aeolian sands are interpreted as the deposits of large transverse dunes, deposited within a north-easterly prevailing wind system.

(ii) Interdune deposits are rare within the Hopeman Sandstone, a fact which coupled with the large scale of aeolian bedforms points toward deposition within a sand saturated aeolian system.

(iii) The large scale of aeolian bedforms is clearly evidenced by large scale trough cross stratification sets (tens of metres thick) exposed in coastal sequences. Superimposition of very large scale sets may result in the development of aeolian sand sequences in which apparently counterdipping foreset fabrics are common, and care should be excersised to ensure that these are not confused with truly opposing foreset fabrics.

(iii) Fluvial horizons are minor and represent sheetflood deposits which flowed northward into the basin of deposition, reworking aeolian deposits.

(iv) The origin of large scale deformation structures is debateable. Groundwater fluctuations and slumping on the flanks of aeolian dunes as a result of undercutting by floodwaters associated with heavy rainfall may both contribute to deformation. However, the principle mechanism favoured is that of air / water escape from dunes during the catastrophic flooding of the Moray Firth Basin by the Zechstein Sea (as described by Glennie and Buller 1983).

## CHAPTER NINE.

### THE PETROLOGY AND DIAGENESIS OF THE HOPEMAN SANDSTONE.

Evaluation of petrology and diagenesis within the Hopeman Sandstone, was accomplished using thin section microscopy, Scanning Electron Microscopy, X-Ray Diffraction analysis of clay sized material, and whole rock geochemical analysis using X-Ray Fluorescence spectroscopy.

#### 9.1 DETRITAL MINERALOGY.

##### 9.1.1 Quartz.

Quartz grains form between 50% and 70% of total rock volume within the Hopeman Sandstone. Monocrystalline quartz having simple straight extinction is the dominant quartz grain type present and forms 63% - 85% of detrital quartz. Polycrystalline quartz grains having greater than three crystal units per grain are very common and constitute 6% - 20% of detrital quartz. Polycrystalline quartz grains of this type frequently display a "stretched" metamorphic texture, or textures with complexly sutured crystal contacts.

Polycrystalline quartz grains having only 2 - 3 crystal units per grain form up to 8% of detrital quartz, whilst monocrystalline grains with strongly undulose extinction are present in volumes up to 15%.

The inferred source area for detrital quartz using four variable quartz provenance diagrams of *Basu et al*

(1975) is one of middle - high rank metamorphic rocks.

See Figure 9.3.2

#### 9.1.2 Feldspar.

Detrital feldspar forms up to 5% of the Hopeman Sandstone, and occurs as potash feldspar and microcline. Feldspar grains are often severely corroded, and display well developed authigenic overgrowth.

#### 9.1.3 Rock Fragments.

Rock fragments form up to 5% of the Hopeman Sandstone, and occur mainly as fine grained quartzitic sandstone clasts, often displaying good intraclastic porosity.

Metamorphic and igneous rock fragments may also be present, and typically form less than 2% of the total clastic constituents. Metamorphic lithologies include highly strained metaquartzites, and less commonly mica schists. Igneous rock fragments occur as granitic lithologies with excellent graphic intergrowths and myrmekitic textures, or as rhyolitic lithologies with spherulitic textures.

Chert clasts are present in minor quantities in some specimens studied.

#### 9.1.4 Heavy minerals and detrital opaques.

Heavy minerals observed within the Hopeman Sandstone include zircons and tourmaline. Mica has been observed within some very fine grained aeolian deposits, but is not common.

Detrital opaques present and identified using reflected light microscopy include haematite, magnetite grains with martite textures, and leucoxene.

## 9.2 AUTHIGENIC MINERALOGY.

### 9.2.1 Quartz.

Authigenic quartz is widespread throughout the Hopeman Sandstone, and forms 1.5% - 30% of total rock constituents. Authigenic quartz occurs as optically continuous overgrowths around grains (see Plate 9.1), or as blocky cements formed by large euhedral crystals extending into secondary pores.

### 9.2.2 Feldspar.

Authigenic feldspar occurs in all samples studied, and forms up to 3% of total rock constituents. Feldspar cements occur as large crystals forming incomplete overgrowths on detrital grains. In terms of a paragenesis, authigenic feldspar forms earlier than quartz cements which often envelop them, (see Plate 9.2).

### 9.2.3 Illitic clays.

Illitic clays occur in the Hopeman Sandstone as poorly developed grain coatings, or as alteration products forming pseudomorphs after silicate clasts. Illite present within grain coating clays is interpreted as representing recrystallised allogenic and early authigenic clays originally of illite / smectite composition.

#### 9.2.4 Kaolinite.

Kaolinitic clays within the Hopeman Sandstone occur as pseudomorphing phases after alkali feldspar, or as porefilling masses of pseudo-hexagonal platelets (often infilling secondary pores).

#### 9.2.5 Calcite.

Calcite cements are rare within the Hopeman Sandstone. When observed, calcite occurs as small areas of nodular, non-ferroan cement which corrodes silicate clasts, and which clearly post-dates authigenic quartz and feldspar (see Plate 9.3). Poikilotopic textures are common within calcite cements. Calcite cements are often themselves corroded, and their removal results in the generation of secondary porosity.

#### 9.2.6 Fluorite.

Fluorite may occur as extensive nodular, and porefilling cements within the Hopeman Sandstone. When present, fluorite cements severely corrode silicate minerals, and post-date quartz, feldspar and calcite cements (see Plate 9.4). Fluorite is the latest authigenic phase to precipitate within the Hopeman Sandstone.

#### 9.2.7 Baryte.

Baryte cements are present at some localities studied, and occur as extensive nodular and porefilling phases which clearly post-date quartz and feldspar. Baryte cements often corrode and replace silicates, and

like fluorite are interpreted as being one of the latest phases to have precipitated.

### 9.3 QUANTITATIVE PETROLOGY.

Quantitative analysis of the Hopeman Sandstone was accomplished by use of simple point counts, X-ray Diffraction analysis of clays, and whole rock geochemical analysis using X-ray Fluorescence spectroscopy.

#### 9.3.1 POINT COUNT ANALYSIS.

Analysis of point count data was used in order to produce standard ternary compositional plots (after *Pettijohn* 1975), and also four variable quartz provenance diagrams (after *Basu et al* 1975). These are reproduced in Figures 9.3.1 and 9.3.2. Point counts were also used in order to produce an estimate of grain size, sorting and packing within the Hopeman Sandstone, and data is summarised in Figure 9.3.3.

The Hopeman Sandstone consists of fine - medium grained, moderate - well sorted, moderately packed aeolian sands (Figure 9.3.3). The sands are compositionally mature, consisting of orthoquartzites subarkoses and sublitharenites (Figure 9.3.1). Porosity within the Hopeman Sandstone is typically high (5% - 35%), and most commonly occurs as oversized, sinuous pores bordering corroded and apparently floating grains. These factors would suggest (by comparison with criteria of *Schmidt et al* 1977) that a significant proportion of

porosity is secondary in nature.

### 9.3.2 SEMI QUANTITATIVE X-RAY DIFFRACTION ANALYSIS OF CLAY SIZED SEDIMENT FRACTIONS WITHIN THE HOPEMAN SANDSTONE.

Semi - quantitative X-ray analysis of clay sized sediment fractions of the Hopeman Sandstone was accomplished using techniques outlined in section 3.4. Descriptions of diffractograms are included in table 9.3.1, and estimates of the composition of the clay sized separates, obtained using techniques outlined in Carver (1971), are presented in table 9.3.2.

Tables 9.3.1 and 9.3.2 indicate that illitic material dominates the clay sized sediment fraction (85% - 100% illite) within the Hopeman Sandstone. The lack of any movement of the 10A and 5A reflections (001 and 002 reflections for "illitic" material) upon glycolation of clay samples indicates that expandable clays are not present within the Hopeman Sandstone (Shrodon 1980). The implications of this are discussed in section 9.4.

### 9.3.3 WHOLE ROCK GEOCHEMICAL ANALYSIS OF THE HOPEMAN SANDSTONE USING X-RAY FLUORESCENCE SPECTROSCOPY.

Whole rock geochemical analysis of samples of the Hopeman Sandstone was carried out in order to quantify its composition, and results are presented in table 9.3.3.

No compositional differences were observed between samples from the Lower and Upper Hopeman

Sandstone divisions of *Glennie and Buller* (1983), suggesting continuity in both the source of detritus, and diagenetic processes operating within the two divisions.

The results of geochemical analysis tabulated in figure 9.3.6 are discussed in further detail in Chapter Ten of this report.

#### 9.4 DIAGENETIC MODEL.

A paragenetic sequence for authigenic mineral phases within the Hopeman Sandstone is shown in figure 9.4.1. The paragenetic sequence is very similar to those obtained for the Bridgnorth and Penrith Sandstones (See Figures 7.4.1 and 5.3.3 - 5.3.4), and a similar diagenetic model is proposed for the Hopeman Sandstone.

Diagenesis commences at deposition by processes similar to those described by *Walker et al* (1978), by infiltration of allogenic clays, and early labile silicate clast dissolution / replacement. Elements released as a result of these early replacement processes (K, Al, Si, Fe, Mg etc) are incorporated into authigenic "illitic" clays, alkali feldspar, kaolinite and quartz. The paragenetic sequence ILLITE - ALKALI FELDSPAR - KAOLINITE - QUARTZ, is identical to that which is observed in the Bridgnorth Sandstone, and it is suggested that the same processes occurred within these two formations.

Precipitation of "illitic" clays and the recrystallisation of allogenic clay coatings occurs under



initially high  $K^+/H^+$  following labile silicate clast dissolution / replacement. Iron released as a result of dissolution / replacement reactions would have been incorporated into haematitic pellicular staining, probably via a precursor ferric hydrate (Walker (1967)). It should be noted that in the Hopeman Sandstone "illitic" material consists of pure illite. No smectite or interlayered clays are present; a feature which may be explained by the thermal effects of later mineralisation upon early illite / smectite clay assemblages.

Following precipitation of early "illitic" clays interstitial solutions were depleted with respect to K, Al, and Si. In particular, the depletion of  $K^+$  relative to  $H^+$  leads to the precipitation of alkali feldspar as authigenic overgrowths (Ali and Turner 1982). Feldspar precipitation causes continued depletion of  $K^+$  within intrastratal solutions, and leads to a phase of kaolinite precipitation within the Hopeman Sandstone.

The precipitation of authigenic silica occurred within interstitial solutions following feldspar and kaolinite authigenesis, when porewaters were sufficiently depleted with respect to  $K^+$  and  $Al^{3+}$ . Extensive silica (and also alkali feldspar) authigenesis within the Hopeman Sandstone implies extensive early dissolution / replacement of labile silicate grains, since this is the proposed source of Si for authigenic overgrowth. The extensive development of secondary porosity within the Hopeman Sandstone partly supports this hypothesis. However, quartz overgrowths are often severely corroded,

indicating that much of the secondary porosity formed following silica authigenesis, by the removal of late stage replacive cements (carbonate, etc).

Carbonate cements (non-ferroan calcite) precipitate from solutions depleted in K, Al, and Si, but enriched in Ca and bicarbonate following the precipitation of early diagenetic phases. Calcite cements occur as poikilotopic nodules which clearly post-date authigenic feldspar and quartz, and which corrode detrital silicates.

Late stage cements within the Hopeman Sandstone include fluorite and baryte, both of which corrode all detrital grains and earlier authigenic phases. Fluorite and Baryte cements within the Hopeman Sandstone are associated with *galena - haematite - fluorite - baryte - calcite* mineralisation effecting pre - Jurassic strata (Permo - Triassic) along the southern Moray Firth coast.

*Peacock* (1968) noted that fractures within fluorite and calcite cemented Hopeman Sandstone were themselves infilled with later fluorite cement, clearly indicating two phases of fluorite deposition. The association between faulting / joints and mineralisation is clearly evidenced by the presence of abundant mineralised faults (approximately east - west) in Permo - Triassic sediments studied. *Moorbath* (1964) quotes a date of 140 +/- 60my for galena mineralisation within the Stotfield Cherty Rock, giving a Jurassic age for mineralisation. This suggests that diagenetic processes

which occur prior to mineralisation are effective largely during the Permo - Triassic. The origin of mineralisation is debateable, and a number of possibilities are outlined by Williams (1974). Magnetic anomalies below the Moray Firth have been interpreted as deep seated granites (Fenning 1968, Dimitropoulos and Donato 1981), and a hydrothermal origin for mineralisation is possible. Alternately, Williams suggested that mineralisation may originate from deep formation waters.

Glennie and Buller (1983) suggest that the interplay between oxidising Rotliegend groundwaters and the strongly reducing conditions of Kupferschiefer deposition might be responsible for the origin of brines leading to the precipitation of sulphide minerals and baryte within the Weissliegend of the North Sea and Poland.

Baryte and fluorite within the Hopeman Sandstone severely corrode silicate grains, and the mineralising fluids which precipitated these minerals might also have contributed to the advanced development of secondary porosity within the Hopeman Sandstone. If the brines causing mineralisation were "hot", then the lack of expandable clays within the Hopeman Sandstone might be explained by the conversion of smectite and mixed layer clays to illite under elevated formation temperatures.

Late stage kaolinite observed within the Hopeman Sandstone is interpreted as a surface weathering product.

## 9.5 CONCLUSIONS.

(i) The Hopeman Sandstone consists of fine - medium grained, moderately well sorted orthoquartzitic sands, sublitharenites and subarkoses. The high degree of mineralogical maturity within the sediments of the Hopeman Sandstone is enhanced by extensive dissolution of labile silicate clasts during diagenesis.

(ii) A paragenetic sequence for authigenic phases present within the Hopeman Sandstone is as follows: Illitic clays, Feldspar, Early Kaolinite, Quartz (major), Calcite, Baryte / Fluorite Mineralisation, Late Kaolinite.

Secondary enhancement of originally high porosities within aeolian sands occurred during early diagenesis via the dissolution / replacement of labile silicate grains; and also during late diagenesis via the removal of calcite cements, and dissolution / replacement of silicate grains during mineralisation.

(iii) The clay sized sediment fraction within the Hopeman Sandstone is dominated by illitic clays. No smectite or mixed layer clays are present. Original infiltrated clays and early diagenetic clays might be expected to have been of illite / smectite composition Walker (1976). The lack of smectites within the Hopeman Sandstone may be explained by either very high K<sup>+</sup> concentrations within early pore fluids, or the conversion of smectite to illite under the thermal effects of mineralisation.

(iv) No compositional differences were observed between samples from the Lower and Upper Hopeman Sandstone divisions of *Glennie and Buller* (1983), suggesting continuity in both the source of detritus, and diagenetic processes operating within the two divisions.

(v) The paragenetic sequence observed within the Hopeman Sandstone may be explained by the evolution with burial of porewater systems enriched in Si, Al, K, and Ca following early labile silicate dissolution.

## CHAPTER TEN.

### THE DIAGENESIS OF LOWER PERMIAN (ROTLIEGEND) DESERT SEDIMENTS - DISCUSSION.

Having described the facies types and diagenesis within Lower Permian sediments studied, it remains to compare the diagenetic sequences observed in different formations, and to try and evaluate the controls on diagenesis within the sediments of different basins.

Rotliegend sediments within offshore U.K. basins studied include strata from aeolian, fluvial, lake margin sabkha and playa lake environments. Rotliegend sediments within onshore U.K. basins studied include strata from aeolian, fluvial and alluvial fan environments.

Aeolian deposits comprise fine - coarse grained, red, bimodal sandstones, typically with high porosities. Fluvial strata are varied and may include poorly sorted red, fine - coarse grained sandstones or less commonly conglomerates. Lake margin sabkha deposits consist of fine grained red - brown siltstones and may be interbedded with red playa lake mudstones. Sediments from sabkha and playa lake environments display the poorest porosities and permeabilities observed within Rotliegend strata. Alluvial fan deposits identified within Rotliegend sequences are varied and include poorly sorted, fine - coarse grained sandstones and breccias.

With regard to the petrographic characteristics of the Rotliegend strata studied, four variable quartz

provenance diagrams (after Basu et al 1975) are all very similar, suggesting continuity in the nature of strata which originally sourced quartz clasts. The similarity in detrital rock fragments present within different formations (i.e. fine grained sandstone clasts, spherulitic rhyolites, metamorphic quartzites, and cherts) also suggests similarity in the nature of strata within source areas. However, these similarities can only be inferred, because the above mentioned lithic clasts are stable clasts remaining after diagenesis, and the degree to which they reflect the original sediment composition may vary greatly between formations.

Paragenetic sequences for authigenic phases within the Lower Permian sediments of onshore basins show remarkable similarity, and a mineralogical sequence consisting of early haematite, illitic clays, feldspar, kaolinite, quartz and calcite is observed in all onshore formations studied.

In the Leman Sandstone Formation of the North Ravenspurn region of the Southern North Sea however, constraints on burial history are readily available, and the paragenetic sequence observed consists of:

SHALLOW BURIAL DEPTH - early quartz, early baryte, non-ferroan dolomite, anhydrite.

INTERMEDIATE BURIAL DEPTH - ferroan dolomite, chlorite.

DEEP BURIAL - secondary porosity generation, kaolinite late quartz, illite, late siderite and baryte.

Differences in facies types present within North

Ravenspurm compared with facies types observed in onshore basins may account for differences in "early" diagenetic sequences observed between offshore and onshore basins.

In North Ravenspurm, the close association of aeolian and fluvial (sheetflood) sediments with the Silverpit Lake and facies of sabkha origin may influence early diagenetic processes. In particular, the migration of sabkha sourced brines into adjacent facies facilitates the early dissolution of labile silicates in alkaline groundwaters, and the precipitation of early evaporite minerals and dolomitic carbonate cements. In addition to this, fluvial sheetfloods appear to promote early silica cementation within the sediments which they deposit.

In the onshore basins studied, aeolian strata dominate the facies types present, with only minor alluvial sediments (deposited predominantly by sheetflood processes across alluvial fans) occupying basin margin locations. Fluvial strata (composed of conglomeratic channel fills and fluvial channel sands) are common in the Vale Of Eden, but are only very poorly developed in other onshore basins studied. The lack of sabkha facies sediments within onshore basins studied results in their sediments being subject to early diagenetic processes which include early labile silicate clast dissolution, and the precipitation of early haematite and clays of "illitic" composition. Al and K dominate over bicarbonate, Ca and Mg in the early porewaters of onshore



Permian sediments, and clay diagenesis is favoured over the precipitation of early carbonates. Early evaporite minerals have been observed within subsurface samples of the Bridgnorth Sandstone, but consist of only very minor amounts of anhydrite and baryte.

In onshore basins studied, "early" carbonate cements have only been observed within Permian sediments of the Eden Valley, and in this case their distribution is clearly facies selective, i.e. early carbonate cements (calcitic) precipitate within alluvial breccias and conglomeratic channel fills. The source of calcium and bicarbonate for the precipitation of these calcite cements is assumed to be the abundant carbonate rocks in source areas, and the distribution of early calcite clearly favours fluvial sands, and those facies which contain abundant carbonate clasts.

The influence of the nature of rocks occurring within source areas and in "marginal" facies upon diagenesis within Lower Permian sediments is illustrated by comparison of diagenesis of sediments within the Vale Of Eden with those present within the Worcester basin. In the Vale Of Eden, it is suggested that extensive dissolution of silicate clasts within carbonate - rich marginal alluvial facies results in the extensive development of quartz overgrowths within aeolian Penrith Sandstones occupying basinward locations.

In the Worcester basin however, sediments within marginal alluvial facies are dominated by clasts which

include quartzites, volcanoclastics and cherts, with only minor carbonate clasts. Thus, by comparison with the Penrith Sandstone, low carbonate clast contents resulted in conditions less suitable for quartz dissolution within marginal facies of the Worcester Basin, and hence a lower Si content within the early porewater system of the Bridgnorth Sandstone. This resulted in only poor development of quartz overgrowths within the Bridgnorth Sandstone.

Extensive quartz overgrowths have also been observed within the aeolian sediments of the Hopeman Sandstone Formation. Carbonate - rich marginal alluvial facies have not been observed within the Permo - Triassic of the Moray Firth Basin, and extensive silica overgrowths within aeolian sediments can not be readily explained by the model invoked for the Penrith Sandstone. However, extensive development of secondary porosity has occurred within the Hopeman Sandstone, a large proportion of which appears to have been generated after the precipitation of authigenic silica. Thus, if an intraformational source of silica is to be proposed for authigenic overgrowths within the Hopeman Sandstone, it is suggested that significant clast dissolution must also have occurred prior to quartz overgrowth. This may reflect the presence of a high proportion of labile silicate clasts within the sediments of the Hopeman Sandstone at deposition.

One of the most obvious differences between

diagenesis within onshore basins studied and the Leman Sandstone in North Ravenspurn, is the presence of well developed authigenic feldspar overgrowths only within Lower Permian sediments of onshore basins.

Authigenic feldspar has been documented within the Leman Sandstone of the Southern North Sea by Arthur *et al* (1986), Glennie *et al* (1978), Lee (1984), and Kessler (1978). It is necessary therefore to compare paragenetic sequences of these authors with those obtained for both onshore Rotliegend strata and also the Leman Sandstone of North Ravenspurn, in order to obtain a general model for Rotliegend diagenesis.

Arthur *et al* (1986) document a paragenetic sequence for authigenic mineral phases within the Leman Sandstone of U.K. Block 49/28 (Sole Pit region) as follows: early haematite, illite / smectite clays, authigenic feldspar, early non-ferroan dolomite, early quartz, anhydrite, illitisation of early clays, late quartz and kaolinite. The illitisation of early clays, and formation of late quartz and kaolinite in this paragenetic sequence are late, deep burial phenomena. The paragenetic sequence haematite, illite / smectite, alkali feldspar, carbonate and quartz however, is essentially the same as that observed within onshore basins studied; and it is significant to note that the facies types present within wells studied by Arthur *et al* are very similar to those observed within onshore basins, i.e. predominantly aeolian strata with only minor fluvial horizons.

Arthur et al (1986) suggest that the development of authigenic alkali feldspar indicates that depletion of  $K^+$  and  $Al^{3+}$  content of porewaters (sourced from labile silicate dissolution / replacement) following the precipitation of illite / smectite clays was not "total", and  $K^+$  remaining in solution was incorporated into authigenic feldspar, i.e. they favour a diagenetic scheme similar to that of Waugh (1978) and Ali and Turner (1982).

The similarity in both paragenetic sequences and facies types (mainly aeolian) of Lower Permian sediments within onshore basins studied and the study area of Arthur et al suggests that similar factors controlled the diagenesis of sediments in these locations. In particular, it should be noted that much of the Rotliegend sediment within onshore U.K. basins was apparently derived from material forming upland areas adjacent to those basins. Rotliegend strata within onshore basins may be regarded as representing "proximal" deposits, and therefore might be expected to contain more alkali feldspar and rock fragments than the Leman Sandstone in North Ravenspurn, which represents a "distal" environmental setting within the Southern Permian Basin. This would also apply for the Leman Sandstone within the Sole Pit region of the Southern Permian Basin studied by Glennie et al (1978), Kessler (1978), Lee (1984) and Arthur et al (1986); which would be expected to represent more "proximal" environmental

settings within the Southern Permian Basin. Thus, in distal settings such as North Ravenspurn, where detrital alkali feldspars would be expected to be present in "lower" quantities, a lower initial potassium content within sediments might result in a totally different paragenetic sequence to that which is observed in onshore basins, i.e. in this case depletion of  $K^+$  following initial illite / smectite precipitation may well be total, resulting in the absence of a later phase of alkali feldspar precipitation.

It is also possible that the lack of sabkha facies in the Permian of onshore U.K. basins resulted in less alkaline porewaters within sediments, and lesser amounts of silicate dissolution than occurs in offshore locations where sabkhas are well developed, e.g. in North Ravenspurn. The  $K^+$  contents of sabkha brines would be expected to be high (Bush 1970). Thus, if more alkaline porewaters occurred in facies adjacent to lake margin sabkhas, then it is possible that  $K^+/H^+$  ratios within these facies were always high, and precipitation of illite / smectite was always favoured over feldspar.

Thus, a model may be proposed to explain why authigenic feldspar is abundant within the Permian of onshore U.K. basins (and North Sea locations where sabkha development is limited), but absent from the Leman Sandstone of North Ravenspurn, where close proximity to the Silverpit Lake resulted in:

(a) The deposition of texturally mature sandstones with a low feldspar content.

(b) The development of abundant lake margin sabkhas.

Kessler (1978) studying wells from U.K. block 48/30 (Sole Pit area) also describes a stratigraphy dominated by aeolian dune and fluvial deposits. Kessler describes the sequence of diagenetic minerals here as: haematite, early authigenic clays and calcite, quartz, and late dolomite.

Like the data of Arthur *et al* (1978), Kesslers results again reflect a basic paragenetic sequence similar to that which occurs in onshore U.K. Rotliegend sediments, i.e. early haematite and illite / smectite, alkali feldspar, and quartz; but with the addition of an early calcite cement within fluvial sandstones.

A similar paragenetic sequence was obtained for authigenic minerals within the Leman Sandstone of Leman Bank and Indefatigable gas reservoirs by Lee (1984). Early haematite, carbonate and anhydrite, alkali feldspar, and after quartz, late clays (chlorite, illite, kaolinite). Lee however, did not favour an intraformational source of potassium for alkali feldspar overgrowths, and suggested that  $K^+$  ions might be derived from the overlying Zechstein or underlying Carboniferous.

Glennie *et al* (1978), studying the Leman Sandstone of Leman Bank and Sole Pit, document the presence of fluvial, aeolian and common adhesion rippled sabkha deposits within the Sole Pit area, and describe sabkhas as being interdune or lake margin type. They describe a

more detailed paragenetic sequence as follows:

EARLY - SHALLOW BURIAL DIAGENESIS: Haematite, illite / smectite clays, early calcite, calcite - dolomite transformations, transformation of plagioclase feldspar to kaolinite, and precipitation of authigenic feldspar.

LATE - BURIAL DIAGENESIS: Quartz, chlorite, and illitic clays, dolomite and anhydrite.

It is suggested in this case that a greater distance from the Silverpit Lake compared to North Ravenspurn is responsible for a sequence of diagenesis which is much more like that observed in onshore basins.

Both Lee (1984) and Glennie *et al* (1978) document a phase of early carbonate authigenesis occurring prior to feldspar authigenesis in the Leman Sandstone. In particular Glennie *et al* suggest that early calcite cements were common within "wadi" sandstones and precipitated in near surface environments. This corresponds with data obtained for the Penrith Sandstone.

Within the Leman Sandstone of the North Ravenspurn area, the products of diagenesis at depth include the development of ferroan dolomite and chlorite, with kaolinite, late quartz, illite, siderite and baryte occurring under deepest burial conditions (at 2Km - 3.5Km). The late stage development of kaolinite, illite and quartz during deep burial of Rotliegend sediments of the Southern North Sea has also been documented by Lutz *et al* (1975), Glennie *et al* (1978), Lee (1984), and Arthur *et al* (1986).

The controls on illite formation have been

documented as temperature (Perry and Hower 1970), potassium activity (Dypvik 1983), and residence time in the illite stability field (Bruce 1984).

Illite is well developed in parts of North Ravenspur, where no expandable clays are observed at all. Here, illitic clays are interpreted as forming both as a result of the illitisation of early grain coating clays, and also as a direct authigenic precipitate. In the Worcester Basin however, late stage illite has not formed in the Bridgnorth Sandstone of the Kempsey Borehole, and early grain coating and authigenic clays are still of illite / smectite composition.

It is suggested that the presence of smectite and mixed-layer clays within the Bridgnorth Sandstone indicates that these sediments were not buried as deeply as the Leman Sandstone in the North Ravenspur reservoir, and have never encountered temperatures suitable for smectite - illite transitions.

Smectite and clays of illite / smectite composition are also present within surface samples of the Penrith Sandstone. The Hopeman Sandstones however, contain no expandable clays. The lack of smectite within the Hopeman Sandstone may indicate deep burial of this formation, or prolonged contact with K<sup>+</sup> rich pore fluids. However, the Hopeman Sandstone also contains late fluorite and baryte mineralisation, and it is possible that the conversion of early authigenic clays to illite might have been facilitated by the presence of



"hot" mineralising fluids.

Late stage kaolinitic cements within Rotliegend sediments of onshore U.K. basins are interpreted as forming largely as a result of uplift into a zone of freshwater weathering.

It should be noted that the products of late, deep burial diagenesis in North Ravenspurn (kaolinite, illite, quartz and siderite) are developed to differing degrees in wells from different structures on U.K. block 43/26. Wells located upon the northern "B" structure which was "closed" earliest are good gas producers. Late diagenesis in the Lemn Sandstone of this structure resulted in the formation of only minor amounts of illite, but large volumes of late kaolinite and quartz. Late stage siderite and abundant secondary porosity are also present within this structure. Comparison of fluid inclusion homogenisation temperatures with horizon temperature / time plots results in interpretation of siderite as having precipitated during the Middle - Late Jurassic.

The Lemn Sandstone within wells located upon the "A" structure of North Ravenspurn however, contains abundant illitic clays, and lesser amounts of kaolinite and quartz than the Lemn Sandstone within "B" structure wells. It is suggested that the early trapping of aggressive Carboniferous - derived fluids associated with the onset of gas emplacement account for the diagenesis observed within the Lemn sandstone of the North

Ravenspurn "B" structure.

A similar model for late stage, burial diagenesis has been proposed by Arthur *et al* (1986) to explain the occurrence of kaolinite within gas producing wells of U.K. block 49/28 (Sole Pit). Arthur *et al* (1986) suggested that the kaolinite content of gas reservoirs was controlled by the CO<sub>2</sub> content of fluids migrating from source rocks. The possibility of this phenomenon occurring in Rotliegend sediments of onshore U.K. basins has also been suggested in this thesis, i.e. in the case of the Penrith Sandstone, where the locations of aeolian sands containing abundant authigenic silica and kaolinite coincide with Namurian and Coal Measure subcrops. Here, high CO<sub>2</sub> content within Carboniferous derived fluids may provide a mechanism for the precipitation of silica, much of which may be derived from clast dissolution / replacement in carbonate rich basin margin facies.

With regard to the timing of diagenetic processes, the following points are relevant.

(i) In the Bridgnorth Sandstone, a scoured and eroded unconformity between this formation and the overlying Kidderminster Formation suggests that much diagenesis occurred during the Permian, prior to deposition of the Kidderminster Conglomerates.

(ii) If Moorbaths (1962) date of 140my  $\pm$  60my for mineralisation within the Hopeman Sandstone is correct, then it suggests that diagenetic processes (of the type common to continental desert sediments) which occurred

within the Hopeman Sandstone were completed by the Jurassic

(iii) In the Southern North Sea, data for the North Ravenspurn region indicates:

(a) Dolomite and late quartz cements precipitated during the late Triassic, following the main phase of basin subsidence.

(b) The range of K-Ar dates obtained for illite separates is  $104 \pm 3$  my to  $203 \pm 4$  my. Samples yield a mean age of 173 my (Lower Jurassic).

(c) Late siderite cements formed during the Middle - Upper Jurassic. Again, the implication is that much of the diagenesis actually occurred during the Permo - Triassic, and was largely completed by the Middle Jurassic.

Compositional quantification of Lower Permian sediments was accomplished using X-ray fluorescence spectroscopy for whole rock geochemical analysis of selected samples. The data produced is presented in Tables 3.7.1 - 3.7.4, 5.1.1, 7.3.4, and 9.3.3. The comparison of aeolian sands from different basins on the basis of geochemical results is problematical.

Comparison of subsurface data obtained for the Bridgnorth Sandstone with data collected from surface samples of the Bridgnorth Sandstone indicates that processes associated with surface weathering result in a very different geochemical "signature" for surface

samples, i.e. surface samples are depleted in Al, Fe, Ca, Mg, Mn and Ti relative to borehole samples. This implies that comparative studies carried out on surface samples from one formation and subsurface samples from another formation would be totally invalid. For this reason, the only valid comparison available between onshore locations studied and wells from North Ravenspurn, was one utilising Bridgnorth Sandstone samples from the Kempsey Borehole (see Table 10.1). Comparison of geochemical data from aeolian sandstones of the Kempsey Borehole with data obtained for aeolian sandstones from the North Ravenspurn "A" structure indicates:

(i) The aeolian Bridgnorth Sandstone contains higher Fe, Mg, K and Ti than aeolian Lemn Sandstone samples from North Ravenspurn.

(ii) The aeolian Bridgnorth Sandstone contains similar Al and Ca contents to aeolian samples from the North Ravenspurn "A" structure. Aeolian sands from the North Ravenspurn "B" structure have lower Ca contents than aeolian strata from the North Ravenspurn "A" structure and onshore material from the Kempsey borehole.

(iii) Samples of aeolian Bridgnorth Sandstone contain lower Si contents than samples of aeolian Lemn Sandstone from North Ravenspurn.

Higher K, Fe, Mg, and Ti contents within the Bridgnorth Sandstone probably occur because this formation is less compositionally mature than the Lemn Sandstone of North Ravenspurn, i.e. aeolian Bridgnorth

Sandstone samples from the Kempsey Borehole consist mainly of sublitharenites, whereas aeolian samples of the Lemn Sandstone consist of both sublitharenites and orthoquartzites, displaying a narrow compositional range. Lower feldspar and lithic clast contents within the Lemn Sandstone probably arise as a result of more extreme diagenesis within this formation; and also because of minor differences in the original composition of these sediments compared to sediments in onshore basins.

The comparison of onshore basins is problematical because most samples studied were collected from surface outcrop. However, if it is assumed that the surface outcrops have undergone the same weathering processes, then comparative studies of surface samples is possible.

Results of comparative studies between surface samples of aeolian strata collected from the Bridgnorth Sandstone, Penrith Sandstone and Hopeman Sandstone are included in Tables 10.2 - 10.4.

Tables 10.2 - 10.4 illustrate major differences in the composition of aeolian Bridgnorth Sandstone samples when compared to aeolian samples of the Penrith and Hopeman Sandstone. Differences in the geochemical composition of these formations may be summarised as follows:

Surface samples of the Bridgnorth Sandstone contain lower Si contents, but higher Al, Fe, Mg, K, and Ti contents than surface samples of the Penrith and Hopeman Sandstone. There is apparently no significant

difference between the Mn contents of the Bridgnorth, Hopeman and Penrith Sandstone, or in the Ca content of the Bridgnorth and Penrith Sandstone. The only significant difference between aeolian Penrith and Hopeman Sandstones is a lower Al content in the latter.

Higher Fe, Mg, Ca, and K in the Bridgnorth Sandstone when compared to the Hopeman Sandstone probably correlates with more extensive grain dissolution / replacement, and the absence of smectite in the clay fraction of the Hopeman Sandstone.

The same argument can be used to explain differences in the composition of the Bridgnorth and Penrith Sandstone. In the case of the Penrith Sandstone, dissolution / replacement of labile silicate clasts in carbonate rich facies at basin margins ultimately leads to the precipitation of silica in basinward locations. Thus in basinward locations enrichment of silica occurs relative to Fe, Mg, Ca, K, and Ti. (This statement broadly applies if either of the models for silica authigenesis within the Penrith Sandstone outlined in Chapter Five are true). This process does not occur in the Bridgnorth Sandstone, where low volumes of carbonate material within marginal alluvial facies results in much less labile silicate clast dissolution.

It should also be noted that grain coating clays are only very poorly developed within the silicified Penrith Sandstone when compared with the Bridgnorth Sandstone. The Penrith Sandstone also contains

significantly lower proportions of feldspar and lithic clasts than the Bridgnorth Sandstone (see Figures 5.1.1 and 7.3.1)

The similarity between the geochemistry of aeolian Penrith Sandstone and Hopeman Sandstone is interesting. Both formations display extensive evidence of clast dissolution / replacement, abundant authigenic silica, a high degree of compositional maturity, relatively low total clay contents, and extensive evidence of the development of secondary porosity. These compositional similarities suggest it is highly likely that the controls on diagenesis within these formations were similar. However, the limited exposure and poor knowledge of the nature of facies within the Lower Permian of the Moray Firth prevents a more detailed interpretation.

In conclusion, it is suggested that lithology, facies type, the location of facies types within a basin, and burial history (inversion etc.) are all important controls upon diagenesis within Rotliegend sediments. In addition to these factors, the nature of sediments flooring the basin may also be important, especially if they contain organic matter, the maturation of which may alter the chemistry of fluids within basin fill sediments.

## REFERENCES.

- Ali, A. D., and Turner P. (1982) "Authigenic K-feldspar in the Bromsgrove sandstone formation (Triassic) of Central England". J. Sed. Pet. Vol. 52, No. 1, p.187-197.
- Anderson, J. G. C. and Owen, T. R. (1980) "The structure of the British Isles" Pub. Pergamon.
- Arthur, T. J., Pilling D., Bush D. and Macchi L. (1986) "The Leman Sandstone Formation in U.K. Block. 49/28 - Sedimentation, Diagenesis and Burial History." In Brooks et al (eds) (1986) "The Habitat of Palaeozoic Gas in N.W. Europe". Geological Society Special Publication. No. 23, p.251-266.
- Basu, A., Young, S. W., Lee, J. and James, W. (1975) "Re-evaluation of the use of undulose extinction and polycrystallinity in quartz for provenance interpretations." J. Sed. Pet. Vol. 45, No 4, p.875-882.
- Benton, M. J. and Walker, A. D. (1985) "Palaeoecology, taphonomy and dating of Permo - Triassic reptiles from Elgin, North-east Scotland." Palaeontology, Vol. 28, p.207-234.
- Berner, R. A. (1971) "Principles of chemical sedimentology." McGraw-Hill, New York.
- Blackwelder, E. (1928) "Mudflow as a geological agent in semi-arid mountains" Bull. Geol. Soc. America., Vol. 39, p.465-486.



- Blandford, (1873) "On the nature and probable origin of the superficial deposits in the valleys and deserts of central Persia". Quart. J. Geol. Soc. Lond., Vol. 29. p.493-501.
- Boulton, W. S. (1933) "The Rocks between the Carboniferous and the Trias in the Birmingham District." Quart. J. Geol. Soc. Lond. Vol. 89, p.53-56.
- Boulton, W. S. (1924) "On a recently discovered breccia bed underlying Nechells, (Birmingham)". Quart. J. Geol. Soc. Lond. Vol. 80, p.434-373.
- Boulton, W. S. (1951) "Permian rocks of the Midlands." Geol. Mag. Vol. 74, p.534-553.
- Brindley, G. W. (1961) "Kaolin, Serpentine, and kindred minerals", In Brown G (ed) "The X-Ray identification and crystal structures of clay minerals". Pub. Min. Soc. Lond.
- Brookfield, M. E. (1977) "The origin of bounding surfaces in aeolian sandstones". Sedimentology, Vol. 24, p.303-332.
- Brookfield, M. E. (1979) "Anatomy of a Lower Permian aeolian sandstone complex, Southern Scotland". Scott. J. Geol., Vol. 30, p.311-339.
- Bruce, C. H. (1984) "Smectite dehydration - its relation to structural development and hydrocarbon accumulation in Northern Gulf of Mexico Basin." Bull. A.A.P.G., Vol. 68, No. 6, p.673-683.
- Bush, P. R. (1970) "Chloride - rich brines from sabkha sediments and their possible role in ore formation".

- Trans. Inst. Min. Metall. B., Vol. 79, p.137-144.
- Bull, W.E. (1964) "Alluvial fans and near surface subsidence in Western Fresno County, California". U.S. Geol. Surv. Prof. Pap. No. 437A, 70p.
- Bull, W. B. (1972) "Recognition of alluvial fan deposits in the stratigraphic record" In Hamblin W. K., and Rigby, J. K., (eds) "Recognition of ancient sedimentary environments". S.E.P.M. Spec. Pub. No. 16, p.63-83.
- Bull, W. B. (1977) "The alluvial fan environment" Prog. Phys. Geogr. Vol. 1, p.222-270.
- Burgess, I. C. (1965) "The Permo - Triassic rocks around Kirkby Stephen, Westmorland". Proc. Yorks. Geol. Soc. Vol. 35, No. 6, p.91-101.
- Burgess, I. C. and Holliday, M. A. (1974) "The Permo-Triassic Rocks of the Hilton Borehole, Westmorland." Bull Geol. Survey of Britain. Vol. 46, p.1-17.
- Burgess, I. C. and Wadge, A. J. (1974) "The Geology of the Cross Fell Area." Pub. British Geological Survey, London.
- Burley, S. D. and Kantorowitz, J. D. (1986) "Thin Section and S.E.M. textural criteria for the recognition of cement dissolution porosity in Sandstones." Sedimentology Vol. 33, p.587-604.
- Carroll, D. (1970) "X-ray identification of clay minerals." Geological Society Of America Special Publication No. 126.
- Carver, R. E. (ed.) (1971) "Procedures in

- sedimentology". John Wiley, New York.
- Chadwick, R. A. (1985) "Permian, Mesozoic and Cenozoic structural evolution of England and Wales in relation to the principles of extension and inversion tectonics." In Whittaker, A. ed. "Atlas of onshore sedimentary basins in England and Wales - Post Carboniferous tectonics and stratigraphy." Pub. British Geol. Survey.
- Chadwick, R. A. (1985) "Seismic reflection investigations into the stratigraphy and structural evolution of the Worcester Basin." Quart. J. Geol. Soc. Lond. Vol. 142, p.187-202.
- Chesher, J. A. and Lawson, D. (1983) "The Geology of the Moray Firth" Rep. Inst. Geol. Sci.
- Chillingarian, G. V., and Wolf, K. H. (1976) "The compaction of coarse grained sediments." Developments in sedimentology 8B. Pub. Elsevier.
- Clemmensen, L. B. and Abrahamsen, K. (1983) "Aeolian stratification and facies association in desert sediments, Arran Basin (Permian) Scotland". Sedimentology, Vol. 28, p.753-780.
- Clemmensen, L. B. (1987) "Complex star dunes and associated aeolian bedforms, Hopeman Sandstone (Permo - Triassic), Moray Firth Basin, Scotland." In Frostic, L. E. and Ried, I. (eds) "Desert sediments: Ancient and Modern." Spec. Pub. Geol. Soc. Lond., No. 35, p.213-231.
- Collinson, J. D. and Thompson, D. B. (1982) "Sedimentary structures" pub. George Allen and

- Unwin. London.
- Colter, V. S. and Ebborn, J. (1978) "The Petrography and reservoir properties of some Triassic Sandstones of the Northern Irish Sea Basin." Quart. J. Geol. Soc. Lond., Vol. 135, p.57-62.
- Cooke, R. U. and Warren, A. (1973) "Geomorphology in deserts" Pub. Univ. Of. California Press, L.A. Calif. 374p.
- Craig, J. R. and Vaughan, D. J. V. (1981) "Ore microscopy and ore petrography" Pub. John Wiley.
- Curtis, C. D. and Spears, D. A. (1971) "Diagenetic development of kaolinite" Clays and Clay Minerals, Vol. 19, p.219-227.
- Doe, T. W. and Dott, R. H. (1980) "Genetic significance of deformed cross bedding - with examples from the Navajo and Weber Sandstones of Utah". J. Sed. Pet., Vol. 50, No 3, p.793-812.
- Deer, W. A., Howie, R. A., and Zussman, J. (1966) "An introduction to the rock forming minerals". Pub. Longman.
- Dimitropoulos, K. and Donato, J. A. (1981) "The Inner Moray Firth Central Ridge, a geophysical interpretation" Scott. J. Geol., Vol. 17, p.27-38.
- Dunham, K. C. (1932) "Quartz dolomite pebbles (whin sill type) in the Upper Brockham." Geol. Mag., Vol. 69, p.425-427.
- Dypvik, H. (1983) "Clay mineral transformations in

- Tertiary and Mesozoic sediments from the North Sea".  
Bull. A.A.P.G., Vol. 67, No. 1, p.160-165.
- Earp, J. R., and Hains, B. A. (1971) "British Regional  
Geology - The Welsh Borderland". Pub. Institute  
Geological Sciences, HMSO Lond.
- Eastwood, T., Whitehead, T.M., and Roberstson, T.  
(1925) "The Geology of the country around Birmingham."  
Mem. Geol. Survey, England and Wales, HMSO, Lond.
- Evamy, B. D. and Shearman, D. J. (1965) "The  
development of overgrowths from echinoderm fragments."  
Sedimentology, Vol. 5, p.211-233.
- Evamy, B. D. (1969) The precipitational environment  
and correlation of some calcite cements deduced from  
artificial staining"  
Sedimentology, Vol 12, p317 - 322.
- Fenning, P. J. (1968) "Geophysical investigations" In  
Peacock, J. D., Berridge, N. G., Harris, A. L., and  
May, F. "The Geology of the Elgin District" Mem.  
Geol. Survey of Great Britain. HMSO Lond. p.140-153.
- Fleet, W. F. (1923) "Notes on the Triassic sands near  
Birmingham with special reference to their heavy  
detrital minerals." Proc. Geol. Assoc., Vol. 34,  
p.114-124.
- Fleet, W. F. (1927) "The heavy minerals of the Keele,  
Enville, Permian and Lower Triassic rocks of the  
Midlands and the correlation of these strata." Proc.  
Geol. Assoc., Vol. 38., p.481-487.
- Folk, R. L. (1974) "Petrology of sedimentary rocks".  
Hemphill Publishing Co. Austin Texas.

- Folk, R. L. and Land, L. S. (1975) "Mg/Ca ratio and salinity: two controls over crystallisation of dolomite". Bull. A.A.P.G., Vol. 59, p.60-68.
- Frostick, L., Ried, I., Jarvis, J. and Eardley, H. (1988) "Triassic sediments of the Inner Moray Firth, Scotland: Early rift deposits." Quart. J. Geol. Soc. Lond., Vol. 145, p.235-248.
- Fryberger, S. G., Ahlbrandt, T. S. and Andrews, S. (1979) "Origin, sedimentary features, and significance of low - angle aeolian "sand sheet" deposits, Great Sand Dunes National Monument and Vicinity." J. Sed. Pet., Vol. 49, p.733-746.
- Fryberger, S. G. and Dean, G. (1979) "Dune forms and wind regime" In McKee, E. D. (ed) "A study of global sand seas" U.S.G.S. Prof. Pap. No. 1052, 137-169.
- Glennie, K. W. (1970) "Desert sedimentary environments". Developments in sedimentology, No. 14, Elsevier.
- Glennie, K. W., Mudd, G. C., and Nataegaal, P. J. C. (1978) "Depositional environment and diagenesis of Permian Rotliegendes Sandstones in Leman Bank and Sole Pit areas of the UK southern North Sea". Quart. J. Geol. Soc. Lond., Vol. 135, p.25-34.
- Glennie, K. W. and Boegner, P. L. E. (1981) "Sole Pit inversion tectonics" In Illing, L. V. and Hobson, G. D. (eds) "Petroleum Geology of the continental shelf of N.W. Europe". Pub. Heyden, London.
- Glennie, K. W. and Buller, A. T. (1983) "The Permian

- Weisslied of North-West Europe. The partial deformation of aeolian dune sands caused by the Zechstein transgression." *Sedimentary Geology*, Vol. 35, p.43-81.
- Glennie, K. W. (1984) "Early Permian - Rotliegend". In Glennie K. W. (ed.) "Introduction to the petroleum geology of the North Sea". Pub. Blackwell, p.41-60.
- Glennie, K. W. (1985) "Early Permian (Rotliegendes) palaeowinds of the North Sea" - Reply. *Sedimentary Geology*, Vol. 45, p.293-313.
- Glennie, K. W. (1987) "Desert sedimentary environments, present and past - A summary." *Sedimentary Geology*, Vol. 50, p.135-165.
- Goldich, S. S. (1938) "A study in rock weathering" *J. Geol.*, Vol. 46, p.17-58.
- Hains, B. A. and Horton, A. (1969) "British Regional Geology - Central England." Pub. Institute Geological Sciences, HMSO, London.
- Hancock, N. J. (1978) "Possible causes of Rotliegend Sandstone Diagenesis in Northern West Germany." *Quart J. Geol. Soc. Lond.* Vol 135, p.35-40.
- Helgeson, H. C., Garrels, R. M. and McKenzie, F. T. (1969) "Evaluation of irreversible reactions in geochemical processes involving minerals and aqueous solutions -II, applications". *Geochem. et Cosmochim. Acta.* Vol. 33, p.455-481.
- Hummel, G. and Kocurek, G. (1984) "Interdune areas of the back island dune field, north Padre Island, Texas." *Sedimentary Geology*, Vol. 39, p.1-25

- Hunter, R. E. (1977) "Basic types of stratification in small aeolian dunes" *Sedimentology*, Vol. 24, p.361-388.
- Hurst, V. J., and Kunkle, A. C. (1985) "Dehydration, rehydration and stability of Kaolinite". "Clays and Clay Minerals", Vol. 33, No. 1.
- Ixer, R. A., Turner, P., and Waugh, B. (1978) "Authigenic iron and titanium oxides in Triassic red-beds: St Bees Sandstone, Cumbria, Northern England". *Geological Journal*, Vol. 14, p.179-192.
- JerzyKiewicz, T., Kijewski, P., Mroczkowski, J. and Teisseyre, A. K. (1976) "Origin of the Weissliegende in the Fore Sudetic Monocline." *Geol. Sudetica.*, XI, p.58-97.
- Kessler, L. G. (II) (1978) "Diagenetic sequence in ancient sandstones deposited under desert climatic conditions". *Quart. J. Geol. Soc. Lond.*, Vol. 135, p.41-49.
- King, W. W. (1883) "Clent Hills Breccia.", *Midland Naturalist*, Vol. 10, p.24-37.
- King, W. W. (1893) "Clent Hills Breccia." *Midland Naturalist*, Vol. 10, p.24-37.
- King, W. W. (1923) "The unconformity below the Trappoid (Permian?) Breccia." *Trans. Worcs. Nat. Club.*, Vol 8, p.3-15.
- Kocurek, G. and Dott, R. H. (1981) "Distinctions and uses of stratification types in the interpretation of aeolian Sand." *J. Sed. Pet.*, Vol. 51, No 2,



p.579- 595.

Kocurek, G. (1981) "Erg reconstruction: The Entrada Sandstone (Jurassic) of Northern Utah and Colorado." Palaeogeography, palaeoclimatology, palaeoecology, Vol 36, p.125-153.

Kocurek, G. (1981) "Significance of interdune deposits and bounding surfaces in aeolian dune sands." Sedimentology, Vol. 28, p.753-780.

Krauskopf, K. B. (1979) "Introduction to Geochemistry ". McGraw-Hill, New York.

Lancaster, N. (1983) "Controls on dune morphology in the Namib sand sea." In: Brookfield, M. and Ahlbrandt, T. S. (eds) "Eolian sediments and processes." Elsevier, Amsterdam. p.261-289.

Lee, M. (1984) "Diagenesis of the Permian Rotliegende Sandstone, North Sea: K/Ar,  $O^{18}/O^{16}$ , and Petrologic evidence". PhD Thesis, Case Western Reserve University.

Lee, M., Aronson, J. L. and Savin, S. M. (1985) "K/Ar, dating of time of gas emplacement in Rotliegendes Sandstone, Netherlands." Bull. a.a.p.g., Vol 69, p.1381-1385.

Longman, M. W. (1980) "Carbonate Diagenetic Textures from Rearsurface diagenetic environments." Bull, a.a.p.g., Vol. 64, No. 4 p. 461-487.

Loope, D. B. (1984) "Discussion: Origin of extensive bedding planes in aeolian sandstones - a defense of Stokes' hypothesis." Sedimentology, Vol 31, p.123-125.

- Lutz, M., Kaasschier, J. P. H. and Van Wijhe, D. H. (1975) "Geological factors controlling Rotliegend gas accumulation in the Mid - European Basin." Proc. 9th World Pet. Cong., Vol. 2., p.93-97.
- Macchi, L. (1987) "A review of Sandstone illite cements and aspects of their significance to hydrocarbon exploration and development." J. Geol. Vol. 4.
- Macchi, L. and Waugh, B. (1984) "The Permo-Triassic rocks of Cumbria." Poro Perm Excursion Guide No. 2.
- Macchi, L. C. (1981) "Sedimentology of the Penrith Sandstone and Brockhams (Permo-Triassic) of Cumbria, N.W. England." Unpub. Ph.D thesis. Univ. of Hull.
- Mader, D. and Yardley, M. J. (1985) "Migration, modification and merging in aeolian systems and the significance of the depositional mechanisms in Permian and Triassic dune sands of Europe and North America." Sedimentology, Vol. 43, p.85-218.
- Marie, J. P. P. (1975) "Rotliegendes Stratigraphy and diagenesis." In Woodland, A. H. (ed) "Petroleum and the Continental of North-West Europe." Vol. 1 Geology. Applied Science Publishers, Barking Essex. p. 205-211.
- McKee, E. D. (1945) "Small scale structures in the Coconino Sandstone of northern Arizona" J. Geol. Vol. 53, p.313-325.
- McKee, E. D. (1982) "Sedimentary Structure in dunes of the Namib Desert South West Africa." Geol. Soc. AM. Bull. Vol. 188, p. 1-64.
- McKee, E. D. (1979) "Sedimentary Structures in dunes."

- In McKee, E. D. (ed) "A Study of Global Sand Seas."  
U.S.G.S. Prof. Pap. Vol.1052, p.83-291.
- McKee, E. D. and Moiola, R. J. (1975) "Geometry and growth of the white sands dune field, New Mexico." J. Res. U.S. Geol. Surv. Vol. 3 p.59-66.
- McKee, E. D. (1966) "Structures of dunes at White Sands National Monument, New Mexico (and comparison with structures of dunes from other selected areas)." Sedimentology. Vol. 7, p. 1-69.
- Mitchell, G. M., Pocock, R. W., and Taylor, J. M. (1961) "The Geology of the country around Droitwich, Abberly and Kiddderminster." Mem. Geol. Survey of Great Britain, HMSO Lond.
- Moorbath, S. (1962) "Lead isotope abundance studies on mineral occurrences in the British Isles." Phil. Trans. Roy. Soc. London. A 254. p. 295-360.
- Mosely, F. (ed) (1978) "The Geology of the Lake District." Occ. Pub. Yorks. Geol. Soc. No. 3.
- Muir - Wood, R. (1985)  
"The seismo tectonics of North - West Europe". In "Earthquake engineering in Britain".  
Pub. Inst. Civil. Engineers.
- Nielson, J. and Kocurek, G. (1987) "Surface processes, deposits, and development of Star dunes: Dumont dune field, California." Bull. Geol. Soc. AM. Vol. 99, p. 177-186.
- Nagtegaal, P. J. C. (1973) "Adhesion ripple and Barchan dune Sands of the recent Namib (S.W. Africa) and Permian Rotliegend (N.W. Europe) deserts. MADOQUA

Series 11, Vol. 2, nos. 63-68, p.5-19.

- Owen, T. R. (1976) "The geological evolution of the British Isles." Pub. Pergamon international library of science, technology, engineering and social studies.
- Peacock, J. D. (1966) "Contorted Beds in the Permo-Triassic Aeolian Sandstones of Moray Shire." Bull. Geol. Survey of Great Britain, Vol. 24, p157 - 167.
- Perry, A. E. Jr. and Hower, J. (1970) "Burial diagenesis in Gulf Coast Pelitic Sediments." Clays and Clay Minerals, Vol. 18, p. 165-177.
- Pettijohn, F. J. (1975) "Sedimentary Rocks". Harper and Row, New York.
- Pettijohn, F. J., Potter, P., and Siever, R. (1973) "Sand and Sandstone." Pub New York, Springer Verlag.
- Phipps, C. B. and Reeve, F. A. E. (1969) "Structural Geology of the Malvern, Abberley and Ledbury Hills." Quart. J. Geol. Soc. Lond. Vol. 125, p.1-37.
- Pocock, R. W. and Wray, D. A. (1925) "Geology of the Country around Wem." Mem. Geol. Survey of Great Britain, HMSO, Lond.
- Poole, E. G. and Whiteman, A.J. (1966) "Geology of the Country around Nantwich and Whitchurch." Mem. Geol. Surv. Great Britain.
- Reynolds, R.C. (1980) "Interstratified Clay Minerals." In Brindley, G. W. and Brown, G. (eds) "Crystal Structures of Clay Minerals and their X-ray Identification." Pub. Min. Soc. London p. 249-303.

- Richardson, L. (1928) "Wells and springs of Warwickshire." Mem. Geol. Survey of Great Britain. HMSO, London.
- Richardson, L. (1930) "Wells and springs of Worcestershire." Mem. Geol. Survey of Great Britain. HMSO, London
- Richter, D. K. and Fuchtbouer, H. (1978) "Ferroan Calcite replacement indicates former Magnesian Calcite Skeletons." Sedimentology 25, p. 843-860.
- Roedder, E. (1984) "Fluid Inclusions". Mineralogical Society of America. Reviews in Mineralogy. Vol. 12.
- Rossel, N. C. (1982) "Clay mineral diagenesis in Rotliegend Aeolian sandstones of the southern North Sea." Clay Minerals, Vol. 17, p.69-78.
- Rubin, D. W. and Hunter, R. E. (1981) "Bedform Climbing in theory and nature." Sedimentology. Vol. 29, p.121-138.
- Schmidt, V., McDonald, D. A. and Platt, R. L. (1977) "Pore geometry and reservoir aspects of secondary porosity in sandstones." Can. Petrol. Geol. Bull. Vol. 25, No. 2, p.271-290.
- Seeman, U. (1979) "Diagenetically formed interstitial clay minerals as a factor in Rotliegend sandstone reservoir quality in the Dutch sector of the North Sea." J. Petrol. Geol. Vol. 3, p.55-62.
- Shepherd, T., Rankin, A. H., and Alderton, D. H. M. (1985) "A Practical guide to Fluid Inclusion Studies." Pub. Blackie.
- Shotton, F. W. (1937) "The Lower Bunter Sandstones of

- North Worcestershire and East Shropshire." Geol. Mag. IXXIV, p. 534-553.
- Shotton, F. W. (1956) "Some aspects of the New Red Desert in Britain." Liverpool and Manchester Geol. Journ. Vol 1, p. 450-465.
- Shrodon, J. (1980) "Precise identification of Illite/Srectite interstratification by X-ray Powell Diffraction." Clays and Clay Minerals, Vol. 28 No. 6 p. 401-411.
- Smith, D. B., Brunstrom, R. G. W., Manning, P. I., Simpson, S., and Shelton, F. W. (1974). "Permian". Geol. Soc. Lond. Special Report no. 5.
- Smith, N. J. P. et al. (1985) "Pre-Permian subcrop map." In Whittaker, A. (ed). "Atlas of onshore sedimentary basins in England and Wales - Post Carboniferous tectonics and Straigraphy." Pub. British Geol. Survey.
- Sorby, (1858) "Microscopic structure of crystals, indicating the origin of minerals and rocks." Quart. J. Geol. Soc. Lond., Vol. 14, No. 1, p.435-500.
- Steele, R. P. (1981) "Aeolian Sand and Sandstone." Unpub. Ph.D. thesis. Univ. of Hull.
- Stokes, S. C. (1968) "Multiple parallel - truncation bedding planes, a feature of wind deposited sandstone formations." J. Sed. Pet. Vol. 38, p. 510-515.
- Underhill, J.R., Gayer, R. A., Woodcock, N. H., Donnelly, R., Jolley, E. J., and Stimpson, I. G. (1988). "The Dent Fault System, Northern England - reinterpreted as

- a major oblique slip fault zone". Quart. J. Geol. Soc. Lond., Vol. 145, p.303-316.
- Versey, H. C. (1939) "The Petrography of the Permian rocks in Southern part of the Vale of Eden." Quart. Journ. Geol. Soc. Lond. Vol. 95, p. 275-298.
- Versey, H. C. (1960) "The Geology of the Appelby district." Pub. Whitehead and Son, Appelby.
- Walker, T. R., Waugh, B. and Crone, A. J. (1978) "Diagenesis in First-cycle desert alluvium of Cenozoic age, Southwestern United States and Northwestern Mexico." Bull. Geol. Soc. AM. Vol. 89, p.146-155.
- Walker, A. D. (1973) "The age of the Cutties Hillock Sandstone (Permo-Triassic) of the Elgin area." Scott. J. Geol. Vol. 9, p. 177-183.
- Walker, T. R. and Harms, J. C. (1972) "Eolian origin of Flagstone Beds. Lyons Sandstone (Permian) type area. Boulder County, Colorado." Mountain Geologist, Vol 9, p. 279-288.
- Walker, T. R. (1967) "Formation of Red Beds in Modern, and Ancient Deserts." Geol. Soc. America Bull., Vol. 78, p.353-368.
- Walker, T. R. (1967) "Diagenetic origin of Continental Red Beds." In Falke, H. (ed) "The Continental Permian in Central, West and South Europe." N.A.T.O. Advanced study Inst. Ser. C. Maths and Physics, sci. Reidel, Dordrecht, Holland. p. 240-282.
- Warrington, G., Audley-Charles, M. G., Elliot, R. E., Evans, W. B., Iuimey-Cook, H. C., Kent, P. E., Robinson, P. L., Shotton, F. W., and Taylor, F. M. "A

- Correlation of Triassic rocks in the British Isles." Spec. Rept. Geol. Soc. London No. 13 p. 78.
- Wasson, R. J. (1977) "Last-glacial alluvial fan sedimentation in the Lower Derwent Valley, Tasmania." Sedimentology. Vol. 24. p. 781-799.
- Waugh, B. (1970) "Petrology, provenance and silica diagenesis of the Penrith sandstones (lower Permian) of northwest England." J. Sed. Pet. Vol. 40, p.1226-1240.
- Waugh, B. (1978) "Authigenic K-Spar in British Permo-Triassic sandstones." J. Geol. Soc. Lond. 135 p51-56.
- Whitehead, T.H. and Eastwood, T. (1927) "The Geology of the Southern part of the South Staffordshire Coalfield." Mem. Geol. Survey of England and Wales. HMSO, London.
- Whitehead, T. H. and Pocock, R. W. (1947) "Dudley and Bridgnorth." Mem. Geol. Survey of England and Wales. HMSO London.
- Williams, D. (1974) "The Sedimentology and Petrology of the New Red Sandstone of the Elgin Basin, N.E. Scotland." Unpub. Ph.D. thesis. University of Hull.
- Williams, R. B. G. (1983) "Introduction to Statistics for Geographers and Earth Scientists." Pub. Macmillan p .349.
- Wills, L. J. (1946) "The palaeogeography of the Midlands." Pub. Hodder and Stroughton, London.
- Wills, L. J. (1956) "Concealed Coalfields - A palaeogeographical study of the stratigraphy and